THE UNIVERSITY OF CALGARY

Spatial Predator-Prey Dynamics: The Effect of Prey Movement and Environmental Heterogeneity

by

Tammy Dee Rosner

A THESIS

SUBMITTED TO THE FACULTY OF GRADUATE STUDIES

IN PARTIAL FULFILMENT OF THE REQUIREMENTS FOR THE

DEGREE OF MASTER OF SCIENCE

DEPARTMENT OF BIOLOGICAL SCIENCES

CALGARY, ALBERTA

JANUARY, 1999

ABSTRACT

Spatially-structured predator-prey models with simple local population dynamics (i.e. the neutrally stable Lotka-Volterra model) predict spatial population heterogeneity and stability only when environmental heterogeneity is present. When the local population model contains biologically realistic features of predators and prey (the Rosenzweig-MacArthur model), spatial structure affects dynamics similarly in heterogeneous and homogeneous environments. This model was tested using the *Ceriodaphnia*-algal interaction with systems consisting of two aquaria in which mixing of algae was manipulated along with heterogeneity in light intensity (which affects the algal carrying-capacity). As predicted by theory, spatial pattern in prey density and depressed *Ceriodaphnia* birth rates were observed in both heterogeneous and homogeneous environments. Partial failure of the model to predict differences among treatments in equilibria, and relationships between Ceriodaphnia birth rate and prey density, might be explained if the *Ceriodaphnia* birth rate was density-dependent, and evidence of this structural theory is provided.

ACKNOWLEDGMENTS

I thank Edward McCauley for his excitement, patience, guidance, and support. Andre M. de Roos and William S. C. Gurney helped me with the modelling components. Michael Vander Meulen and Susan Watson gave me hands-on instruction on maintaining cultures, setting up the experiment and sampling. Emma Pyke, Marianne Wallace, and Ken Nelson assisted with the experiment. John R. Post, Robert Woodrow, and Richard L. Walker provided valuable criticism. Graduate students in the Ecology Division provided support and encouragement.

TABLE OF CONTENTS

LIST OF TABLES

LIST OF FIGURES

LIST OF SYMBOLS

Symbol	Description	Units
A_a	prey density in patch-a (algal density in tank-a)	µg Chl-*a* / L
A_b	prey density in patch-b (algal density in tank-b)	µg Chl-*a* / L
A or A_{mix}	prey density (algal density) in a system with only a single prey population	µg Chl-*a* / L
$\overline{A}$	average algal concentration between two tanks in a metapopulation or non-metapopulation	µg Chl-*a* / L
C	predator density (*Ceriodaphnia* density) in a metapopulation or non-metapopulation	# / L
C_{mix}	predator density when prey are mixed between two patches (non-metapopulation)	# / L
t	time	day
r	intrinsic rate of increase of prey	1/day
r_a	intrinsic rate of increase of prey in environment-a	1/day
r_b	intrinsic rate of increase of prey in environment-b	1/day
r_{mix}	intrinsic rate of increase of prey when they population is distributed equally in environment-a and environment-b	1/day
k	carrying capacity of prey	µg Chl-*a* / L
k_a	carrying capacity of prey in environment-a	µg Chl-*a* / L
k_b	carrying capacity of prey environment-b	µg Chl-*a* / L
k_{mix}	carrying capacity of prey when they population is distributed equally in environment-a and environment-b	µg Chl-*a* / L
f	attack rate of predator	L/#/day
e	conversion efficiency	# / µg Chl-*a*
d	death rate parameter of predator ($d=d_1+d_2$)	1/day
d_1	predator per capita maintenance rate	1/day
d_2	predator per capita death rate	1/day
g	predator maximum per capita ingestion rate	µg Chl-*a* / # /day
h	half saturation constant of predator functional response	µg Chl-*a* / L
m	predator per capita migration rate	1/day
I	predator per capita ingestion rate	µg Chl-*a* / # /day
b	predator per capita birth rate	1/day

Overview of Chapters

Spatial structure can have a large effect on predator-prey interactions. Two features which have been shown to affect spatially-structured populations in theory are the degree of connectedness of local populations and the amount of spatial environmental variability. Chapter 1 reviews some of the theoretical research that has been done on the effects of these two factors.

Chapter 2 describes a model and provides original analyses of the situation where local dynamics posses a moderate amount of biological realism (the Rosenzweig-MacArthur model) and spatial structure is incorporated in a way which can be replicated precisely in an experimental setting. The chosen spatial structure has complete mixing of the predator population between two patches and complete isolation of the prey population in the two patches. The model describing this system is compared to the case where both prey and predator are completely mixed over both patches. The comparison is made both in the presence and in the absence of environmental heterogeneity in the prey growth rate. A number of very interesting predictions about spatially-structured predator-prey interactions are developed from this analysis.

Chapter 3 provides necessary information required to test the model in a specific experimental system, which has *Ceriodaphnia dubia* as the predator and a multi-species assemblage of algae as the prey. The expected equilibria for spatially structured and unstructured experimental systems are determined from detailed information on the biology of *Ceriodaphnia,* and algae-only systems of the experiment. As well, specific predictions about the effect of spatial structure on the relationship between algal density and the *Ceriodaphnia* birth rate are derived, and methods to test these predictions are described.

Chapter 4 presents the experiment and results which test the predictions developed in the previous chapters. The movement of individuals in the experiment is precisely controlled and corresponds directly to the representation of spatial structure incorporated into the models of the previous chapters. Although fundamental predictions are realized there are a number of deviations from predictions that, because the spatial structure has been so carefully controlled, must arise because fundamental features of the biology of the interacting populations have not been accurately represented in the model. A description of the decessary properties of these features is given.

CHAPTER ONE: Two-Patch Predator-Prey Models

INTRODUCTION

The earliest models describing predator-prey interactions assumed that populations were mixed and that interaction rates were determined by the law of mass action. In real populations, individuals do not mix over the entire range of the population and mass action is only expected to occur locally. In this case, it is useful to think of the population as a group of local populations (sub-populations or patches), whether they are spatially isolated or not, for which the law of mass action holds for each well mixed local population. The population is then a metapopulation or a group of local populations. Dynamics of local populations are dictated by migration, colonization or dispersal, in addition to the usual processes described for isolated, well mixed, populations. Metapopulation dynamics arise from the sum of the dynamics of these local populations.

Currently, the term metapopulation has been primarily used to describe systems where individual sub-populations are destined to become extinct (i.e., there is no population regulation at a local scale), and when migration is rare enough that it is only important when an empty region of habitat is colonized (Hanski and Simberloff, 1997). In these cases, within-patch dynamics need not be modelled explicitly and the number or proportion of patches in a given state (ie. populated or extinct) is described by the model equations. The term metapopulation was first coined to describe such a system by Levins (1969). The definition of metapopulation however, accurately describes a large range of possible spatial structures and dynamics, and a number of other model formulations could easily be considered metapopulations. In many spatially structured models, the balance between independence and connectedness of local populations can give rise to dynamics at the "metapopulation scale" that are not present for a single isolated local population and can be similar for a variety of methods of modelling spatial structure (Taylor, 1988).

My thesis focuses on spatially structured predator-prey systems where: (1) local populations occupy discrete patches, (2) migration is common and can be described by per capita rates, (3) "within patch" dynamics are modelled explicitly, and (4) isolated patches, although they may show unstable dynamics, do not go extinct. This chapter reviews some aspects of theory for this type of metapopulation for predator-prey interactions and describes some examples that are relevant to this thesis.

If local populations all have equal densities at all times then a non-metapopulation

(spatially unstructured) model is sufficient to describe dynamics. Heterogeneity, or pattern, in prey and predator density can arise from internal or external mechanisms. If isolated populations diverge from one another when they have identical starting densities or if per capita migration rates are different among patches, then an external source of heterogeneity is present. Internal sources of heterogeneity include fixed differences in the environment between patches which give rise to variation in prey or predator vital rate parameters (Nisbet, Briggs, Gurney, Murdoch, and Stewart-Oaten, 1992), stochasticity in vital rates which is independent between patches (Reeve, 1988), or bias in migration between patches (Nisbet *et al.*, 1992). If isolated patches have identical dynamics, and migration is not density-dependent or biased, but heterogeneity in prey or predator density can be maintained among linked patches, then the source of this heterogeneity must be internal. When there is more than a single isolated patch, there may be dynamics possible where population densities are not equal in all patches simply because the local populations are somewhat independent. The mechanisms which allow pattern to persist through time without an external source of heterogeneity may be system-specific. The delays inherent in discrete time models can produce spatially non-static but persistent pattern (Hassell, Comins, and May, 1992; Adler, 1993). If there is sufficient non-linearity in vital rate functions then a number of different patterns of prey distribution can result in an equilibrium in predator and prey densities (de Roos, McCauley, and Wilson, 1998).

When a source of heterogeneity is present, dynamics will always have the potential to be different from those observed in a single isolated patch. In the case where the source of heterogeneity is internal, the solutions for the single population model are still present for the metapopulation model and occur when initial conditions in all local populations are identical. Because alternative solutions exist in the metapopulation model, there is also the possibility that dynamics of the metapopulation model are more stable than those of the corresponding non-metapopulation model. Stability is expected to arise because population trajectories of local populations are somewhat independent. Because of this, migration serves as a form of density-dependence where the net emigration rate from a local population tends to be high if the local population has high density, and negative if it has low density (Nisbet *et al.* 1992). In addition to this effect, independence of local populations tends to make the fluctuations in average density for the metapopulation less than they are in any local population. Therefore, when single population dynamics are unstable and metapopulation dynamics are stable, stability usually takes on one of two forms. Local

populations may display approximately the same dynamics as mixed systems but patches (or regions) are asynchronous and therefore the metapopulation is more stable (de Roos, McCauley and Wilson, 1991 for a system without explicit patches; Hassel *et al.*, 1992). Alternatively, dynamics at a local scale may become more stable and different among patches (Nisbet *et al.*, 1992; de Roos *et al.*, 1998).

Both internal and external sources of heterogeneity are observed in natural populations and therefore it is important to understand how they affect metapopulation dynamics individually and how they interact. The effect of external heterogeneity is relatively easy to understand. Differences in the environment among patches cause a difference in parameter values between patches which results in a cascade of effects: (1) different dynamics at a local scale, (2) interactions between local populations, and (3) metapopulation dynamics. When only internal sources of heterogeneity are present, the factors which give rise to differences in local dynamics may be difficult to identify. In the next section, two examples of predator-prey metapopulation models are given. In the first, metapopulation dynamics are primarily dictated by an external source of heterogeneity in the prey per capita growth rate. In the second example, there is no external heterogeneity and heterogeneity can arise solely from non-linearities in the vital rate functions. These examples, along with the model studied in Chapter 2, form a theoretical foundation for the experiment that is the topic of Chapter 4 which contrasts metapopulation and non-metapopulation dynamics both when an external source of heterogeneity is present and when it is absent. All models described here are shown in Table 1.1.

The experimental system that I have chosen has the fresh water herbivore *Ceriodaphnia* as the predator (C) and algae as the prey (A). Nisbet, McCauley, Gurney, Murdoch, and de Roos (1997) have shown that despite the fact that Cladocera, such as *Ceriodaphnia*, have size structured populations, several characteristics of their dynamics may be captured by the Rosenzweig-MacArthur model, which is a Lotka-Volterra type model with logistic growth of the prey, a type II functional response of the predator, and constant conversion efficiency of ingested food by predators.

In nature, *Ceriodaphnia* move over much larger distances than their algal prey (Cuddington and McCauley, 1994). Thus, the prey migration rate will be much less than the predator migration rate in the experiment. There is one superior choice of prey and predator migration rates. Consider the following experimental design. The control system (a system with no metapopulation structure) could consist of two habitat patches with

complete mixing of predators and prey between the two patches. The metapopulation systems would have the migration rate of prey and predator lowered to finite values. If only the prey population had reduced mixing then this would give a better understanding of metapopulations, because only one factor differed between the metapopulation and non-metapopulation systems. Prey mixing could actually be reduced to zero. In this case, the model describing population dynamics does not appear to be a metapopulation model because migration is not present. There would be a single well-mixed predator population feeding on two isolated prey populations. However, prey would still be linked through their common predator, and the behavior of this model would probably be very similar to the case where prey have a low rate of diffusive migration and predators have a high rate of diffusive migration. The model of this special case will be referred to as a "separation of scales" model, but because it is not fundamentally different from metapopualtion models, it will be considered a metapopulation model.

The model for *Ceriodaphnia* has an internal source of heterogeneity, the nonlinearities in prey growth and predator ingestion rates, however, external sources of heterogeneity are also of interest. In order to develop a more complete understanding of these factors, the equilibria and local stability of metapopulations with two patches will be described. First the dynamics of a model with a weak internal source of heterogeneity (the Lotka-Volterra model) is described when external heterogeneity is absent or present. Next the dynamics of a model with a strong internal source of heterogeneity (the Rosenzweig-MacArthur model) is studied. In both models, the case where predators are mixed over both patches is compared to the case where predator migration is finite and diffusive. In Chapter 2, the model with a strong internal source of heterogeneity is studied when there is also external heterogeneity.

METHODS

Some of the results presented here are taken from the literature but in many cases additional analysis was needed. Linear stability analysis was used to determine the dynamics near equilibria. This technique uses a linear approximation of the model to determine whether small deviations from an equilibrium decay or grow over time. This can be determined from the eigenvalues of the coefficient matrix of the linearized model. If all of the eigenvalues of the coefficient matrix have negative real parts then the equilibrium is locally stable. If the eigenvalues cannot be determined explicitly then the Routh-Hurrwitz

Table 1.1. Models reviewed in Chapter 1. The model in the first row describes prey (A - #/L) and predators (C - #/L) in a single isolated patch or mixed over two patches equally well. The models in the second row describes: prey in patch-a (A_a - #/L), prey in patch-b(A_b - #/L), predators in patch-a (C_a - #/L), and predators in patch-b (C_b - #/L). The models in the third row describe: prey in patch-a (A_a - #/L), prey in patch-b (A_b - #/L), and predators in both patches (C - #/L). For the Lotka-Volterra models the parameters are: r_a-intrinsic rate of increase of prey in habitat-a(1/day), r_b-intrinsic rate of increase of prey in habitat-b (1/day), f -attack rate of predator (L/#/day), e -conversion efficiency (-), d-per capita predator death rate (1/day), m - migration rate (1/day). For the Rosenzweig-MacArthur model: r - intrinsic rate of increase of prey (1/day), k - carrying capacity (#/L), g - maximum ingestion rate (1/day), h - half saturation constant (#/L), e - conversion efficiency (-), d - predator per capita death rate (1/day), m - migration rate (1/day).

	Lotka-Volterra	Rosenzweig-MacArthur
Complete mixing, non-metapopulation model	$\frac{dA}{dt} = \frac{r_a + r_b}{2}A - fAC \qquad \frac{dC}{dt} = efAC - dC$	$\frac{dA}{dt} = rA\left(1 - \frac{A}{k}\right) - \frac{gAC}{h + A} \qquad \frac{dC}{dt} = e\frac{gAC}{h + A} - dC$
Diffusive predator migration, metapopulation model	$\frac{dA_a}{dt} = r_a A_a - fA_a C_a \qquad \frac{dA_b}{dt} = r_b A_b - fA_b C_b$ $\frac{dC_a}{dt} = efA_a C_a - dC_a - m(C_a - C_b)$ $\frac{dC_b}{dt} = efA_b C_b - dC_b - m(C_b - C_a)$	$\frac{dA_a}{dt} = rA_a\left(1 - \frac{A_a}{k}\right) - \frac{gA_a C_a}{h + A_a} \qquad \frac{dA_b}{dt} = rA_b\left(1 - \frac{A_b}{k}\right) - \frac{gA_b C_b}{h + A_b}$ $\frac{dC_a}{dt} = e\frac{gA_a C_a}{h + A_a} - dC_a - m(C_a - C_b)$ $\frac{dC_b}{dt} = e\frac{gA_b C_b}{h + A_b} - dC_b - m(C_b - C_a)$
"Separation of scales", metapopulation model	$\frac{dA_a}{dt} = r_a A_a - fA_a C \qquad \frac{dA_b}{dt} = r_b A_b - fA_b C$ $\frac{dC}{dt} = \frac{ef}{2}(A_a + A_b)C - dC$	$\frac{dA_a}{dt} = rA_a\left(1 - \frac{A_a}{k}\right) - \frac{gA_a C}{h + A_a} \qquad \frac{dA_b}{dt} = rA_b\left(1 - \frac{A_b}{k}\right) - \frac{gA_b C}{h + A_b}$ $\frac{dC_a}{dt} = \frac{eg}{2}\left(\frac{A_a C}{h + A_a} + \frac{A_b C}{h + A_b}\right) - dC$

criteria (for the coefficients of the characteristic equation of the coefficient matrix) for stability can be used. For a more in depth description of this technique see Gurney and Nisbet (1998) or May (1973). MAPLE V Release 3 (Waterloo Maple Software and the University of Waterloo) was used for algebraic manipulations. All of the local stability analyses for this chapter are given in Appendix I.

In some cases, the expressions for the equilibria or the stability criteria were too difficult to evaluate. In this event, the stability boundaries in parameter space were determined using CONTENT (CONTinuation EnvironmeNT, Yu. A. Kuznetsov and V.V. Leviten, Centrum voor Wiskcunde en Informatica (CWI)). This program computes eigenvalues of the model and identifies special points where eigenvalues or functions of eigenvalues and equilibrium values change sign. A more detailed description of the methods used by this program is given in Kuznetsov (1995).

For the "separation of scales" models, the effect of mixing occurring once daily rather than continuously was investigated using STAMS SOLVER (University of Strathclyde). This program uses a fourth order Runge-Kutta method of integration to produce the trajectory of the state variables over time. It also allows for state variables to be periodically reset. No effect of a periodic mixing interval on qualitative aspects of the equilibria and their stability was found, and therefore only the results of the models with continuous mixing are given.

Results and Discussion

Lotka-Volterra Model

The Lotka-Volterra model has a constant prey per capita birth rate and a linear functional response of the predator. This model has a neutrally stable equilibrium. The system oscillates with an amplitude which is dependent on initial conditions.

When the Lotka-Volterra model is used as the "within patch" model for a two-patch metapopulation model with diffusive migration and heterogeneity in the prey growth rate, the dynamics are quite different. There are three possible equilibria with predators present, which can be distinguished by the equilibrium prey density in each patch (Table 1.2): (1) positive prey density in both patches, (2) prey density zero in one patch, and (3) prey density zero in the other patch. In the equilibrium with positive prey density in both patches, the prey and predator density are higher in the patch with the higher prey growth rate. The average prey density is lower than in the non-metapopulation model and the equilibrium

Table 1.2. Equilibria and stability conditions for the non-metapopulation and metapopulations models with heterogeneity in prey growth rate between patches when the "within patch" dynamics are described by the Lotka-Volterra model. Parameter definitions are given in Table 1.1.

	Equilibrium	Condition for equilibrium to be positive	Stability condition
Complete mixing, non-metapopulation model	$A^* = \frac{d}{ef} \quad C^* = \frac{r_a + r_b}{2f}$	Always	Never - the equilibrium is neutrally stable
Diffusive predator migration, metapopulation model	$A_a^* = \frac{1}{ef}\left(d + m - m\frac{r_b}{r_a}\right) \quad C_a^* = \frac{r_a}{f}$ $A_b^* = \frac{1}{ef}\left(d + m - m\frac{r_a}{r_b}\right) \quad C_b^* = \frac{r_b}{f}$	For $r_b > r_a$: $m < \frac{d}{\left(\frac{r_b}{r_a} - 1\right)}$	Predator and prey densities in each patch are positive and $r_a \neq r_b$
	$A_a^* = 0 \quad C_a^* = \frac{m}{d+m}\frac{r_b}{f}$ $A_b^* = \frac{d}{ef}\left(1 + \frac{m}{d+m}\right) \quad C_b^* = \frac{r_b}{f}$	Always (except for the zero prey patch)	$r_b > r_a \quad m > \frac{d}{\left(\frac{r_b}{r_a} - 1\right)}$
"Separation of scales", metapopulation model	$A_a^* = 0 \; A_b^* = \frac{2d}{ef}$ $C^* = \frac{r_b}{f}$	Always	This equilibrium is neutrally stable but some of the deviation from equilibrium decays for: $r_b > r_a$
	Same as above with the roles of A_a and A_b reversed	Same as above with the roles of A_a and A_b reversed	Same as above with the roles of A_a and A_b reversed

predator densities are the same as they would be if the patches were isolated. This equilibrium is always stable as long as population densities in each patch are positive (Table 1.2). The difference between the prey densities increases with migration rate, but if the migration rate is too high then one of the prey densities may become negative. In this case, the equilibrium with the zero prey density in the patch with the lower prey growth rate is stable. The alternative equilibrium, where prey density is zero in the patch with higher prey growth rate, is always unstable (Table 1.2). This model was studied by Nisbet *et al.* (1992) and it was shown that the rate of damping of fluctuations increases with the degree of asynchrony in density between patches, which in turn increases with the degree of heterogeneity in the growth rates. They show that when prey density is somewhat independent between patches, this can introduce spatial density-dependence and stability.

Although one of the equilibria of the diffusive metapopulation model is always stable even for a high predator migration rate, the corresponding equilibrium of the "separation of scales" model is always unstable. One of the conditions for stability of the diffusive model is that the predator density in the high growth rate patch is greater than in the low growth rate patch. It can be seen from the equilibria in Table 1.2 that for a finite migration rate this condition is always satisfied, but as the migration rate increases, the predator density approaches equality in the two patches. This is confirmed in the stability analysis of the equilibrium for the "separation of scales" model (Appendix I). The system is neutrally stable, like its non-metapopulation counterpart. The stability analysis also shows, however, that some component of the deviation from equilibrium of the initial conditions decays away at a rate that is proportional to the difference between the prey growth rates.

External sources of heterogeneity can have a stabilizing effect in Lotka-Volterra metapopulations even if this effect is not strong enough to result in a stable equilibrium in the "separation of scales" model. The local stability, and equilibria when there is no heterogeneity in growth rates, are the same as for the non-metapopulation model (see Table 1.2 for the special case when $r_a=r_b$). However, the equilibria and their local stability do not show the complete picture. Jansen (1995) showed that there are some differences between the dynamics of the non-metapopulation and diffusive metapopulation model even when there is no heterogeneity of parameters. Jansen's results are summarized in the following paragraph.

As described, the equilibrium is neutrally stable when the prey growth rate is equal in the two patches. This means that near equilibrium, populations fluctuate with an

amplitude that is dictated by the initial conditions. In the case of the non-metapopulation model, this is also true far away from equilibrium. In the metapopulation model with diffusive migration, a large amplitude, unstable limit cycle may exist if the prey migration rate is low or zero and the predator migration rate is relatively high. So, if the initial starting density is far away from equilibrium then the amplitude of the fluctuations will diverge from the initial amplitude. This can result in a decrease in the amplitude of oscillation and populations densities can move toward the neutrally stable region near the equilibrium. Therefore, fluctuations are bounded, and population density does not reach low levels. Although the system is still technically unstable, the metapopulation structure has a stabilizing influence on the system. The important of this effect can be is illustrated by adding a type II functional response to the interaction. In the absence of self-regulation of the prey, this is an extremely destabilizing influence. In the non-metapopulation model oscillations diverge over time. In the diffusive metapopulation model, the same bounded neutrally-stable fluctuations that occur for the Lotka-Volterra model are observed. Details of how this relative stability comes about are given in Jansen (1995). But a critical component is that when the oscillations diverge from the unstable limit cycle, the densities of the two prey populations diverge and therefore there is a weak internal source of heterogeneity in this system.

Rosenzweig-MacArthur Model

The Rosenzweig-MacArthur model is a more biologically realistic model than the Lotka-Volterra model. It has logistic growth of the prey, which has a stabilizing influence on the dynamics. It also has a type II functional response of the predator, rather than a linear functional response, which has a destabilizing influence on dynamics. The resulting non-metapopulation model has a stable equilibrium if the carrying-capacity is low enough or the predator death rate is high enough (Table 1.3). If these conditions do not occur then the equilibrium is unstable (Rosenzweig, 1971) and a stable limit cycle is present (Hastings, 1978). Instability occurs when the prey equilibrium is such that a perturbation of the prey above the equilibrium will cause the prey density to increase, because the increase in the ingestion rate is not proportional to the increase in the prey per capita growth rate which results in "prey escape cycles" (de Roos, Metz, Evers, and Leipoldt, 1990). Dynamics of this model when incorporated into a metapopulation structure are much more complex than in the case of the Lotka-Volterra model. Even local stability analysis is not always possible

Table 1.3. Equilibria and stability conditions for the non-metapopulation and metapopulations models when the "within patch" dynamics are described by the Rosenzweig-MacArthur model. Parameter definitions are given in Table 1.1.

	Equilibrium	Condition for equilibrium to be positive	Stability condition
Complete mixing, non-metapopulation model	$A^* = \frac{hd}{eg-d} \qquad C^* = \frac{r}{g}\left(1-\frac{A^*}{k}\right)\left(h+A^*\right)$	$A^* < k \qquad k > \frac{dh}{eg-d}$ (The two are equivalent)	$A^* > \frac{k-h}{2} \qquad k < h\frac{eg+d}{eg-d}$ (The two are equivalent)
Diffusive predator migration, metapopulation model	$A_a^* = A_b^* = \frac{hd}{eg-d}$ $C_a^* = C_b^* = \frac{r}{g}\left(1-\frac{A_a^*}{k}\right)\left(h+A_a^*\right)$	$A_a^* < k \qquad k > \frac{dh}{eg-d}$ (The two are equivalent)	$A_a^* > \frac{k-h}{2} \qquad k < h\frac{eg+d}{eg-d}$ (The two are equivalent)
	$A_a^* = 0 \quad A_b^* = \frac{hd(d+2m)}{eg(m+d)-d(d+2m)}$ $C_a^* = \frac{m}{d+m}C_b^* \qquad C_b^* = \frac{r}{g}\left(1-\frac{A_b^*}{k}\right)\left(h+A_b^*\right)$	Probably similar to the "separation of scales" model (see text)	Probably similar to the "separation of scales" model (see text)
	Same as above with the roles of A_a and A_b reversed	Same as above with the roles of A_a and A_b reversed	Same as above with the roles of A_a and A_b reversed

Table 1.3. Continued.

	$A_a^* = \frac{k}{2} + \frac{h(2m+d)}{2(eg-(2m+d))} + D$ $A_b^* = \frac{k}{2} + \frac{h(2m+d)}{2(eg-(2m+d))} - D$ $D = \frac{1}{2}\sqrt{\left(k - \frac{h(2m+d)}{(eg-(2m+d))}\right)\left(k + \frac{2hm(eg+d)}{(eg-d)(eg-(2m+d))} - \frac{hd}{(eg-(2m+d))}\right)}$ $C_a^* = \frac{r}{g}\left(1 - \frac{A_a^*}{k}\right)\left(h + A_a^*\right)$ $C_b^* = \frac{r}{g}\left(1 - \frac{A_b^*}{k}\right)\left(h + A_b^*\right)$	Probably similar to the "separation of scales" model (see text)	Probably similar to the "separation of scales" model (see text)
	Same as above with the roles of A_a and A_b reversed	Same as above with the roles of A_a and A_b reversed	Same as above with the roles of A_a and A_b reversed
"Separation of scales" metapopulation model	$A_a^* = A_b^* = \frac{hd}{eg-d}$ $C^* = \frac{r}{g}\left(1 - \frac{A_a^*}{k}\right)\left(h + A_a^*\right) = \frac{r}{g}\left(1 - \frac{A_b^*}{k}\right)\left(h + A_b^*\right)$	$A_a^* < k$ $k > \frac{dh}{eg-d}$ (The two are equivalent)	$A_a^* > \frac{k-h}{2} \quad k < h\frac{eg+d}{eg-d}$ (The two are equivalent)

Table 1.3. Continued.

	$A_a^* = 0\ A_b^* = \dfrac{h2d}{eg-2d}$ $C^* = \dfrac{r}{g}\left(1-\dfrac{A_b^*}{K}\right)\left(h+A_b^*\right)$	$A_b^* < k$	$A_b^* < k-h$ $A_b^* > \dfrac{k-h}{2}$
	Same as above with the roles of A_a and A_b reversed	Same as above with the roles of A_a and A_b reversed	Same as above with the roles of A_a and A_b reversed
	$\dfrac{eg}{2}\left(\dfrac{A_a^*}{h+A_a^*}+\dfrac{A_b^*}{h+A_b^*}\right)-d=0$ (1.1) $A_a^* = \dfrac{k-h}{2}+\dfrac{1}{2}\sqrt{(k+h)\left(k-h\dfrac{eg+d}{eg-d}\right)}$ $A_b^* = \dfrac{k-h}{2}-\dfrac{1}{2}\sqrt{(k+h)\left(k-h\dfrac{eg+d}{eg-d}\right)}$ $C^* = \dfrac{r}{g}\left(1-\dfrac{A_a^*}{k}\right)\left(h+A_a^*\right) = \dfrac{r}{g}\left(1-\dfrac{A_b^*}{k}\right)\left(h+A_b^*\right)$ (1.2)	$\dfrac{hd}{eg-d} < \dfrac{k-h}{2}$ $\dfrac{h2d}{1-2d} > k-h$	$k(eg-2d)(eg-d)$ $\times\left(2d(k+h)-eg(k-h)\right)$ $+2r(2dk-(k-h))$ $\times\left[d(k+h)-eg(k-h)\right] > 0$
	Same as above with the roles of A_a and A_b reversed	Same as above with the roles of A_a and A_b reversed	Same as above with the roles of A_a and A_b reversed

algebraically. Analysis of the diffusive model was done by Jansen (1994) and only a brief description of his results will be given here. The major focus will be on the "separation of scales" model which is relevant to the following chapters. de Roos *et al.* (1998) analyzed the "separation of scales" model with no environmental heterogeneity for a large number of patches and results that are applicable to two patch models with some elaboration will be given here.

The Rosenzweig-MacArthur "separation of scales" model has at most 5 equilibria with positive predator density. The equilibria and their existence and stability conditions are shown in Table 1.3. The first equilibrium is homogeneous and is the same as the non-metapopulation model equilibrium, and it has the same local stability properties. The second and third equilibria are symmetrical (i.e. if one of the equilibria is $A_a^*=x$, $A_b^*=y$, and $C^*=z$ then the other is $A_a^*=y$, $A_b^*=x$, and $C^*=z$) and have positive prey density that is unequal in the two patches. The last equilibria are again symmetrical and have prey density equal to zero in one of the patches. Figure 1.1 shows the possible prey equilibria. When the prey density is positive in both patches at equilibrium, an expression for the two prey equilibrium values can be obtained from equation 1.2 (Table 1.3). This expression results in two possible relationships between prey density in the two patches. These are shown in bold in Figure 1.1. Additional equilibria occur where one of the two patches has no prey and the equilibrium will fall on the horizontal or vertical axis. The predator differential equation gives another expression for the two prey equilibrium densities (equation 1.1 in Table 3) which are shown with curves for different values of the predator death rate. Equilibria occur when the curve for the chosen death rate intersects one of the bold lines or one of the axes. The non-metapoplation model has a single prey population but if this population is considered to be two identical populations, then the equilibrium for the non-metapopulation model occurs where the curve intersects the positively sloped bold line in Figure 1.1.

The equilibria that exist and their stability change with decreasing death rate (Figure 1.2). When the predator death rate is high, there is only one equilibrium. This is the stable equilibrium with equal prey density in the two patches. When the death rate decreases, the homogeneous equilibrium becomes unstable and the two symmetrical heterogeneous equilibria with positive prey density in both patches become possible. The condition for stability of these equilibria is given in Table 1.2, but it is interesting to note that the stability of this equilibrium is dependent on characteristics of the equilibrium with prey equal to zero

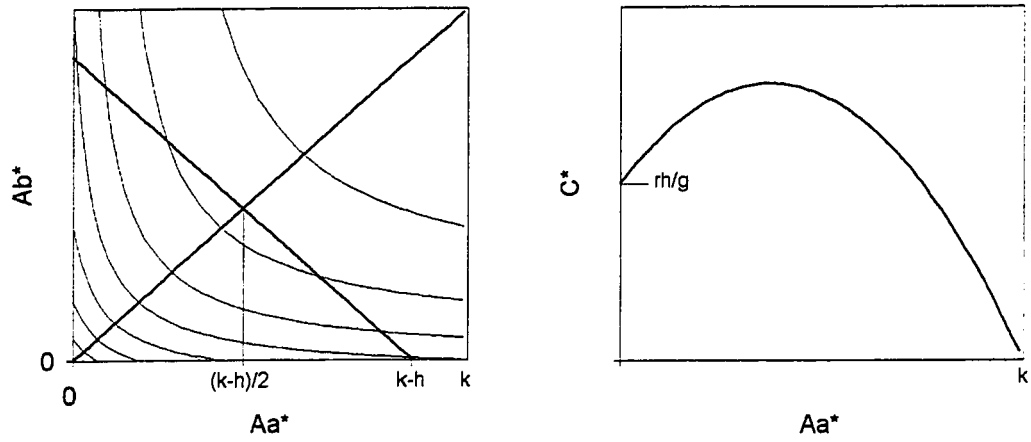

Figure 1.1 Prey and predator equilibria for the Rosenzweig-MacArthur "separation of scales" model. In the left frame, the curves show equation 1.1 (Table 1.3) for a number of values of d and the bold lines are for equation 1.2 (Table 1.3). The right frame shows the predator equilibrium as a function of the prey equilibrium in the first patch.

in one of the patches. It is necessary that the death rate be small enough that predators can be supported when prey density in one of the patches is zero. Thus, the equilibrium is stable for the value of d at which the homogeneous equilibrium becomes unstable only if the carrying capacity is small enough (the exact value is shown in Table 1.3). In this case the equilibrium becomes unstable for some values of d only if the prey growth rate is extremely high. (Figure 1.2). If the carrying capacity is higher, then the heterogeneous equilibrium is unstable for the death rate when the homogeneous equilibrium becomes unstable but becomes stable for lower values of the death rate (Figure 1.2). As the prey growth rate increases, a lower death rate is required for stability of this equilibrium. As the death rate increases further, the density in the low density patch becomes negative. When d is greater than this point, the equilibrium with prey density equal to zero in one patch, is unstable, and it becomes stable at the same point when the other heterogeneous equilibrium becomes negative. The lower stability boundary for the equilibrium with one patch having no prey is at the same prey density as the lower stability boundary for the homogeneous equilibrium but occurs at one half of the death rate. There are a number of non-equilibrium features of the model, including stable heterogeneous limit cycles, that are described in de Roos *et al.* (1998).

Results for the model with diffusive migration of predators are taken from Jansen (1994) and are remarkably similar to the model with complete mixing of predators. Again

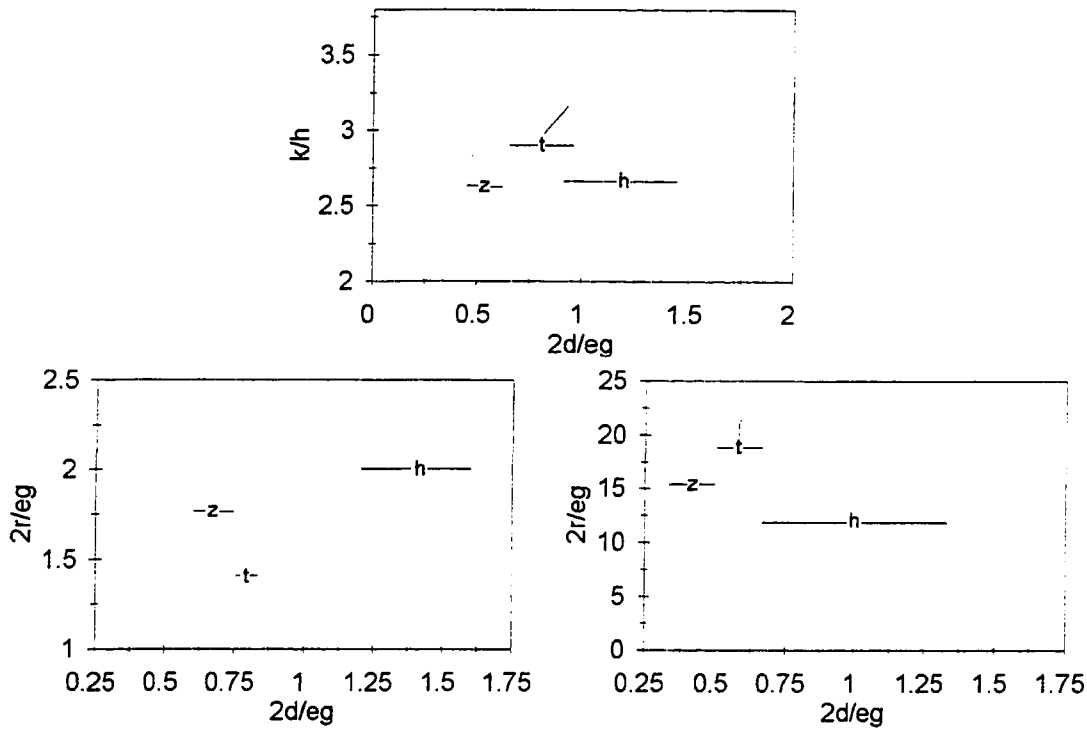

Figure 1.2. The stability boundaries for the Rosenzweig-MacArthur "separation of scales" model. The top frame is for 2r/eg=1 and varying k and d. The bottom frame on the left is for k/h=4 and varying r and d. The bottom frame on the right is for k/h=2 and varying r and d. The letters refer to the type of equilibrium: the homogeneous equilibrium that is the same as for the non-metapopulation model (h), the two heterogeneous equilibria with positive prey density in both patches (t), and the two heterogeneous equilibria with zero prey density in one of the patches (z). The lines from each letter point to the stability boundaries for the equilibria.

a total of 5 different equilibria are possible and they are analogous to those for the "separation of scales" model (Table 1.3). In the region where the homogeneous equilibrium is unstable a range of dynamics can be observed. Limit cycles are associated with all of the equilibria and may be stable for some parameter combinations. Also, the first or second pair of equilibria can be stable with the stable equilibrium switching from one type to the other with a change in parameter values.

In this model, heterogeneity in prey density can arise without external heterogeneity. Often, these heterogeneous equilibria are stable when the homogeneous equilibrium is unstable. The dynamics of this model do not depend on the fact that predators are completely mixed because results from both spatially structured models are very similar.

SUMMARY AND CONCLUSION

External heterogeneity is stabilizing in metapopulations where "within patch" dynamics are described by the Lotka-Volterra model. The diffusive metapopulation model without external heterogeneity does have dynamics which are different from those of the non-metapopulation model but the dynamics of both models are neutrally stable near equilibrium. When heterogeneity is added to the model, a stable equilibrium is introduced. If the migration rate is very high then the equilibrium has zero prey density in one of the patches. The "separation of scales" model with external heterogeneity does not have a stable equilibrium, however there is evidence that it has stabilizing features which are not present in the non-metapopulation model.

When the 'within patch' model is the Rosenzweig-MacArthur model, then external heterogeneity is not necessary to produce heterogeneity and stability in the metapopulation models. The "separation of scales" model and the diffusive metapopulation model both have 5 possible equilibria, some of which can be stable when the equilibrium of the non-metapopulation is stable. Four of these equilibria are heterogeneous and represent pattern formation of prey ("separation of scales" model) or prey and predator (diffusive model) in the absence of underlying environmental heterogeneity.

The "separation of scales" model, which has appeal for use in experiment, is not fundamentally different from the diffusive metapopulation model. Therefore, experiments which separate the scales of prey and predator can be expected to have general implications.

Because internal and external sources of heterogeneity affect metapopulations in similar ways, it might be expected that adding external heterogeneity to a model with a strong internal source of heterogeneity would reinforce the factors which promote pattern formation and stability. In the following chapter it will be shown that for the Rosenzweig-MacArthur "separation of scales" model this is not generally the case.

CHAPTER 2: The Effect of Environmental Heterogeneity on the Rosenzweig-MacArthur "Separation of Scales" Model

INTRODUCTION

The previous chapter shows that heterogeneity can arise in metapopulation models of predator-prey interactions as a result of heterogeneity of the environment or internal features of the predator-prey interaction. This chapter describes a "separation of scales" metapopulation model (complete mixing of predators and complete isolation of the two prey populations) when both heterogeneity of the environment and internal sources of heterogeneity are present. This model is compared to: (1) the non-metapopulation counterpart and (2) the metapopulation model without heterogeneity.

In order to make the desired comparisons meaningful, the parameters of the non-metapopulation model and the homogeneous metapopulation model need to be chosen carefully because the prey growth parameters have a large effect on the dynamics of all three models. The appropriate choice of parameters for the non-metapopulation model and the homogeneous metapopulation model can be made by formulating a model of a homogeneously mixed prey population in a heterogeneous environment. This is done in the first section of this chapter and the following sections formulate the non-metapopulation model and the homogeneous metapopulation model. In the fourth section, the heterogeneous metapopulation model is described and the equilibria and their local stability are compared to the other two. In the fifth section, the implication of the metapopulations structure to the "Paradox of Enrichment" (Rosenzweig, 1971) are given. In the last section, equilibria are compared among the models, and features are described that will be important in the subsequent experimental chapters. The methods used in this chapter are the same as for the first chapter and the derivation of results is given in Appendix II.

LOGISTIC GROWTH IN A HETEROGENEOUS ENVIRONMENT

Before the predator-prey model is formulated, it is necessary to understand how the prey population behaves when some fraction of the population experiences one environment while the other portion experiences a different environment. This causes the parameters of the model to be different in the two environments.

There are two types of patches with different environments and only prey present. The population in environment-a (A_a) and environment-b (A_b) in isolation are described by:

$$\frac{dA_a}{dt} = r_a A_a\left(1-\frac{A_a}{k_a}\right) \quad (2.1.1) \qquad \frac{dA_b}{dt} = r_b A_b\left(1-\frac{A_b}{k_b}\right) \quad (2.1.2)$$

One important assumption of many spatially structured models is that migration and local dynamics can be described independently. That is, when an individual enters an environment or patch it behaves in the same way as all others in that environment. Therefore if a prey population is homogeneously mixed, but one half of the population is in one type of environment and the other half is in the other type of environment, then the model for the well-mixed population is:

$$\frac{dA_{mix}}{dt} = \frac{1}{2}r_a A_{mix}\left(1-\frac{A_{mix}}{k_a}\right)+\frac{1}{2}r_b A_{mix}\left(1-\frac{A_{mix}}{k_b}\right) \quad (2.2)$$

or, by defining a different set of parameters, by:

$$\frac{dA_{mix}}{dt} = r_{mix} A_{mix}\left(1-\frac{A_{mix}}{k_{mix}}\right) \quad (2.3.1)$$

$$k_{mix} = \frac{(r_a + r_b)k_a k_b}{r_b k_a + r_a k_b} \quad (2.3.2) \qquad r_{mix} = \frac{r_a + r_b}{2} \quad (2.3.3)$$

There are several features of this simple model which are noteworthy. The equilibrium prey density is not simply the average of the two carrying capacities. It depends on the intrinsic rate of increase in the two environments if they are different. Also, the equilibrium is above the carrying capacity of one of the environments. Therefore, there is some question as to whether this model will capture the dynamics of prey near equilibrium. However, it may accurately capture the dynamics when the population is below the carrying capacity of both environments, where the prey equilibria of the predator-prey models are found unless the predator death rate is very high. Regardless of these possible inaccuracies, it is the correct choice given the assumptions of the metapopulation models that have been chosen.

The above model can be derived by assuming that the two environments are isolated and prey are mixed between environments at regular intervals. The model arises from taking the limit as the interval between mixing gets small. This process is shown in

Appendix II. In this case, it is assumed that mixing of prey between environments does not alter the parameters in each environment. If migration is small but finite, then the dynamics are very similar to the limiting case. If the assumptions are not met, then the equilibrium of the derived mixed model will not be right, but it is expected that the equilibrium will always be between the carrying capacity of the two environments.

THE NON-METAPOPULATION PREDATOR-PREY MODEL

Using the derived equation for a mixed prey population in different habitats, the non-metapopulation predator-prey model is:

$$\frac{dA_{mix}}{dt} = \frac{r_a}{2}A_{mix}\left(1-\frac{A_{mix}}{k_a}\right) + \frac{r_a}{2}A_{mix}\left(1-\frac{A_{mix}}{k_b}\right) - \frac{gA_{mix}C_{mix}}{h+A_{mix}} \quad (2.4.1)$$

Or:

$$\frac{dA_{mix}}{dt} = r_{mix}A_{mix}\left(1-\frac{A_{mix}}{k_{mix}}\right) - \frac{gA_{mix}C_{mix}}{h+A_{mix}} \quad (2.4.2)$$

$$\frac{dC_{mix}}{dt} = e\frac{gA_{mix}C_{mix}}{h+A_{mix}} - dC_{mix} \quad (2.4.3)$$

This model is exactly the same as the non-metapopulation model described in Chapter 1 except for the added significance of the parameters r_{mix} and k_{mix}. The equilibrium of this model is:

$$A^*_{mix} = h\frac{d}{eg-d} \quad (2.5.1)$$

$$\begin{aligned} C^*_{mix} &= \frac{r_{mix}}{g}\left(1-\frac{A^*_{mix}}{k_{mix}}\right)\left(h+A^*_{mix}\right) \\ &= \frac{r_a}{2g}\left(1-\frac{A^*_{mix}}{k_a}\right)\left(h+A^*_{mix}\right) + \frac{r_b}{2g}\left(1-\frac{A^*_{mix}}{k_b}\right)\left(h+A^*_{mix}\right) \end{aligned} \quad (2.5.2)$$

The prey equilibrium does not depend on prey parameters and therefore is the same as if

the patches were isolated. The predator equilibrium is positive if $A_{mix}^* < k_{mix}$ but a sufficient condition is that $A_{mix}^* < k_a$ and $A_{mix}^* < k_b$. As with the equilibrium, a sufficient condition for stability can be written in terms of two conditions, each of which depend on the parameters of a single patch:

$$A_{mix}^* > \frac{k_a - h}{2} \quad (2.6.1) \qquad \text{And} \qquad A_{mix}^* > \frac{k_b - h}{2} \quad (2.6.2)$$

This shows that if the patches have positive prey density and are stable in isolation, then the mixed system will also be stable. Likewise, if the equilibria of the two isolated patches are both unstable, then the mixed system is also unstable.

THE HOMOGENEOUS METAPOPULATION MODEL

In Chapter 1, a "separation of scales" metapopulation model with identical parameters in each patch was described. One of the questions being asked here is how external heterogeneity affects a metapopulation model with an internal source of heterogeneity. External heterogeneity is introduced through the prey growth parameters, which can have a dramatic effect on the dynamics of the non-metapopulation model. The goal is to compare homogeneous and heterogeneous metapopulation models when dynamics are the same for the corresponding non-metapopulation model. The desired homogeneous model is:

$$\frac{dA_a}{dt} = r_{mix} A_a \left(1 - \frac{A_a}{k_{mix}}\right) - \frac{g A_a C}{h + A_a} \quad (2.7.1) \qquad \frac{dA_b}{dt} = r_{mix} A_b \left(1 - \frac{A_b}{k_{mix}}\right) - \frac{g A_b C}{h + A_b} \quad (2.7.2)$$

$$\frac{dC}{dt} = \frac{e}{2}\left(\frac{g A_a C}{h + A_a} + \frac{g A_b C}{h + A_b}\right) - dC \quad (2.7.3)$$

Again, this model is exactly the same as the homogeneous metapopulation model described in Chapter 1 but the parameters r_{mix} and k_{mix} have special significance. Comparison of these two metapopulation models is mainly of theoretical interest in studying the effects of external heterogeneity on metapopulation dynamics. In an experimental situation, it would be difficult to produce heterogeneous and homogeneous metapopulations with identical corresponding non-metapopulations. From a practical point of view, the effect of introducing heterogeneity by increasing or decreasing prey growth parameters in one of the patches is of interest, keeping in mind the effect of this on the corresponding non-

metapopulation model. Therefore, the models will also be compared when both patches of the homogeneous metapopulation model have the same parameters as one of the patches of the heterogeneous metapopulation model.

THE HETEROGENEOUS METAPOPULATION MODEL

When prey growth rates differ between patches then the metapopulation model that corresponds to the above-mentioned non-metapopulation model and homogeneous metapopulation model is:

$$\frac{dA_a}{dt} = r_a A_a\left(1-\frac{A_a}{k_a}\right) - \frac{gA_aC}{h+A_a} \quad (2.8.1) \qquad \frac{dA_b}{dt} = r_b A_b\left(1-\frac{A_b}{k_b}\right) - \frac{gA_bC}{h+A_b} \quad (2.8.2)$$

$$\frac{dC}{dt} = \frac{e}{2}\left(\frac{gA_aC}{h+A_a} + \frac{gA_bC}{h+A_b}\right) - dC \quad (2.8.3)$$

There can be as many as 5 equilibria with positive predator density for any set of parameter values. These equilibria each roughly correspond to one of the equilibria of the homogeneous metapopulation model. One equilibrium has prey density very close to equal in both patches. There are two with positive prey density in each patch and with large differences between patches, and there are two with zero prey density in one of the patches. An in depth description of these equilibria, their stability, and how they can be displayed graphically, follows.

Assuming that the prey equilibrium densities are positive in both patches, equations 2.8.1 and 2.8.2 each give an equation for the predator equilibrium value in terms of the prey equilibrium value in one of the patches:

$$C^* = \frac{r_a}{g}\left(1-\frac{A_a^*}{k_a}\right)\left(h+A_a^*\right) \quad (2.9.1) \qquad C^* = \frac{r_b}{g}\left(1-\frac{A_b^*}{k_b}\right)\left(h+A_b^*\right) \quad (2.9.2)$$

Equation 2.8.3 gives the relationship between the prey equilibrium density in each patch:

$$\frac{eg}{2}\left[\frac{A_a^*}{h+A_a^*} + \frac{A_b^*}{h+A_b^*}\right] - d = 0 \quad (2.10)$$

Equation 2.10 does not specify a specific prey density for which the predator birth and

death rates are equal as does the non-metapopulation model. Rather, it specifies the relationship between the two "within patch" prey densities required to balance the predator birth and death rates.

Equations 2.8.1 and 2.8.2 can be combined while simultaneously eliminating C*. The resulting equation can be recognized as a hyperbola after it has been manipulated into the following form:

$$\frac{r_a}{k_a}\left[A_a^* - \left(\frac{k_a - h}{2}\right)\right]^2 - \frac{r_b}{k_b}\left[A_b^* - \left(\frac{k_b - h}{2}\right)\right]^2 = \frac{r_a}{k_a}\left(\frac{k_a + h}{2}\right)^2 - \frac{r_b}{k_b}\left(\frac{k_b + h}{2}\right)^2 \quad (2.11)$$

The intersections of the graphs of equation 2.10 and 2.11 (in the A_a*- A_b* plane) gives the prey equilibrium values. Equations 2.8.1 or 2.8.2 can then be used to estimate the corresponding predator equilibrium. Varying prey intrinsic rate of increase or prey carrying capacity in either patch does not affect equation 2.10. Varying the death rate of the predator, or varying prey the intrinsic rates of increase while keeping the ratio of the two intrinsic rates of increase constant, does not affect equation 2.11. Given that A_a* is put on the abscissa and A_b* on the ordinate, equation 2.11 specifies a hyperbola opening upwards and downwards if the right side of the equation is negative, and opening to the left and right if it is positive (Figure 2.1). If the right-hand side of the equation is zero (this occurs when r_a=r_b and k_a=k_b) then this equation specifies the two diagonal lines of the homogeneous model shown in Figure 1.1. If there is not much difference between the parameters of the two patches then the hyperbola passes very close to these diagonal lines. Analysis of this model will be restricted to the case where the right-hand side of equation 2.11 is negative (when the hyperbola opens upward and downward) without loss of generality. If the prey parameters are such that the hyperbola opens to the left and the right then the values of the prey parameters in each patch can be exchanged to give a hyperbola that opens upward and downward. Some important points of these equations are given in Table 2.1.

Figure 2.1 shows the graph of equation 2.11 for a specific value of the intrinsic rate of increase and carrying capacity for each patch. Only the intrinsic rate of increase or the carrying capacity differs between patches and the other parameter is equal between patches. Each graph also shows equation 2.10 for a number of values of the predator death rate. Where equation 2.10 intersects the bold hyperbola there is an equilibrium for the parameter values which specify the two curves. The non-metapopulation model can

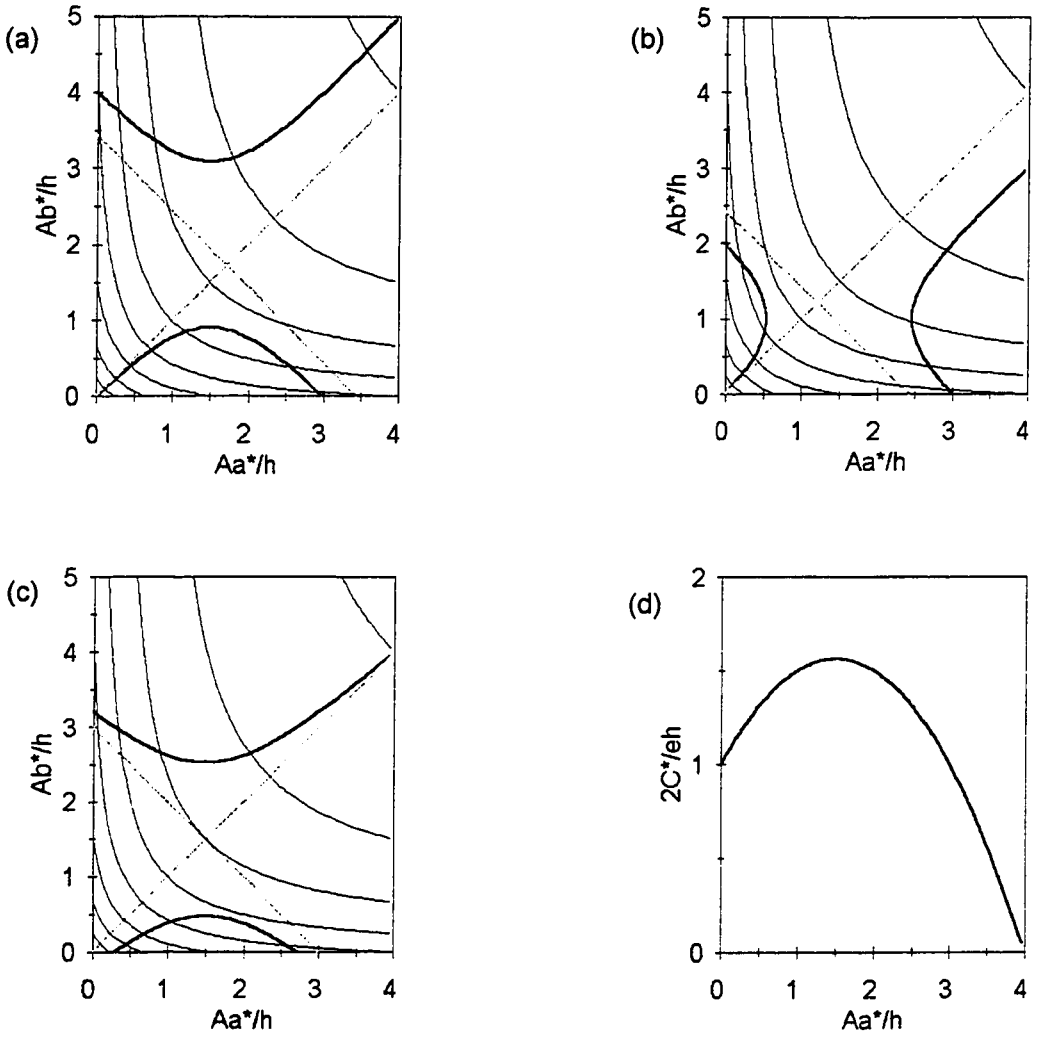

Figure 2.1. Prey (A_a^*,A_b^*) and Predator (C^*) equilibria of the heterogeneous metapopulation model. For (a) and (b) the solid grey diagonal lines represent the heterogeneous solution to equation 2.11 when both patches have a carrying capacity equal to k_a or k_b. For (a), (b) and (c), the bold grey lines represent equation 2.11 when the carrying capacity in both patches is equal to k_{mix}. The multiple solid black curves represent equation 2.10 and starting from the top right corner are for 2d/eg equal to:1.6, 1.4, 1.2, 1.0, 0.8, 0.6, 0.4, and 0.2. The bold black line represents equation 2.10 when parameters are not equal between patches. In all graphs $k_a/h=4$. In (a): $k_b/h=5$ and $2r_a/eg=2r_b/eg=1$. In (b): $k_b/h=3$ and $2r_a/eg=2r_b/eg=1$. In (c): $k_b/h=4$, $2r_a/eg= 1$, and $2r_b/eg=1.2$. In (d) the predator equilibrium density is shown as a function of prey equilibrium density in patch-a and applies to a),b) and c).

Table 2.1. Some important points on the equilibrium curves of the heterogeneous metapopulation model.

Point	Importance
$A_a^* = k_a \; A_b^* = k_b$	The upper part of the hyperbola passes through this point on the right. To the right of this point the predator density is negative.
$A_a^* = \frac{k_a - h}{2}$	The minium of the upper part of the hyperbola and the maximum of the lower part of the hyperbola occur at this value of A_a^*.
$A_b^* = \frac{k_b - h}{2}$	The line of symmetry between the upper and lower parts of the hyperbola.
$A_b^* = \frac{k_b - h}{2} + \sqrt{\left(\frac{k_b - h}{2}\right)^2 + \frac{k_b}{r_b}(r_b - r_a)}$ if $r_a=r_b$ this reduces to: $A_b^* = k_b - h$	The intersection of the upper part of the hyperbola with the A_b^* axis.
$A_a^* = \frac{k_a - h}{2} + \sqrt{\left(\frac{k_a - h}{2}\right)^2 + \frac{k_a}{r_a}(r_a - r_b)}$ if $r_a=r_b$ this reduces to: $A_a^* = k_a - h$	The intersection of the right branch of the lower part of the hyperbola with the A_a^* axis.

be interpreted as representing two identical patches with identical prey and predator densities, and in this case the prey equilibrium of the non-metapopulation model occurs when equation 2.10 intersects the positively sloped diagonal line. The prey equilibrium of the corresponding homogeneous metapopulation model occurs when equation 2.10 intersects either of the two diagonal lines.

Equation 2.10 intersects the upper part of the hyperbola once at most (equilibrium #1). If it intersects this curve on the right branch then the equilibrium is close to the homogeneous equilibrium of the homogeneous model in the stable region, and the equilibrium is also stable. If equation 2.10 intersects the left branch of this curve, the equilibrium corresponds to the heterogeneous equilibrium (with positive prey density in both patches) of the homogeneous model. This equilibrium becomes stable if the death rate becomes low enough, as with the corresponding equilibrium of the homogeneous

model. As the death rate increases further, this equilibrium becomes negative and the equilibrium with prey density equal to zero in patch-a becomes stable, again, as is seen in the homogeneous metapopulation model (Figures 2.2 and 2.3).

If the death rate is low enough then equation 2.10 will intersect the lower part of the hyperbola (Figures 2.1-2.3). Again the equilibria produced by the lower part of the hyperbola corresponds to equilibria of the homogeneous metapopulation model. The limit point, when equation 2.10 just touches the lower part of the hyperbola, always occurs on the right branch of the curve, but as the death rate decreases the equilibrium with a higher prey density in patch-a (equilibrium #2) will be on the right branch of the hyperbola and the equilibrium with the lower prey density in patch-a (equilibrium #3) will be on the left branch of the hyperbola. On the right branch of the hyperbola, the equilibrium corresponds to the heterogeneous equilibrium of the homogeneous model with positive prey density in both patches (as does equilibrium #1 on the left branch of the upper part of the hyperbola). Again, this equilibrium becomes stable when the death rate is low enough, and negative if the death rate is even lower. On the left branch, the equilibrium corresponds to the homogeneous equilibrium of the homogeneous model in the unstable region, and equilibria on this part of the curve are also unstable.

The only equilibria which can be written explicitly in a simple form are the two equilibria with prey density equal to zero in one of the patches. If the prey density in patch A is zero (equilibrium #4) then the predator equilibrium density is independent of equation 2.8.1 and the resulting equilibrium is:

$$A_a^* = 0 \quad (2.12.1) \qquad A_b^* = \frac{2hd}{eg - 2d} \quad (2.12.2) \qquad C^* = \frac{r_b}{g}\left(1 - \frac{A_b^*}{k_b}\right)\left(h + A_b^*\right) \quad (3.12.3)$$

Alternatively the prey density in patch-b may be zero (equilibrium #5) to give the following equilibrium:

$$A_a^* = \frac{2hd}{eg - 2d} \quad (2.13.1) \qquad A_b^* = 0 \quad (2.13.2) \qquad C^* = \frac{r_a}{g}\left(1 - \frac{A_a^*}{k_a}\right)\left(h + A_a^*\right) \quad (2.13.3)$$

As with the homogeneous model, these equilibria become stable when the corresponding equilibria with positive prey density in each patch become negative. The lower stability boundaries of these equilibria depend only on the growth rate parameters of the patch

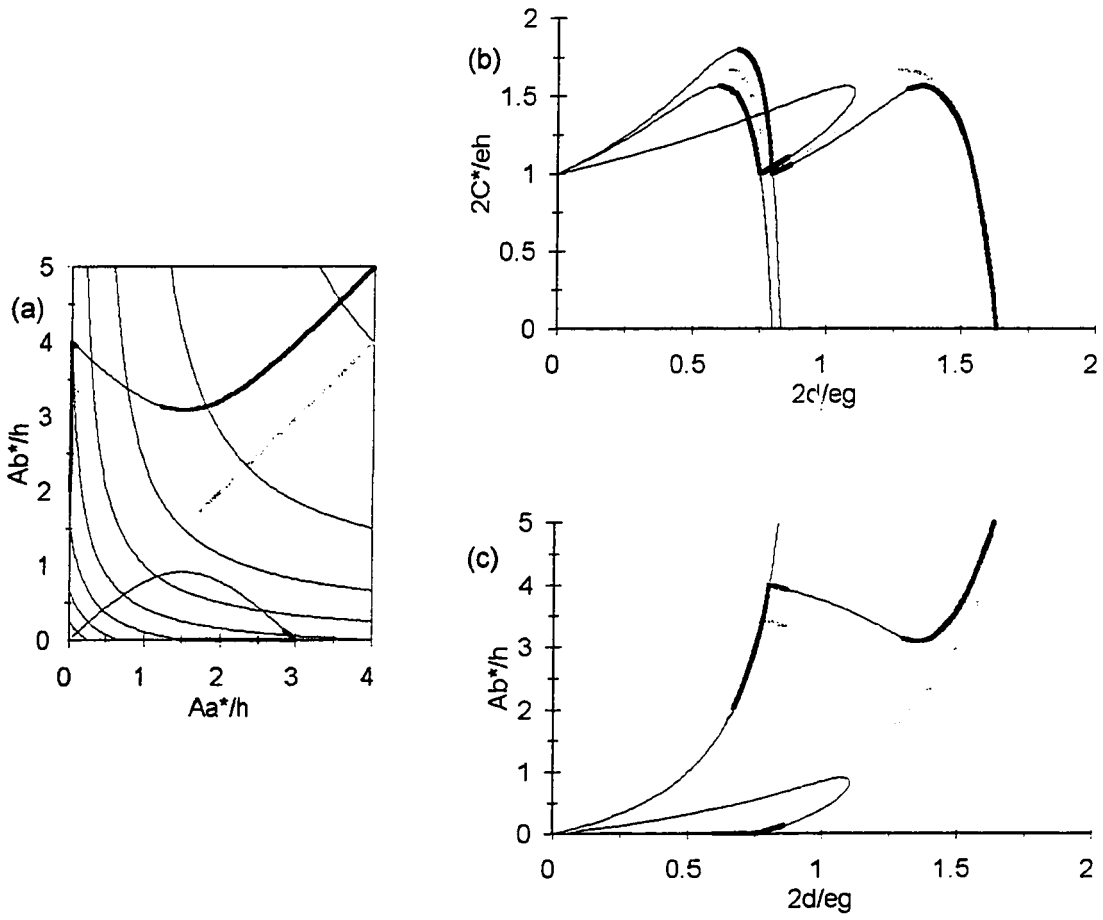

Figure 2.2. Equilibria and their stability properties for the homogeneous and heterogeneous metapopulation models as a function of predator death rate when ther is a difference in the prey carrying capacity (k) between patches. Parameter values are: $2r_a/eg=2$ $r_b/eg=1$, $k_a/h=4$, $k_b/h=5$. In (a) curves for equations 2.10 and 2.11 are as in Figure 2.1 and stable equilibria are marked in bold. In (b) and (c) grey is for the homogeneous model, black is for the heterogeneous model. Stable equilibria are shown in bold.

where prey density is not zero and occur at one half of the death rate of the boundary for an isolated patch.

The results for the heterogeneous model are very similar to those for the homogeneous model, however, there are some important differences. Figure 2.2 and 2.3 show that when the non-metapopulation model or the homogeneous metapopulation model have a death rate which results in stability of the homogeneous solution, then equation 2.10 can intersect the upper part of the hyperbola to the left of the minimum. It is possible, however, for this equilibrium to be stable for this value of d. This is the equilibrium that is

analogous to the stable homogeneous equilibrium of the non-metapopulation or homogeneous metapopulation models in this region but it does not become unstable for $A_a^* < (k_a - h)/2$ (i.e. it becomes unstable somewhere on the left branch, rather than at the minimum, of the upper part of the hyperbola). However, this equilibrium does become unstable at higher values of the death rate than the corresponding equilibrium of the homogeneous metapopulation or non-metapopulation models. In a similar way, equilibrium #3, the left most equilibrium of the lower curve is always unstable even if it occurs on the right branch of the lower part of the hyperbola. Another difference between the homogeneous and heterogeneous metapopulation models is that if the intrinsic rate of increase is much higher in patch-a than in patch-b of the heterogeneous model, then the lower part of the hyperbola does not attain positive values and these equilibria are not possible. When this occurs, the equilibrium with no prey in patch-b is always unstable.

Although the results of the heterogeneous and homogeneous metapopulation models are similar qualitatively, there are quantitative differences when there are differences in carrying capacity between patches. In the examples shown, equilibrium #1 of the heterogeneous model always becomes unstable at a higher value of the predator death rate than the corresponding equilibrium of the non-metapopulation or homogeneous metapopulation models (Figure 2.4). Equilibrium #1 becomes stable again at a higher value of the predator death rate than the corresponding equilibrium of the homogeneous metapopulation model and equilibrium #2 becomes stable at a lower value of the predator death rate than the corresponding equilibrium of the homogeneous metapopulation model. Equilibrium #4 becomes unstable at a higher value of the predator death rate and equilibrium #5 becomes unstable at a lower predator death rate than the corresponding equilibrium of the homogeneous model. In general, there is no increase in stability, or introduction of new features when heterogeneity is added to the model, only a shift in the equilibria and stability boundaries. Figure 2.4 shows that this is true for a wide range of parameters.

When the carrying capacity in both patches is small, equilibria #1 and #2 and the corresponding equilibria of the homogeneous model are always stable and therefore stable equilibria exist for a large continuous range of the predator death rate. The stable range is twice that of the non-metapopulation model. If the carrying capacity in patch-a is held constant at a low value, and the carrying capacity in patch-b is increased then the

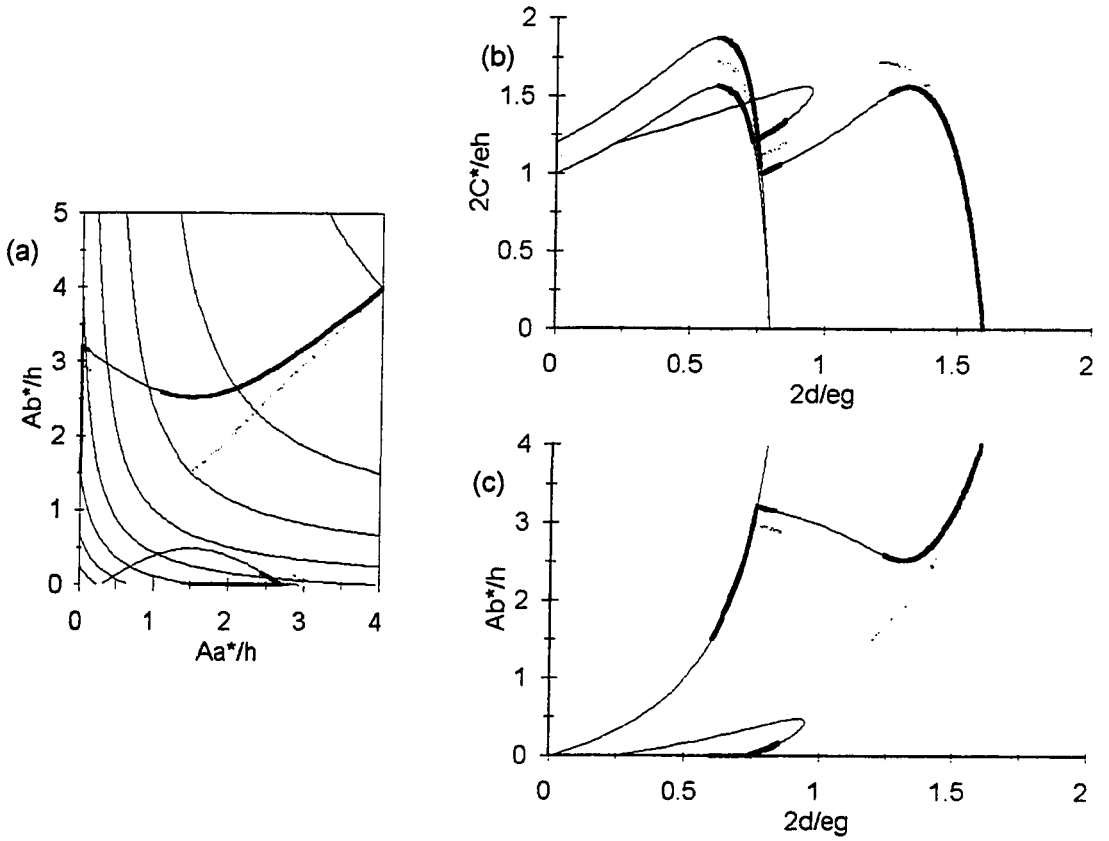

Figure 2.3. Equilibria and their stability properties for the homogeneous and heterogeneous metapopulation models as a function of predator death rate when there is a difference in the intrinsic rate of increase (r) between patches. Parameter values are: $k_a/h=k_b/h=4$, $2r_a/eg=1$ and $2r_b/eg=1.2$. In (a) curves for equations 2.10 and 2.11are as in Figure 2.1 and stable equilibria are marked in bold. In (b) and (c) grey is for the homogeneous model, black is for the heterogeneous model. Stable equilibria are shown in bold.

equilibrium becomes unstable for some values of the predator death rate. For the corresponding equilibrium of the homogeneous model, this happens at a much higher value of the carrying capacity in patch-b (Figure 2.4).

When there is a difference in the intrinsic rate of increase between patches, differences in the stability boundaries between homogeneous and heterogeneous metapopulation models are very similar to the results when there are is a difference in carrying capacity between patches (Figures 2.3 and 2.5). Equilibrium #1 becomes unstable at a higher death rate than the corresponding equilibrium of the homogeneous model and becomes stable again at a lower death rate. Equilibrium #2 can become stable at a higher or lower death rate than the corresponding homogeneous equilibrium but is positive only

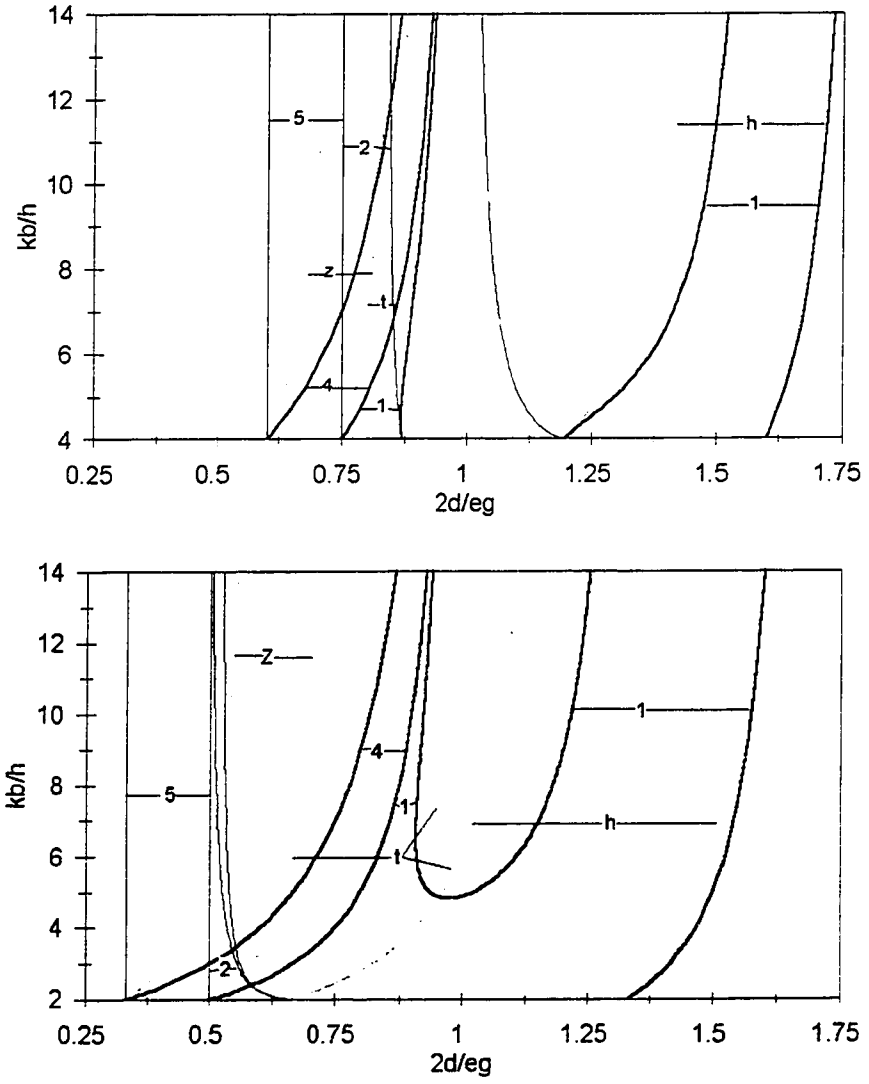

Figure 2.4 Stability boundaries of homogeneous and heterogeneous metapopulation models when k_b and d vary. Top frame is for $k_a/h=4$. Bottom frame is for $k_a/h=2$. The bold grey lines are for the homogeneous model and the letters point to the boundaries of stability for that equilibrium. The equilibria of the homogeneous model are: the homogeneous equilibrium that is the same as for the mixed model (h), the two heterogeneous equilibria with positive prey density in both patches (t), and the two heterogeneous equilibria with zero prey density in one of the patches (z). The bold black lines are for equilibria #1 and #4 of the heterogeneous model and The solid black lines are for equilibria #2, #3 and #5. The number of the equilibrium points to its stability boundaries.

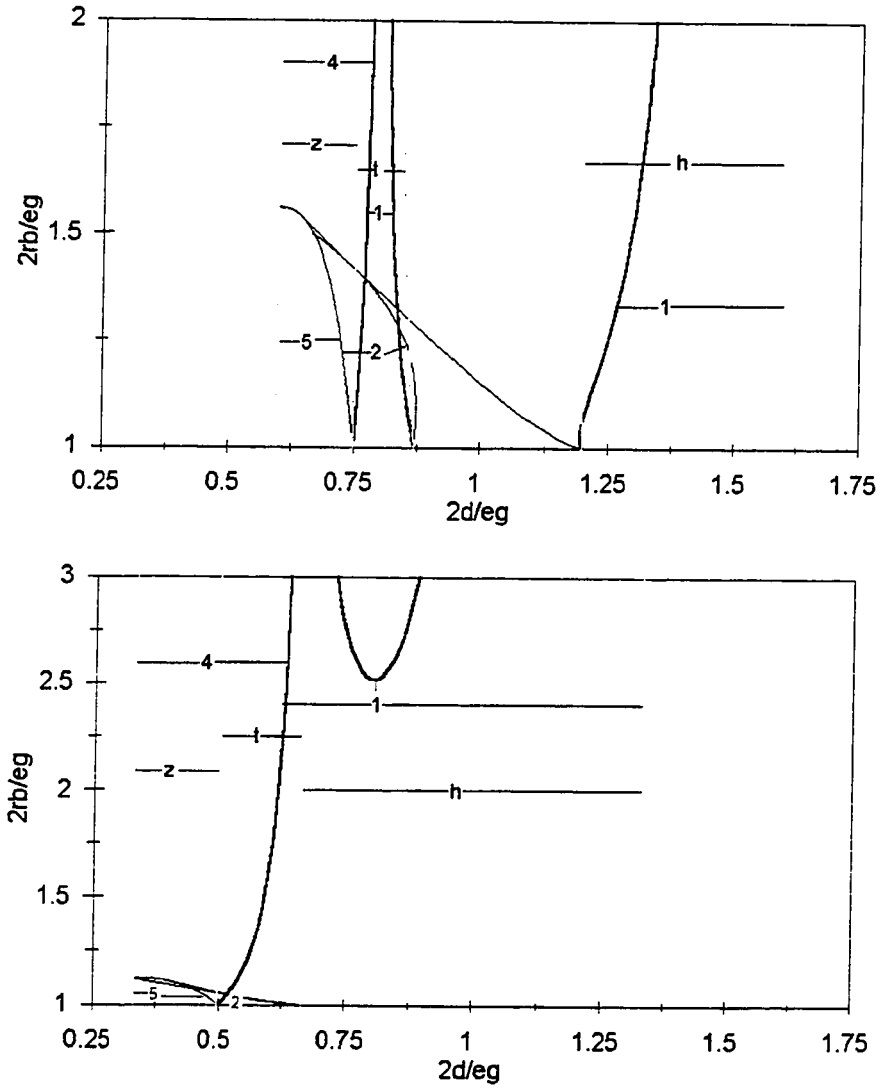

Figure 2.5 Stability boundaries of homogeneous and heterogeneous metapopulation models when r_b and d vary. Top frame is for $k_a/h=4$. Bottom frame is for $k_a/h=2$.Curves, lines,numbers, and letters are as in Figure 2.4.

when the difference in the prey intrinsic rate of increase between patches is small. The equilibria with prey density equal to zero in one of the patches has the same lower stability boundary for both patches and this coincides with that of the homogeneous model.

THE PARADOX OF ENRICHMENT

The non-metapopulation model has been used to demonstrate the paradox of enrichment. Investigating the effect of increasing prey carrying capacity in one of the patches of the homogeneous model is of interest because this enriches the system but also introduces external heterogeneity. Enrichment of patch-b affects the 5 equilibria in different ways (Figure 2.4). The homogeneous equilibrium is destabilized in the same way, but at a smaller value of k_b, as the equilibrium of the non-metapopulation model. The heterogeneous equilibrium with a higher prey density in patch-b can be stabilized if it is in the unstable region or destabilized if it is in the stable region. The stability boundary of the equilibrium with higher prey density in patch-a changes very little with enrichment.

One of the most interesting effects of enrichment on the equilibrium with higher prey density in patch-b is that, if d is within a certain range, the prey density in patch-b will increase with enrichment but the prey density in the other patch and predator density will not change very much. This is in strong contrast to the non-metapopulation model where the prey equilibrium density is not affected by enrichment but predator density increases.

COMPARISON OF EQUILIBRIA

In addition to the differences in stability between the metapopulation and the corresponding non-metapopulation model, there are a number of other features which are of interest for the experiment investigated in Chapter 4. The requirements for predators to be in equilibrium are different between the metapopulation and non-metapopulation models, but do not differ between the homogeneous and heterogeneous metapopulation models. The required relationships for metapopulation and non-metapopulation models respectively are:

$$\frac{eg}{2}\left[\frac{A_a^*}{h+A_a^*}+\frac{A_b^*}{h+A_b^*}\right]-d=0 \qquad (2.14) \qquad eg\frac{A_{mix}^*}{h+A_{mix}^*}-d=0 \qquad (2.15)$$

In the non-metapopulation model, the predator equation determines the prey equilibrium values. In the metapopulation this equation only specifies the relationship between the two prey equilibrium values. Because the predator death rate is a constant, the per capita birth

rate at equilibrium must be the same in both models as with per capita ingestion rate. The result is that the prey equilibrium density and the predator per capita ingestion rate must either be equal in both patches, and this value must be equal to that of the non-metapopulation model, or that ingestion and birth must be lower than the non-metapopulation model in one of the patches and higher in the other. Equating the per capita ingestion rates of the two models gives:

$$\frac{A_a^*}{1+A_a^*}+\frac{A_b^*}{1+A_b^*}=2\frac{A_{mix}^*}{1+A_{mix}^*} \quad (2.16)$$

Equation 2.16 can be put in a form which demonstrates the relationship between the average prey equilibrium density of the metapopulation model to the prey equilibrium density of the non-metapopulation model:

$$\frac{A_a^*+A_b^*}{2}=A_{mix}^*+\frac{1}{2}\frac{(A_a^*-A_b^*)^2}{A_a^*+A_b^*+2h} \quad (2.17)$$

The average prey equilibrium of the metapopulation model is always equal to or higher than the equilibrium of the non-metapopulation model because the proportion of prey consumed per predator per unit time decreases with prey density, and an increase in prey density does not increase ingestion as much as an equal decrease in density decreases ingestion.

There is an interesting corollary to the above result. Given a specific average prey density, ingestion will be maximized if prey density is equal in the two patches and will decrease with an increase in the difference between the two prey densities. If the magnitude of the difference in prey density between the two patches is bounded, then when prey density is high the ingestion rate in both patches will be very close to the maximum ingestion rate. This results in an average functional response on average prey density to rise less steeply, but to have the same maximum, as the average functional response when prey density is equal in both patches. If the functional response was calculated only on the basis of the average prey density, then the maximum ingestion rate (g) would not be affected but the half saturation constant (h) would appear to be higher if there was differences in prey density between the two patches.

The differences between the predator equilibrium of the metapopulation model when prey density is positive in both patches and non-metapopulation model can be put in the

following form:

$$C^*_{mix} - C^* = \frac{1}{g^2 C^*} \frac{r_a}{k_a} \frac{r_b}{k_b} \frac{\left(h + A_a^*\right)^2 \left(h + A_b^*\right)^2}{\left(h + A_a^* + A_b^*\right)^2} \left(A_b^* - A_a^*\right)\left(A_b^* - A_a^* - k_b + k_a\right) \quad (2.18)$$

From this it can be seen that the predator equilibrium in the non-metapopulation model is always smaller than the predator equilibrium in the metapopulation model (when prey density is positive in both patches) if the carrying capacities are equal in both patches. If the intrinsic rate of increase is equal in the two patches then this equation can be put in a different form:

$$\begin{aligned} C^*_{mix} - C^* &= \frac{r_a}{g k_a} \frac{\left(h + A_a^*\right)\left(h + A_b^*\right)}{A_b^*\left(2h + A_a^* + A_b^*\right)^2} \left(A_b^* - A_a^*\right)^2 \left(k_a - h - A_a^*\right) \\ &= \frac{r_b}{g k_b} \frac{\left(h + A_a^*\right)\left(h + A_b^*\right)}{A_a^*\left(2h + A_a^* + A_b^*\right)^2} \left(A_a^* - A_b^*\right)^2 \left(k_b - h - A_b^*\right) \end{aligned} \quad (2.19)$$

It can be shown that the prey equilibria are either both greater than or both less than $(k_i - h)/2$, where the i refers to the patch in question. Therefore, the predator equilibrium of the metapopulation model is only greater than that of the non-metapopulation model if the prey density is very high. Numerical analysis shows that for many parameter values, this difference in the predator equilibria is very small (Figure 2.2 and Figure 2.3).

When prey density is zero in one of the patches of the metapopulation model, then predator equilibrium density can be higher or lower than the equilibrium of the non-metapopulation model (Figure 2.2 and 2.3). In this region the non-metapopulation equilibrium is always unstable but the limit cycle should center around this unstable equilibrium and so average predator density should be higher in the metapopulation.

CONCLUSION

Adding external heterogeneity to the model does not increase the overall stability; it only causes a shift in the stability boundaries. It can be argued that in some cases adding external heterogeneity can be destabilizing.

The focus of metapopulation theory has been the relative stability of metapopulation and non-metapopulation models but there are a number of other features which can be tested experimentally. It was found that prey parameters affect the prey equilibria of the metapopulation model but not the non-metapopulation model. The average equilibrium between the two patches should always be larger in the metapopulation than in the non-metapopulation. Also, the average predator ingestion rate should be lower in the metapopulation for the same average prey density. Predator equilibrium density can only be much larger in the metapopulation than in the non-metapopulation if prey density is equal to zero in one of the patches of the metapopulation or the prey density is very large.

Specific predictions about the stability properties and range of patterns that can be observed depend on parameters values for any given experimental system. Predictions made about average functional responses can only be tested if the ingestion rate can be measured for the experimental systems. The following chapter provides the necessary information required to link the theoretical models in this chapter to the experiment studied in Chapter 4.

CHAPTER 3: The Transition From Theory to Experiment

INTRODUCTION

In order to apply the models from Chapter 2 to the *Ceriodaphnia*-algal interaction a number of considerations need to be addressed. First, the range of dynamics and equilibrium patterns in metapopulations are diverse and depend on parameter values. The predictions of the model can be clarified by using parameter estimates from the literature and supporting experiments. The second consideration is that interesting predictions were made about the differences in average ingestion rate between metapopulations and non-metapopulations. It would be difficult to measure ingestion directly but a method of testing these predictions, which involves estimating parameters from the experimental systems, will be described. The third consideration is that in Chapter 2 it was assumed that the functional response, conversion efficiency, death rate and prey growth did not differ between metapopulations and non-metapopulations. This assumption can also be evaluated using parameter estimates from the experimental system. The fourth consideration is how to evaluate whether or not pattern occurs in metapopulations. There are a number of approaches that will be used and these are described.

In the experimental systems, the predator is *Ceriodaphnia dubia* and the prey are a multi-species assemblage of algae. All systems consist of 2 aquaria (patches), and metapopulation or non-metapopulations were created by manipulating the mixing of water, algae and *Ceriodaphnia,* to produce systems that were represented by the models in Chapter 2 (see the Methods section of Chapter 4 for a complete description of the mixing protocols). Heterogeneous systems were created by manipulating light intensity, which affects algal growth parameters, and there was one high-light tank and one low-light tank. Homogeneous systems had two low-light tanks.

EXPECTED DYNAMICS AND EQUILIBRIUM PATTERNS

Algal parameters

"Algae only" tanks were run at the same time as the experimental treatments. It was observed that the effect of increasing light level could be interpreted as a *decrease* in algal carrying-capacity (k). There was little difference in the estimated carrying-capacity between the two high-light tanks, with both having a carrying-capacity of about 3 ± 0.5 µg Chl-a /L. There was a large difference between the two low-light tanks with estimates of 10 ± 5 µg Chl-a /L and 40 ± 5 µg Chl-a /L. The lower value is used, but predictions are not

qualitatively altered by values throughout this range. It was assumed that the intrinsic rate of increase (r) was not affected by light intensity and a value of 1.0 /day (as was used in Nisbet, McCauley, de Roos, Murdoch, and Gurney, 1991). The algal growth parameters are summarized in Table 3.2.

***Ceriodaphnia* parameters**

Ceriodaphnia dubia has been used for toxicological as well as ecological studies and therefore a complete set of parameters could be derived from the literature. All of the parameters of the model are readily interpreted biologically with the exception of the death rate parameter of the model (d) which is actually the sum of two components: the actual death rate (d_2) and a component that represents ingested energy that is not converted to new offspring (d_1). This arises because it is expected that a proportion of ingested energy is converted to new offspring only when ingestion is above a certain threshold, which results in the following relationship between the birth rate and the ingestion rate (I):

$$b = eI - d_1 \quad (3.1)$$

In order to parameterize the model, a number of assumptions were made. It was assumed that egg production only takes place when somatic growth is positive (i.e. when the respiration rate is less than the ingestion rate), and that the proportion of carbon in prey that was not assimilated was negligible. There is empirical support for both of these assumptions for cladocera (McCauley, Murdoch, Nisbet, and Gurney, 1990; Porter, Gerritsen, and Orcutt, 1982). Although, *Ceriodaphnia* size is not constant, individuals were assumed to be 0.7 mm long and have a dry weight of 3.74 µg. This is the maximum length and weight of the smallest adult size class. An egg was assumed to have a dry weight of 0.68 µg. Dry weight of *Ceriodaphnia* was estimated by the relationship: ln(W)=2.11+2.22*ln(L) (Anderson and Benke, 1994). Body carbon is approximately 42% of dry weight (McCauley 1984) and chlorophyll-*a* was converted to algal carbon following known conversion factors (Murdoch, Nisbet, McCauley, de Roos, and Gurney, 1998). Some parameters are temperature sensitive, and the temperature relationship was used to estimate the parameter value at the experimental temperature (21 °C).

The parameters of the functional response were estimated from experiments on filtration rate. Estimates of the death rate, threshold ingestion rate, and conversion efficiency followed Nisbet *et al.* (1991). The death rate was estimated from the average

life span. The threshold ingestion rate for reproduction was estimated from the starvation time, assuming that an individual dies at 50% of its normal body weight. The conversion efficiency was calculated from maximum growth rates and other parameters. A summary of the data used for parameter estimation is given in Tables 3.1 and Table 3.2 summarizes the parameters used for the predictions in the following section.

Expected dynamics based on literature derived parameter estimates

Although there are expected differences in pattern between treatments, the chlorophyll-*a* concentrations of all treatments (heterogeneous and homogeneous, metapopulation and non-metapopulation) are expected to fall on the same equilibrium curve derived from the predator growth equation:

$$\frac{1}{2}\left(\frac{eg}{h+A_a^*}A_a^* + \frac{eg}{h+A_b^*}A_b^*\right) - d = 0 \quad (3.2)$$

In the non-metapopulations there is the added condition that A_a=A_b. Equation 3.2 requires that if pattern formation occurs in metapopulations but not in non-metapopulations, then the average chlorophyll-*a* concentration at equilibrium will be higher in metapopulations. For the parameters in Table 3.3, this difference in average chlorophyll-*a* concentration is expected to be quite small. An equally important expectation from this relationship is that when pattern occurs at equilibrium, one patch must be higher than, and one must be lower than, the chlorophyll-*a* concentration when there is no pattern formation.

Heterogeneous systems

The parameter estimates given in Table 3.3 result in the equilibrium curves from the prey equations given in Figure 3.1 for the heterogeneous metapopulation (black bold) and non-metapopulation models (positively sloped grey bold). Although the corresponding homogeneous metapopulation is not represented in the experiment, the equilibrium curve for this system is also shown (negatively sloped grey bold). The regular black line shows the equilibrium curve from the predator equation (equation 3.2) derived from *Ceriodaphnia* parameters.

For these parameter estimates, there are no stable equilibria, and the only equilibria that exist for the metapopulation model are those with zero prey density in one of the patches. For a slightly lower value of d, the equilibrium with higher prey density in the high-light (low carrying-capacity) tank, and either zero or non-zero prey density in the low

Table 3.1 Information about *Ceriodaphnia* individuals and populations from the literature and supporting experiments that was used to estimate parameter values.

Quantity	Relationship to parameter of the model	Value	Reference
F - filtration rate	$F = \frac{g}{h + A}$	g=0.05938 µg Chl-a / individual /day h = 1.4129 µg Chl-a / L	Mourelatos and Lacroix (1990)
L - average life span	$L = 1/d$	L=45.8 days gives: d = 0.022 / day	Anderson and Benke (1994)
s - starvation time	$0.5 = e^{-resp*s}$ death from starvation at 50% of normal body weight	s = 2.73 days resp = 0.254 µg C/µg C/ day = 0.399 µg C/adult/ day = 0.01662 µg Chl-a/adult/day	Appendix III
r_m - maximum growth rate	$r_m = e(g - resp) - d_2$ $eg - d_1 - d_2$	r_m = 0.23 / day	Kirk and Gilbert (1990)
r_m - maximum growth rate		r_m = 0.5 / day	Cowgill and Milazzo (1991)
r_m - maximum growth rate		r_m = 0.28 / day	Matveev and Balseiro (1990)
r_m - maximum growth rate *C. lacustris*		r_m = 0.31 / day	Pace, Porter, and Feig (1983)
r_m - maximum growth rate		r_m = 0.33 / day gives: e = 8.23 individuals / µg Chl-a d_1= 0.1368 /day	the average of the above estimates

Table 3.2 Parameter estimates for the *Ceriodaphnia*-algal system used to develop predictions about dynamics and equilibria of metapopulations and non-metapopulations. Parameter values were derived from information in Table 3.1 and from the section on algal parameters.

Parameter	estimate of value for *Ceriodaphnia dubia*
h	1.41 µg Chl-*a* / L
e	8.23 individuals / µg Chl-*a*
g	0.0593 µg Chl-*a* / individual / day
d_1	0.137 / day
d_2	0.022 / day
r	1 / day
k high-light	3 µg Chl-*a* / L
k low-light	10 µg Chl-*a* / L
k_{mix} when light is heterogeneous	4.6 µg Chl-*a* / L

light tank can exist and may be stable.

In this region, the average algal equilibrium is greatest for the equilibrium with zero prey density in the low -light patch, followed by the other equilibrium of the metapopulation model and the non-metapopulation model equilibrium. For the predator equilibrium density, the reverse order is observed with the highest equilibrium density for the non-metapopulation model.

Homogeneous systems

Figure 3.2 shows the equilibrium curves from the prey equations (black bold) for the metapopulation model. The equilibrium of the non-metapopulation model falls on the positively sloped line. The curve is equation 3.2 as in Figure 3.1. Because the carrying-capacity is so high, both the metapopulation and non-metapopulation equilibria are well into the unstable region. The only pattern that is possible in the metapopulation has zero prey density in one of the patches.

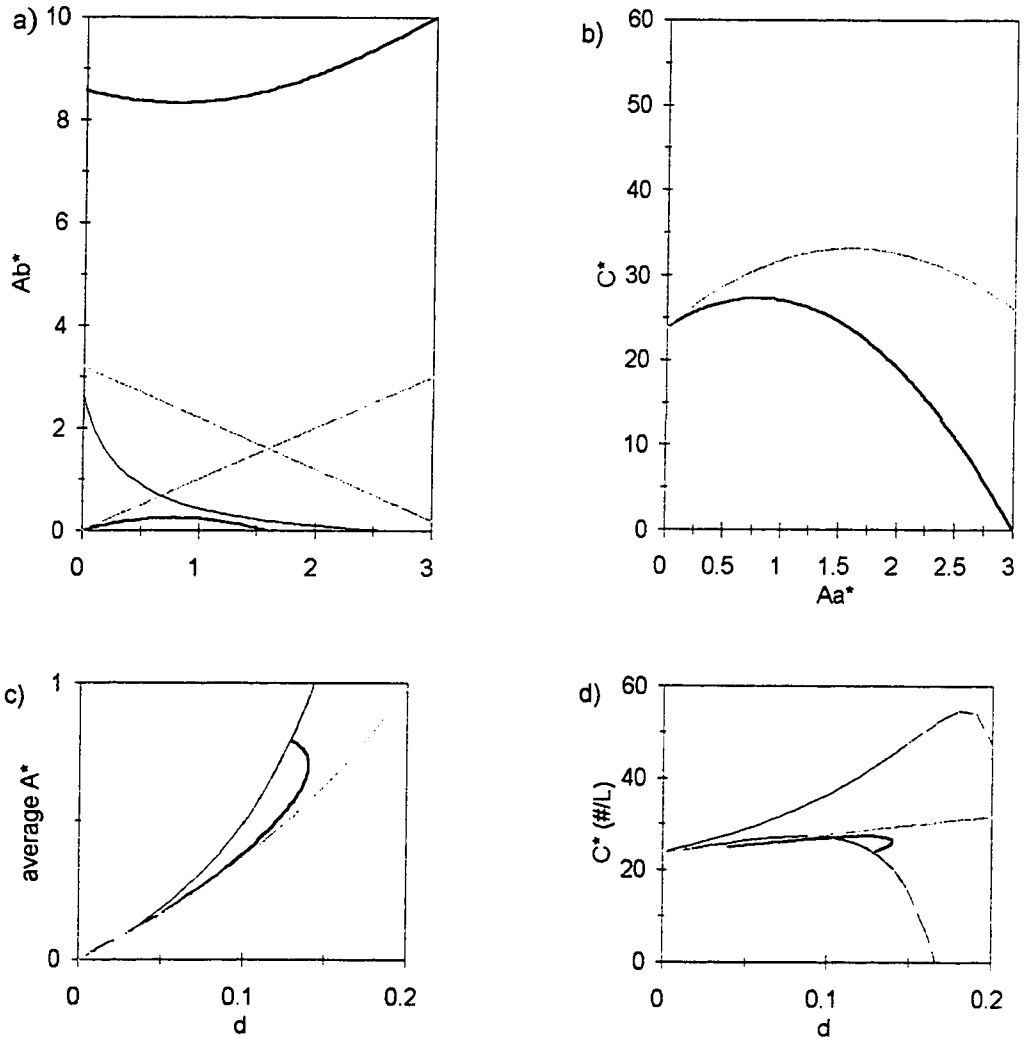

Figure 3.1. Equilibria of the heterogeneous metapopulation and non-metapopulation models for parameter values from Table 3.2. (a) Equilibrium curves from the prey equations for the heterogeneous metapopulation model (bold black), the homogeneous metapopulations model (grey bold), and the non-metapopulation model (positively sloped bold grey) as well as the equilibrium curve for the predator equation (solid black). (b) Predator equilibrium as a function of the prey equilibrium in the high light patch for the metapopulation model (black) and the nonmetapopulation model (grey). (c) The average equilibrium prey density as a function of the parameter d for the non-metapopulation model (grey), the equilibrium with prey positive in both patches of the metapopulation model (bold black), the equilibrium of the metapopulation model with zero prey in one patch (solid black). (d) as in (c) but for *Ceriodaphnia* density and the upper black curve is for the equilibrium with zero prey density in the low-light (high carrying-capacity) tank, and the lower black curve is for equilibrium with zero prey density in the high-light tank.

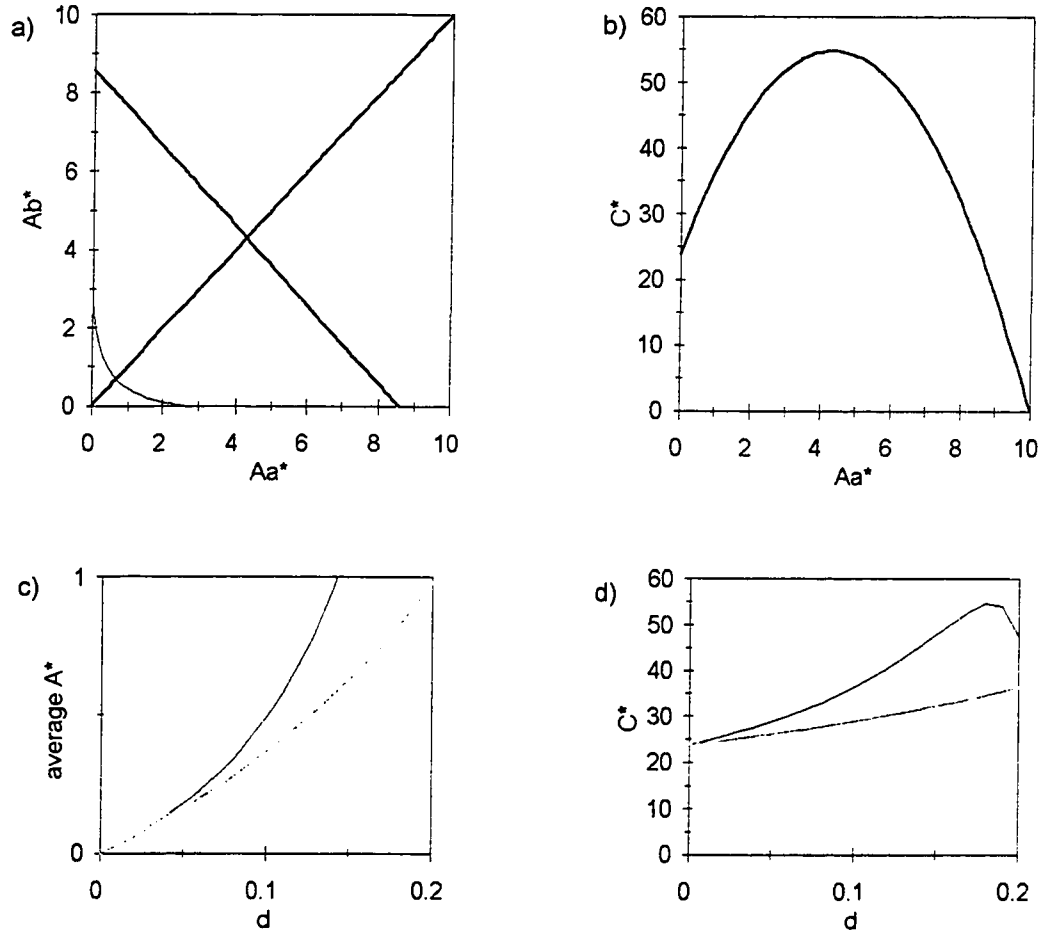

Figure 3.2. Equilibria of the homogeneous metapopulation and non-metapopulation models for parameter values from Table 3.2. (a) Equilibrium curves from the prey equations for the metapopulation model (bold), and the non-metapopulation model (positively sloped bold black) as well as the equilibrium curve for the predator equation (solid black). (b) Predator equilibrium as a function of the prey equilibrium in one of the patches. (c) The average equilibrium prey density as a function of the parameter d for the non-metapopulation model (grey), and the equilibrium of the metapopulation model with zero prey in one patch (black). (d) as in (c) for *Ceriodaphnia* equilibrium values.

TESTING PREDICTIONS ABOUT AVERAGE INGESTION RATE

The theoretical ingestion rates for non-metapopulations and metapopulations respectively are:

$$I = \frac{gA}{h + A} \quad (3.3) \qquad \text{And} \qquad I = \frac{1}{2}\left(\frac{gA_a}{h + A_a} + \frac{gA_b}{h + A_b}\right) \quad (3.4)$$

In Chapter 2, an interesting relationship between these two expressions and related experimental predictions were discussed. When there is a difference in the chlorophyll-*a* concentration between the two patches of the metapopulation, the average functional response on average chlorophyll-*a* concentration would have the same maximum ingestion rate, but a lower half saturation constant, than the functional response in the non-metapopulation model. Comparisons between ingestion in metapopulations and non-metapopulations is important for testing the theory, but, ingestion is not easily measured in population experiments. However, the birth rate is easily estimated and is expected to be linearly related to ingestion (equation 3.1). The per capita birth rate of *Ceriodaphnia* at time t can estimated using the following relationship:

$$b_t = \ln\left(\frac{E_t}{N_t} + 1\right) \Big/ D \quad (3.5)$$

where b is the birth rate, E is the number of eggs, N is the population size, and D is the egg stage duration time (Paloheimo, 1974). This estimate strictly assumes that the death rate is equal for juveniles and adults and that the population has a stable age distribution. Violation of these two assumptions does not greatly affect the estimate (Taylor and Slatkin, 1981). It also assumes that the birth rate is constant over time and the estimate can be quite sensitive to this assumption (Taylor and Slatkin, 1981). The egg stage duration (2 days) was estimated from experiments on individuals (Appendix III).

The hypothesized difference in ingestion rates between metapopulations and non-metapopulation can be quantified by estimating parameters from the following model:

$$b = \frac{eg}{h + \bar{A}}\bar{A} - d_1 \quad \text{(Model I - 3.6)}$$

Where $\overline{A}$ is the average chlorophyll-*a* concentration between the two tanks. Model I should give a higher estimate of h in metapopulations than in non-metapopulations.

TESTING THE ASSUMPTION THAT PARAMETERS ARE INDEPENDENT OF POPULATION SPATIAL STRUCTURE

In the last section it was shown that there are expected differences in the relationship between average chlorophyll-*a* and the birth rate (equation 3.5). The relationship that is expected to fully capture the relationship between the birth rate chlorophyll-*a*, and estimate the 'true' parameter values in all treatments is:

$$b = \frac{1}{2}\left(\frac{eg}{h + A_a}A_a + \frac{eg}{h + A_b}A_b\right) - d_1 \quad \text{(Model II - 3.7)}$$

Note that if A_a=A_b then Model II reduces to Model I. Parameters estimated using Model II should not differ between metapopulations and non-metapopulations. Although only the product eg can be estimated, rather than each parameter, this product, as well as h, and d_1 can still be compared between metapopulations and non-metapopulations. Parameters estimated using Model II can be used to graph what the birth rate curve would be expected to look like when prey density is equal in both patches (no pattern) and there should be no difference between these curves in non-metapopulation and metapopulation systems.

Another parameter that can be estimated is the predator death rate (d_2). Because the systems are closed, the death rate of *Ceriodaphnia* can be deduced from the birth rate and the population growth rate. The average population growth rate between two sampling periods (r_t) can be estimated by:

$$r_t = \frac{\ln(N_t / N_{t+\Delta t})}{\Delta t} \quad (3.8)$$

Where N_t is population density and t is time. The death rate (d_2) is then the difference between the birth rate and the growth rate:

$$r = b - d_2 \quad (3.9)$$

TESTING FOR PATTERN

The section on expected dynamics describes the range of expected pattern at equilibrium. The degree of difference in chlorophyll-*a* concentration between the two tanks cannot be expected to be constant throughout the time series and statistical methods

(Methods section of Chapter 4) will be used to determine whether or not pattern is observed thoughout the time series. An additional method can be used to evaluate the relative amount of pattern in metapopulations and non-metapopulations. Model I and Model II are identical when the chlorophyll-*a* concentration is the same in both patches but very different when there is pattern, so estimates of the functional response by the two models should be very different in metapopulations but not in non-metapopulations.

CONCLUSION

A number of the results from the model investigation in Chapter 2 can be tested for the chosen experimental system. Parameter estimates suggest that pattern formation (but *not necessarily stability*) *can occur in both heterogeneous and homogeneous* metapopulations. Criteria have been developed to test predictions about differences in ingestion rate between metapopulations and non-metapopulations over the range of chlorophyll-*a* concentrations. A critical assumption was made when the spatially structured model was formulated, that parameters of the model are not affected by the spatial structure, and this assumption can be tested.

CHAPTER 4: The Effect of Algal Movement and Environmental Heterogeneity on *Ceriodaphnia*-Algal Dynamics

INTRODUCTION

In this experiment, the movement of *Ceriodaphnia* and algae are carefully controlled in order to duplicate the two spatial structures described for the models in Chapter 2. Metapopulations and the corresponding non-metapopulation populations will be compared in two situations: (1) when environmental heterogeneity is present (heterogeneous systems), and (2) when it is absent (homogeneous systems). The homogeneous systems have a substantially higher average carrying capacity than the heterogeneous systems and this results in a higher *Ceriodaphnia* density and a greater tendency towards oscillation; however, a number of predictions described in Chapter 3 are the same for both heterogeneous and homogeneous systems. Generally, there should be differences between metapopulations and non-metapopulations in the degree of pattern formation, the relationship between *Ceriodaphnia* birth rate and average chlorophyll-*a* concentration between patches, and equilibria.

METHODS

Experimental Design

A single 'patch' consisted of a 20 L tank. Tanks were filled with filtered, UV sterilized Big Hill Spring water and were topped up periodically with distilled water. Tanks were enriched with 2 ml of 121.4 g / L stock solution of $NaNO_3$ and 2 ml of 4.36 g / L stock solution of $KHPO_4$ to increase primary productivity. Air bubblers were put in the tanks. All tanks were inoculated with 2 ml of a concentrate of *Chlamydomonas reinhardtii* and 2 mL of a concentrate of *Selenastrum* sp. for 5 consecutive days. Algal concentrates contained approximately 10^7 cells/ mL. Tanks were all left in high light for 24 hours a day in order for the algal populations to become established. An equal number of juvenile (1-5) *Ceriodaphnia* was then added to each tank daily for 5 days. After *Ceriodaphnia* were established, all tanks were mixed with one another to try to make initial conditions the same in all tanks.

Tanks that were designated low light had a neutral density screening placed over them; this filter did not alter light quality as measured by the PAR spectrum (photosynthetically available radiation). High- and low- light tanks had light intensities of 72 and 26 $\mu E/m^2/s$ respectively at the water surface. Temperature, pH and water hardness

were monitored weekly throughout the experiment. On day 97, the entire experiment had to be relocated to another laboratory, and it appears as though this created a perturbation to the systems. Other than the observation that all systems are stable in the long term, only the first part of the data was used (i.e. before the perturbation).

Non-metapopulation and metapopulation systems consist of two tanks. In the metapopulation systems, one half of the contents of each tank was removed each day and sieved through a 35 µm mesh to remove the *Ceriodaphnia*. The sieved *Ceriodaphnia* were introduced into the opposite tank while the water and algae were returned to the original tank. In the non-metapopulation systems, one half of the contents of each tank was removed each day and introduced to the opposite tank (as opposed to just the *Ceriodaphnia* as in the metapopulation treatment), after the contents had been sieved through a 35 µm mesh. This process ensured that effects due to the process of sieving were the same in both non-metapopulation and metapopulation systems.

Non-metapopulation and metapopulation systems were compared in both homogeneous and heterogeneous light. When light was homogeneous, both tanks had low light-levels, which resulted in a high carrying capacity (Chapter 3). When light was heterogeneous, one tank had high light and one tank had low light, which resulted in a relatively low carrying capacity.

Ceriodaphnia samples were taken every 2 days up to day 20 of the experiment and chlorophyll-*a* samples were taken every 4 days. After day 20, *Ceriodaphnia* samples were taken every 3 days and Chlorophyll-*a* samples were taken every 6 days. To estimate *Ceriodaphnia* density, a 0.5 L sample was taken from each tank just prior to migration, sieved through a 35 µm mesh, and counted under a dissecting microscope. The number in each of 5 size classes was counted as well as the number of eggs. After the sample was counted, the individuals were returned to their tank. This method of estimating *Ceriodaphnia* density does not introduce any mortality to the populations (Lynch, Weider, and Lampert,1986; McCauley *et al.*, 1990).

Chlorophyll-*a* was used as an estimate of algal biomass. A 250 ml sample was taken from the water column of each tank before migration and vacuum extracted onto a GFC filter. Samples were frozen for later analysis. When the samples were analyzed, they were ground in 6 mL of 90% acetone, an additional 6 mL of 90% acetone was added, and then the samples were extracted overnight at 4°C. They were then centrifuged and the

supernatant was used to estimate chlorophyll-*a* concentration. The fluorescence of total chlorophyll-*a* and phaeophyton was measured using a Turner fluorometer; the sample was then acidified, and fluorescence was measured again in order to correct the chlorophyll-*a* estimate for phaeophyton.

Data analysis

Pattern formation in chlorophyll-*a*

Three tests were used to evaluate the degree of pattern formation in the systems and all of them were performed on the difference in chlorophyll-*a* concentration between patch tank-a and tank-b over the first 97 days. The proportion of positive differences was tested against the null hypothesis that the proportion is 0.5 to determine if the chlorophyll-*a* concentrations was consistently higher in one of the tanks (test of proportions). Alternatively, if one tank is not always greater than the other the difference may still be correlated in time. There are two ways of evaluating this. First, the number of runs of positive and negative differences can be tested to determine whether the sign of the difference is independent between consecutive sampling periods (positive and negative runs test). A second method that can be used to test for the independence of consecutive differences is to test the number of runs above and below the median difference (runs above and below the median). The test of proportions is a two-tailed test because the alternative hypothesis is that the tanks have different chlorophyll-*a* concentrations: either tank may be greater than the other. The two runs tests are one-tailed tests because the alternative hypothesis is that the number of runs is less than if the differences are independent (i.e. the difference in chlorophyll-*a* concentrations between the two tanks is correlated over time). A type II error rate of α=0.05 was used for all tests and a positive result from any of these tests indicated pattern formation.

***Ceriodaphnia* vital rate and parameter estimates**

The birth and death rates of *Ceriodaphnia* were estimated as described in Chapter 3. In order to get a relationship between birth rate and chlorophyll-*a*, it is necessary to have an estimate of both of these factors at the same point in time. In the experiment, chlorophyll-*a* and *Ceriodaphnia* were never measured on the same day, the sampling interval changed and sequence of chlorophyll-*a* and *Ceriodaphnia* samples changed. An estimate for chlorophyll-*a* for every day of the experiment was obtained by linear interpolation of the natural log-transformed chlorophyll-*a* estimates. An estimate of birth

rate for every day of the experiment was obtained by linear interpolation of the estimated birth rates.

To compare treatments effectively, the birth rate curve from the period when chlorophyll-*a* appears to be approaching equilibrium was used, specifically, the period where the chlorophyll-*a* dropped below 2 ug/L to day 40. The reason that this was done is because the transient in the size structure of the *Ceriodaphnia* needed to be omitted. The time period that was used includes the first peak in *Ceriodaphnia* density, and density varies between 200 / L and 800 / L.

The parameters were estimated by non-linear regression of equations 3.6, 3.7 and 3.9. The birth rate curves for the third replicate of the metapopulation systems could not be fit successfully over the desired time period, as there is a lot more oscillation in chlorophyll-*a* in this replicate over the relevant time period. Parameter estimates were taken during the time period to day 25 for this replicate.

Equilibrium estimates

Equilibrium chlorophyll-*a* concentrations were estimated using the average of the observed values over the time period of day 40 to day 80,which is a different time period from that used for parameter estimates.

Differences between treatments in parameter estimates, birth rate curves, and equilibrium estimates

Developing parametric tests for the predictions concerning the differences in parameter estimates and birth rate curves is beyond the scope of this thesis. If the Mann-Whitney *U*-test (non-parametric) is used, a significant result (for a type II error rate of α=0.05), with three replicates, in two treatments, can only be achieved for a one tail test, and occurs when all observations of one treatment are ranked higher than all observations of the other treatment. When this occurs, the result is statistically valid; however, in many cases there are qualitatively different results within a treatment which are of interest. For example, treatments may differ in the degree of pattern formation, and the effect of this on other factors will be evaluated. In these cases, whether or not these results are "real" will be judged subjectively and will be taken to be of a preliminary nature.

For equilibrium estimates, the standard error was used as an indication of differences among replicates and treatments. Because the observations used for the equilibrium estimates are correlated in time, the standard error is biased as an estimate of

variation, but is used as an approximation.

RESULTS

Graphs of *Ceriodaphnia* density, *Ceriodaphnia* birth rate, and chlorophyll-*a* in each tank are shown in Figures 4.1 to 4.4. Density is shown per 0.5 liters (the sample volume) to facilitate the interpretation. Since populations are mixed randomly in tanks prior to sampling, the estimate of the density per sample volume is expected to follow a Poisson distribution, and therefore the variance is equal to the mean.

Pattern formation in chlorophyll-*a*

Heterogeneous systems

There was significant pattern formation in all of the metapopulation systems. The negative and positive runs test was significant for two replicates of the metapopulation treatment and could not be used in the third replicate because there was only one observation with a higher chlorophyll-*a* concentration in the high light tank which was in itself a very significant result (test of proportions). There was not significant pattern formation in the non-metapopulation systems (Table 4.1).

Homogeneous systems

At least one of the tests had a positive result for pattern formation in all but the first replicate of the non-metapopulation systems (Table 4.2). Two replicates from each treatment have a significant proportion of positive differences, and one from each treatment have a significant number of positive and negative runs. All three metapopulations, and none of the non-metapopulations, had a significant number of runs above and below the median, which indicates that there was some difference in the quality of pattern between metapopulation and non-metapopulations.

Birth rate curves and parameter estimates from the time series

Heterogeneous systems

Graphs of the per capita birth rate as a function of the chlorophyll-*a* concentration are presented in Figure 4.5. It is clear that the birth rate was lower in metapopulations than non-metapopulations over the range of chlorophyll-*a* concentrations.

Table 4.3 (b) shows parameter estimates using Model I (equation 3.6). There does seem to be a trend towards a higher value of h and a lower value of the quantity eg/h in the metapopulation systems, but this is not consistent. The curves produced by these parameter estimates show more clearly that birth rate is depressed for all replicates when

chlorophyll-*a* is between 0.1 and 1 µg / L.

Table 4.3 (c) shows parameter estimates using Model II (equation 3.7). The difference in the quantity eg/h is much more pronounced when Model II is used. The birth rate curves for Model II in Figure 4.7 are estimated assuming that there are differences in chlorophyll-*a* concentration between systems, but are shown for the case where chlorophyll-*a* is homogeneous (i.e. the 'true' birth rate curve). The difference in this 'true' birth rate curve between treatments (except for the second replicate of the metapopulations), illustrates that the parameters differ between metapopulations and non-metapopulations; instantaneous differences in chlorophyll concentration between tanks are insufficient to explain depressed birth rates in these metapopulations.

It was also predicted that Model I and Model II would give the same parameter estimates for non-metapopulations. Deviation between Model I and Model II in the birth rate curves is larger for metapopulations than non-metapopulations (Figure 4.7).

There was no difference in death rates between non-metapopulation and metapopulation systems (Table 4.3 (b)). Most replicates had an observed death rate very close to 0.02 / day but the third replicate of the non-metapopulation systems has a value of 0.006 / day and the third replicate of the metapopulation systems had a death rate of 0.04 /day (Table 3 (b)).

Homogeneous systems

For the most part, homogeneous systems appear to be less stable than heterogeneous systems over this time period. The third replicate of the non-metapopulation systems displays extremely atypical dynamics.

Graphs of the birth rate as a function of the chlorophyll-*a* concentration are given in Figure 4.6. As with heterogeneous systems, the birth rate curves for metapopulations appear to be depressed compared to non-metapopulations.

Table 4.4 shows parameter estimates using Model I (Table 4.4 (b)). With the exception of the first replicate of the metapopulation systems, there was a consistent difference in the quantity eg/h between treatments and a trend toward a higher value of h in the metapopulations. This one replicate did not show pattern formation during the period of time where parameters were estimated and appears to be similar to the non-metapopulation systems (Figure 4.4). This is consistent with theory. Later in the time series this replicate did develop pattern. This replicate will be shown to be somewhat

different from the others and similar to the non-metapopulations in some other characteristics.

Table 4.5 shows parameter estimates using Model II (Table 4.4 (c)). Again the quantity eg/h was larger in the non-metapopulations and again there were differences in the birth rate curves (with the exception of the first metapopulation replicate).

There was no significant difference in death rate between treatments. The death rate of all but one of the replicates was very close to 0.01 / day. The second replicate of the non-metapopulation systems had a death rate of 0.03 /day. In general, the death rate was about half the value found in the heterogeneous systems (Table 4.4 (a)).

Equilibrium estimates

Three of the parameters estimated from the experimental data (e*g, h, d_2) are very close to those estimated from the literature, but the parameter d_1 is somewhat smaller than the literature estimates. The chlorophyll-*a* equilibrium values are all lower than they were expected to be (which is consistent with a lower value of d_1), but the qualitative aspects of the equilibria discussed in Chapter 3 are not affected by this deviation. Average chlorophyll-*a* concentration between the two tanks at equilibrium were higher in the homogeneous (higher average carrying capacity) systems than in the heterogeneous (lower average carrying capacity) systems. This difference was not expected, especially for the non-metapopulation systems. There are no consistent differences in *Ceriodaphnia* parameter estimates between heterogeneous and homogeneous systems but there does appear to be a trend towards differences in parameter estimates that would result in the observed differences in chlorophyll-*a* equilibrium values.

Ceriodaphnia equilibrium values were about 10 times higher than they were expected to be. These differences were probably not caused by *Ceriodaphnia* parameters (e, g, h, d_1, or d_2) because the estimates were relatively similar to the literature derived values and chlorophyll-*a* equilibrium estimates are close to the predicted values. These observed equilibria would require a value of r of at least 5 / day, which is beyond biological realism. A dramatically larger than estimated carrying capacity could also account for this observation. However, parameter estimates already predict instability, increasing the carrying capacity increases this instability, and these experimental systems are stable.

In spite of the above mentioned deviations in equilibria from model predictions, further details of the equilibria will be described within the context of the experimentally

derived parameters.

Heterogeneous systems

As predicted, there is much more pattern in metapopulation systems than in non-metapopulation systems at equilibrium.

The equilibria from the metapopulation systems had a varying amount of heterogeneity but all appear to fall on the equilibrium curve (equation 3.2) (Figure 4.9). None of the equilibria of metapopulations has a chlorophyll-*a* equilibrium value equal to zero in one of the patches and this type of equilibrium can be excluded from consideration. The only other type of equilibrium predicted to occur in this region of parameter space is the one with higher chlorophyll-*a* concentration in the low carrying-capacity (high-light) tank but only one of the equilibria is of this type. The other two have a higher equilibrium chlorophyll-*a* concentration in the high carrying-capacity (low-light) tank. For the estimated carrying capacities, these two types of equilibria can never both occur for the same *Ceriodaphnia* parameters, or even if there is a moderate amount of variation in *Ceriodaphnia* parameters. If the carrying capacity in the high density patch is somewhat lower than estimated, then both of these equilibria can occur for *Ceriodaphnia* parameters that are close to those observed. If parameter values are such that both of these equilibria can occur, then there should be a higher *Ceriodaphnia* equilibrium in the metapopulation with a higher chlorophyll-*a* in the high-light (low carrying-capacity) tank and this is what is observed.

Two of the observed average equilibrium chlorophyll-*a* values in the non-metapopulation systems were much smaller than those observed in the metapopulation systems and do not appear to fall on the same equilibrium curve (equation 3.2) (Figure 4.9). This is in contrast to the predictions, but is consistent with the observed differences in the quantity eg/h between treatments. The model predicts that non-metapopulations should have a higher *Ceriodaphnia* equilibrium density than metapopulations for the estimated parameters, but if there are differences in parameter values between metapopulations and non-metapopulations then this effect will override the above prediction. The effects of varying parameters on average chlorophyll-*a* concentration and *Ceriodaphnia* density at equilibrium are summarized in Table 4.5. Any parameter change which makes the quantity eg/h smaller will increase the equilibrium values of chlorophyll-*a* and *Ceriodaphnia*. This is what is observed. These two replicates with a lower average chlorophyll-*a* concentration

also have lower *Ceriodaphnia* densities.

One of the equilibria of the non-metapopulations falls on the same equilibrium curve as the metapopulations (equation 3.2) (Figure 4.9). Assuming that there are no differences in parameters among these four systems, and that parameter values are such that all of these equilibria can occur, the predicted order of increasing magnitude of *Ceriodaphnia* density is: metapopulation system with chlorophyll-*a* concentration higher in the low-light tank, metapopulation system with chlorophyll-*a* concentration higher in the high light tank, non-metapopulation system. The observed order of increasing magnitude of *Ceriodaphnia* density is: metapopulation system with chlorophyll-*a* concentration higher in the low-light tank, non-metapopulation system, metapopulation system with chlorophyll-*a* concentration higher in the high-light tank. This coincidence of two types of equilibria in the metapopulations and the extremely high density of *Ceriodaphnia* in the equilibrium with a higher chlorophyll-*a* concentration in the high light tank cannot be captured by the model.

Homogeneous systems

Only one replicate of the metapopulation systems appears to have a large difference in chlorophyll-*a* between the two patches (i.e. shows pattern) at equilibrium (Figure 4.10). Two replicates of the non-metapopulation system had quite large differences in equilibrium chlorophyll-*a* concentration between the two tanks. This probably occurred because these systems had not completely stabilized when the equilibrium was estimated.

There was a large amount of variation in average equilibrium chlorophyll-*a* concentration and there was no consistent difference between treatments even though the estimates of the quantity eg/h were higher in metapopulations than in non-metapopulations as was found in the heterogeneous systems.

Ceriodaphnia equilibrium estimates were much higher in metapopulation systems than in non-metapopulation systems. The effects of differences in parameters between metapopulations and non-metapopulations seems to outweigh the prediction that metapopulations will have smaller *Ceriodaphnia* equilibrium densities than non-metapopulation when parameters are the same in the two systems. It is unclear why differences in *Ceriodaphnia* density between systems were so pronounced while large differences in average chlorophyll-*a* concentration were not observed.

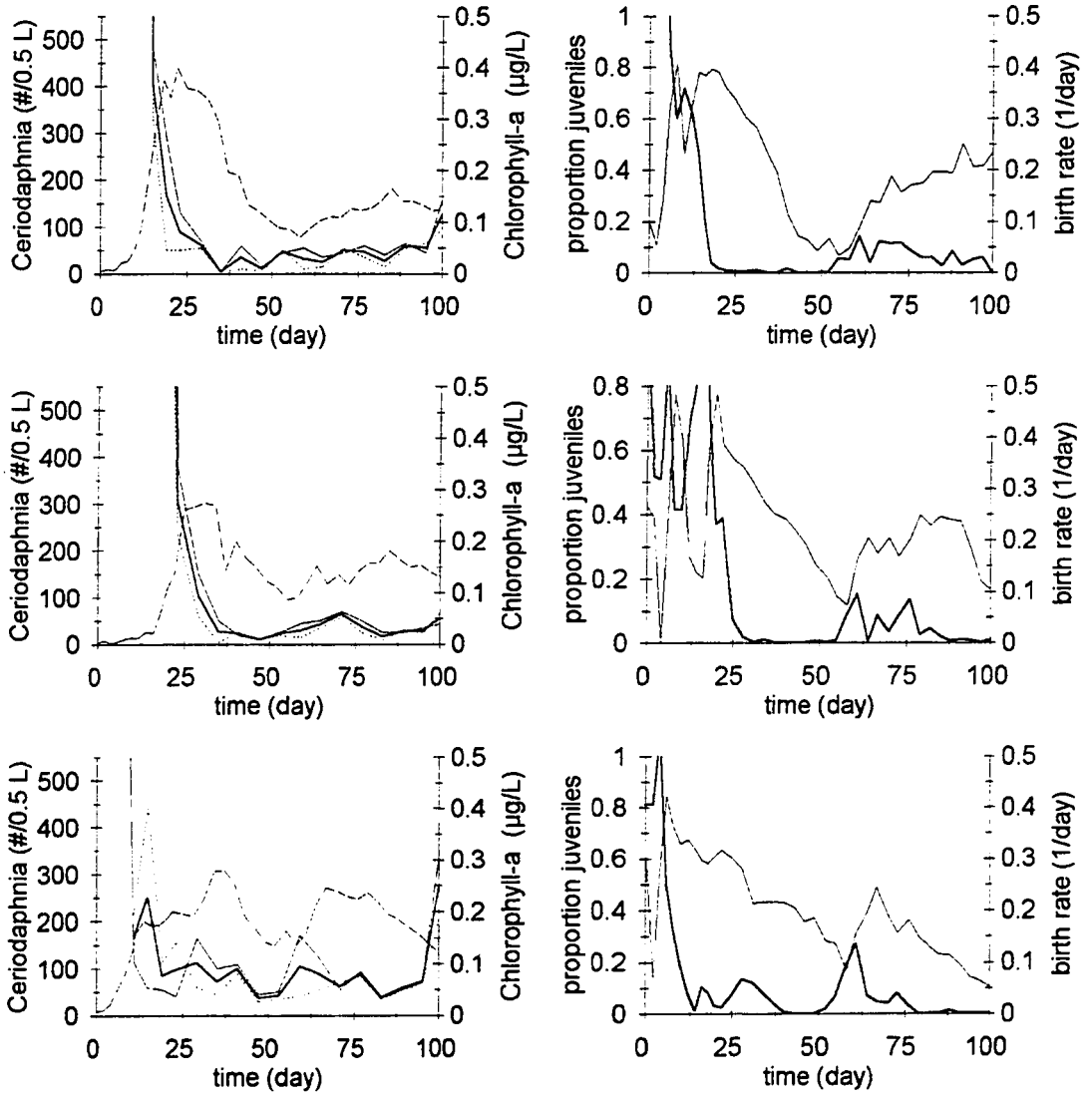

Figure 4.1. Time series for three replicates of the non-metapopulation systems in heterogeneous light. The left column shows *Ceriodaphnia* density (dashed), average chlorophyll-*a* concentration (bold), chlorophyll-*a* concentration in the low-light tank (solid) and chlorophyll-*a* concentration in the high-light tank (dotted). The second column shows the proportion juveniles (solid) and the per capita *Ceriodaphnia* birth rate (bold).

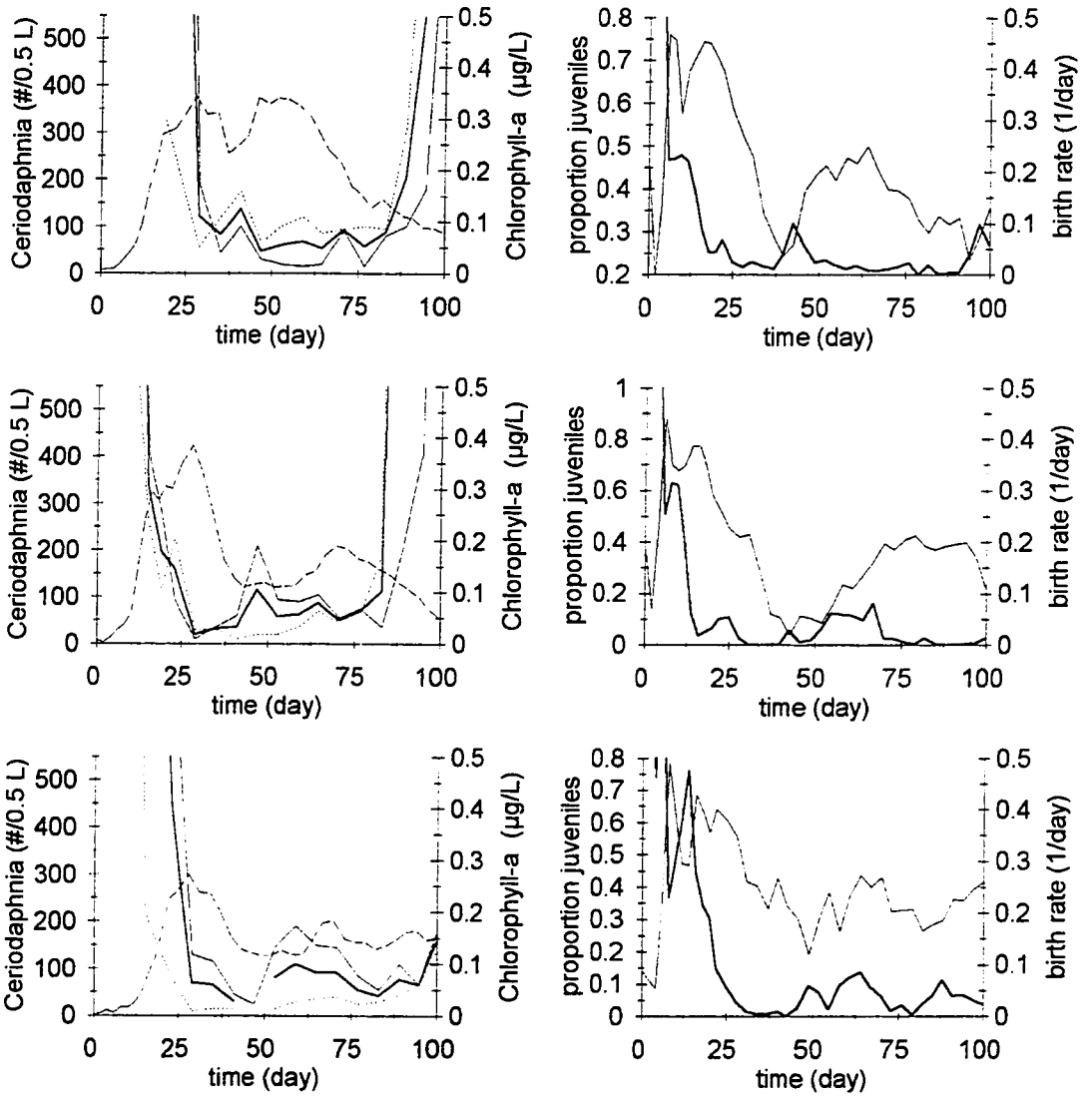

Figure 4.2. Time series for three replicates of the metapopulation systems in heterogeneous light. The left column shows *Ceriodaphnia* density (dashed), average chlorophyll-*a* concentration (bold), chlorophyll-*a* concentration in the low light tank (solid) and chlorophyll-*a* concentration in the high light tank (dotted). The second column shows the proportion juveniles (solid) and the per capita *Ceriodaphnia* birth rate (bold).

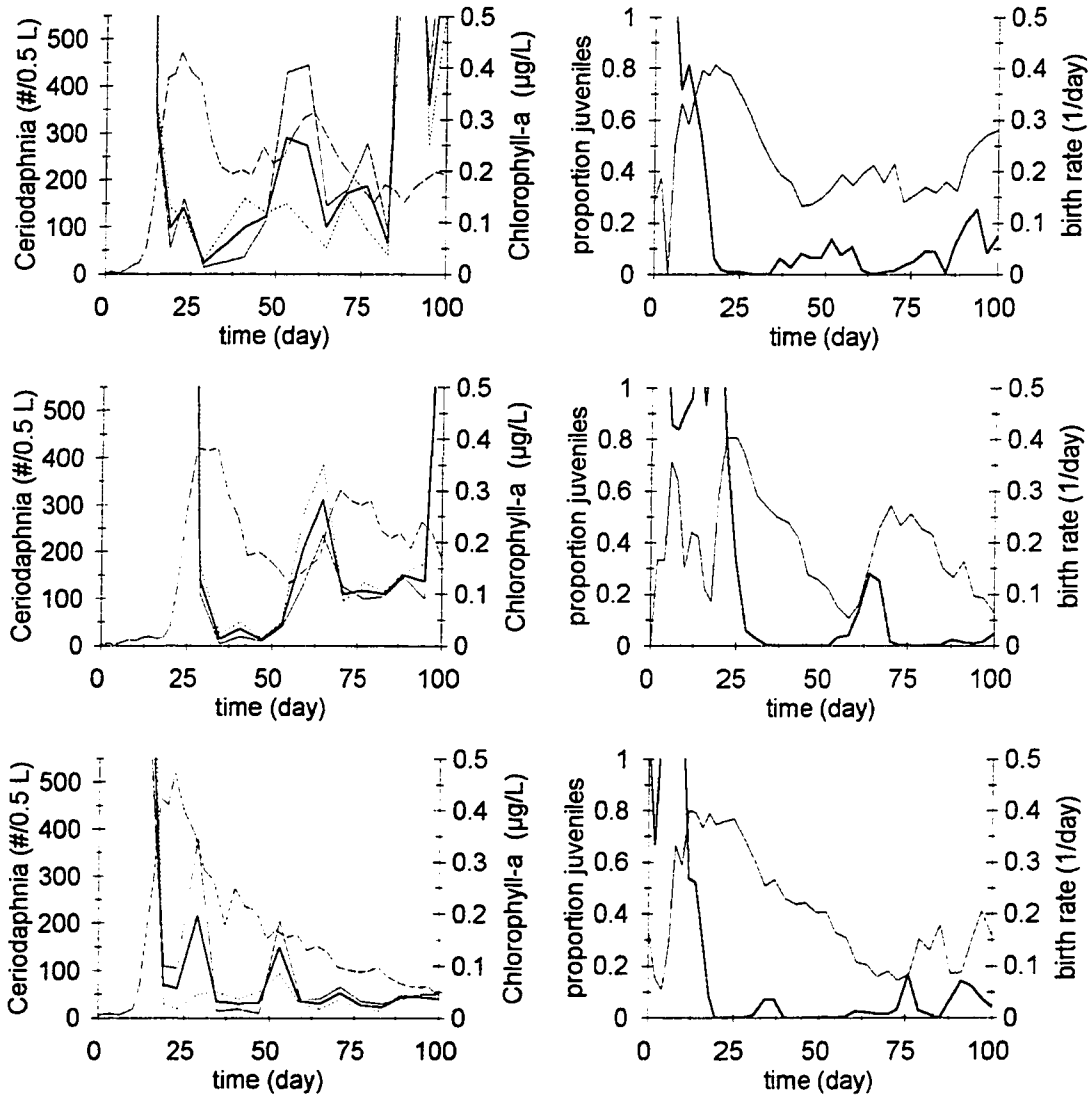

Figure 4.3. Time series for three replicates of the non-metapopulation systems in homogeneous light. The left column shows *Ceriodaphnia* density (dahed), average chlorophyll-*a* concentration (bold), chlorophyll-*a* concentration in tank-a (solid) and chlorophyll-*a* concentration in the tank-b (dotted). The second column shows the proportion juveniles (solid) and the per capita *Ceriodaphnia* birth rate (bold).

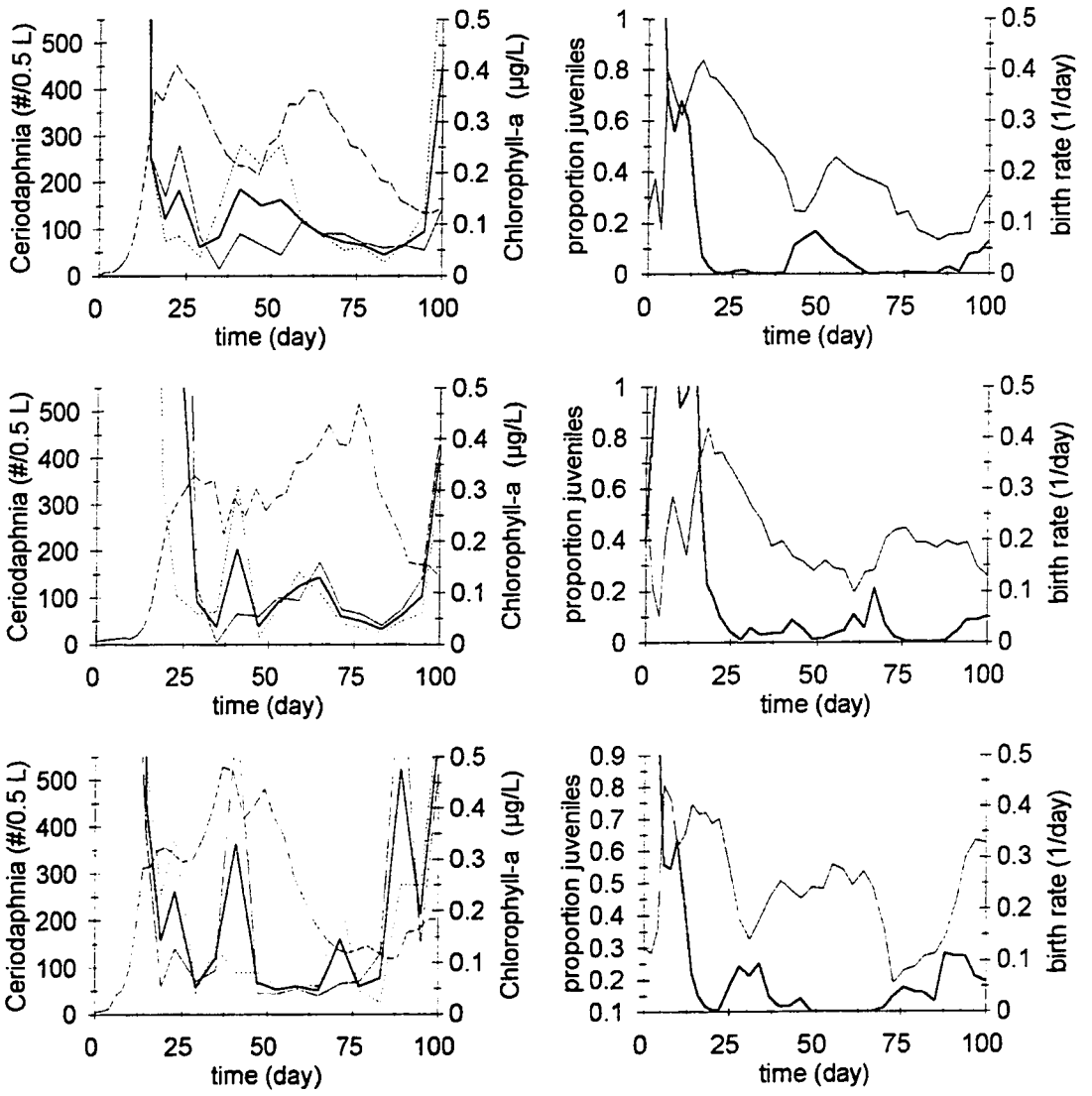

Figure 4.4. Time series for three replicates of the metapopulation systems in homogeneous light. The left column shows *Ceriodaphnia* density (dashed), average chlorophyll-*a* concentration (bold), chlorophyll-*a* concentration in tank-a (solid) and chlorophyll-*a* concentration in the tank-b (dotted). The second column shows the proportion juveniles (solid) and the per capita *Ceriodaphnia* birth rate (bold).

Table 4.1. Results of the tests for pattern formation in the heterogeneous systems. The quantity being tested is the chlorophyll-*a* concentration in the low-light tank minus the chlorophyll-*a* concentration in the high-light tank. a) Positive and negative runs test and test of proportions. b) Runs above and below the median. c) Summary of significant results. * indicates a significant result.

a)	# of negative differences	# of positive differences	# of positive and negative runs	test of proportions critical values (α=0.05) two-tail	Positive and negative runs test critical values (α=0.05) one-tail
non-meta 1	5	14	10	4,15	5
non-meta 2	6	13	9	4,15	5
non-meta 3	6	13	6	4,15	5
meta 1	13	6	3*	4,15	5
meta 2	9	11	5*	5,15	6
meta 3	1*	17	2	4,14	-

b)	# of observations below the median	# of observations above the median	# of runs above and below the median	Runs above and below the median test critical values (α=0.05) one-tail
non-meta 1	10	10	12	6
non-meta 2	10	10	9	6
non-meta 3	8	9	6	5
meta 1	9	9	9	6
meta 2	10	10	5*	6
meta 3	9	9	5*	6

c)	Test of proportions	Positive and negative runs test	Runs above and below the median test
non-meta 1			
non-meta 2			
non-meta 3			
meta 1		*	
meta 2		*	*
meta 3	*	-	*

Table 4.2. Results of the tests for pattern formation in the homogeneous systems. The quantity being tested is the chlorophyll-*a* concentration in tank-a minus the chlorophyll-*a* concentration in tank-b. a) Positive and negative runs test and test of proportions. b) Runs above and below the median. c) Summary of significant results. * indicates a significant result.

a)	# of negative differences	# of positive differences	# of positive and negative runs	test of proportions critical values (α=0.05) two-tail	Positive and negative runs test critical values (α=0.05) one-tail
non-meta 1	9	11	8	5,15	6
non-meta 2	15	5*	5*	5,15	5
non-meta 3	5*	15	7	5,15	5
meta 1	9	11	5*	5,15	6
meta 2	3*	17	5	5,15	3
meta 3	15	5*	7	5,15	5

b)	# of observations below the median	# of observations above the median	# of runs above and below the median	Runs above and below the median test critical values (α=0.05) one-tail
non-meta 1	10	10	10	6
non-meta 2	10	10	13	6
non-meta 3	9	9	8	6
meta 1	9	9	5*	6
meta 2	10	10	5*	6
meta 3	10	10	5*	6

c)	Test of proportions	Positive and negative runs test	Runs above and below the median test
non-meta 1			
non-meta 2	*	*	
non-meta 3	*		
meta 1		*	*
meta 2	*		*
meta 3	*		*

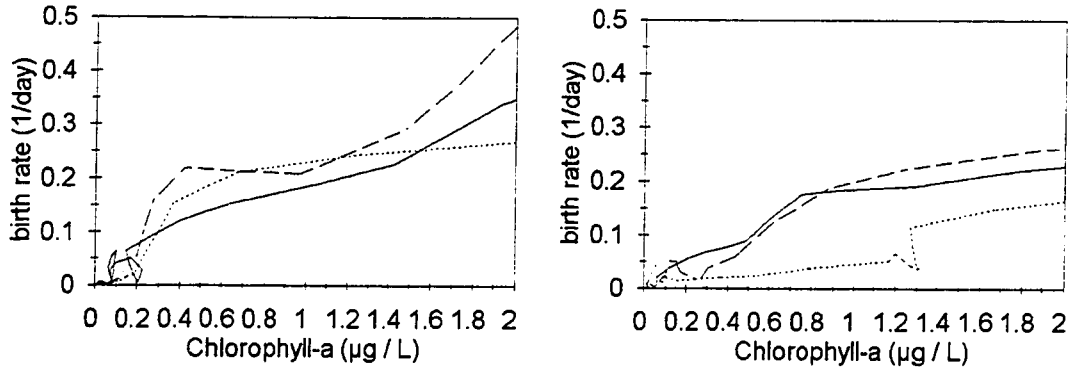

Figure 4.5. *Ceriodaphnia* per capita birth rate as a function of the average chlorophyll-*a* concentration between the two tanks in the heterogeneous systems. On the left are the birth rate curves of the three replicates of the non-metapopulation systems. On the right are the birth rate curves of the three replicates of the metapopulation systems. Data points were obtained by linear interpolation of the birth rate and by linear interpolation of the natural-log transformed chlorophyll-*a* concentrations. Connected points are sequential in time.

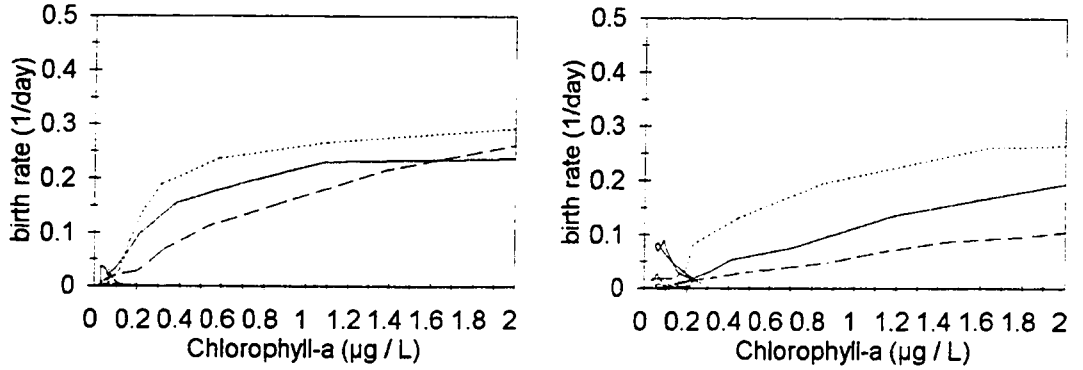

Figure 4.6. *Ceriodaphnia* per capita birth rate as a function of the average chlorophyll-*a* concentration between the two tanks in the homogeneous systems. On the left are the birth rate curves of the three replicates of the non-metapopulation systems. On the right are the birth rate curves of the three replicates of the metapopulation systems. Data points were obtained by linear interpolation of the birth rate and by linear interpolation of the natural-log transformed chlorophyll-*a* concentrations. Connected points are sequential in time.

Table 4.3. Parameters of the birth rate curves and equilibrium estimates for systems in heterogeneous light. (a) equilibria estimates. (b) parameter estimates using Model I and death rate estimates. (c) parameter estimates using Model II.

(a)	non-meta 1	non-meta 2	non-meta 3	meta 1	meta 2	meta 3
chlorophyll-*a* low-light tank (μg / L)	0.04094	0.03509	0.08447	0.03769	0.08967	0.10201
chlorophyl-*a* high-light tank (μg / L)	0.02339	0.02469	0.05263	0.09617	0.03444	0.02274
chlorophyl-*a* average (μg / L)	0.03216	0.02989	0.06855	0.06693	0.06205	0.06238
Ceriodaphnia density (# / L)	250	296	430	576	306	304
birth rate (1/day)	0.02811	0.02798	0.02902	0.02491	0.02914	0.03482

(b)	non-meta 1	non-meta 2	non-meta 3	meta 1	meta 2	meta 3
eg	0.6658	0.5402	0.6203	1.1748	0.8253	0.3711
h	1.7173	0.8721	1.9933	20.0000	3.7914	1.0230
d_1	0.0130	0.0217	0	0	0	0.0090
d_2	0.0224	0.0269	0.0058	0.0226	0.0216	0.0415
eg/h	0.387	0.619	0.313	0.059	0.218	0.363

(c)	non-meta 1	non-meta 2	non-meta 3	meta 1	meta 2	meta 3
eg	0.6168	0.5540	0.5752	0.1437	1.0799	0.6403
h	1.4895	0.8640	1.7255	1.0008	5.0368	1.8245
d_1	0.0137	0.0207	0	0	0	0.0083
eg/h	0.414	0.641	0.666	0.144	0.214	0.351

Table 4.4. Parameters of the birth rate curves and equilibrium estimates for systems in homogeneous light. (a) equilibria estimates. (b) parameter estimates using Model I and death rate estimates. (c) parameter estimates using Model II.

(a)	non-meta 1	non-meta 2	non-meta 3	meta 1	meta 2	meta 3
chlorophyll-*a* tank-a (μg / L)	0.21182	0.08577	0.05393	0.07342	0.08252	0.12411
chlorophyl-*a* tank-b (μg / L)	0.11111	0.13125	0.03899	0.14555	0.10136	0.08707
chlorophyl-*a* average (μg / L)	0.16147	0.10851	0.04646	0.10949	0.09194	0.10559
Ceriodaphnia density (# / L)	500	454	326	608	764	588
birth rate (1/day)	0.02714	0.02618	0.01141	0.02618	0.02704	0.01217

(b)	non-meta 1	non-meta 2	non-meta 3	meta 1	meta 2	meta 3
eg	0.5135	0.6287	0.4772	0.5350	0.2110	2.499
h	0.6292	2.5787	1.2679	1.2373	2.3096	20
d_1	0.0345	0.0035	0.0088	0.0342	0	.0060
d_2	0.0101	0.0307	0.0133	0.0115	0.0127	0.0101
eg/h	0.816	0.244	0.376	0.423	0.091	0.125

(c)	non-meta 1	non-meta 2	non-meta 3	meta 1	meta 2	meta 3
eg	0.5156	0.6350	0.4183	0.5609	0.3003	2.6765
h	0.6221	2.5592	0.9187	1.3118	3.0451	20
d_1	0.0339	0.0034	0.0112	0.0321	0	0.0078
eg/h	0.829	0.248	0.455	0.428	0.108	0.134

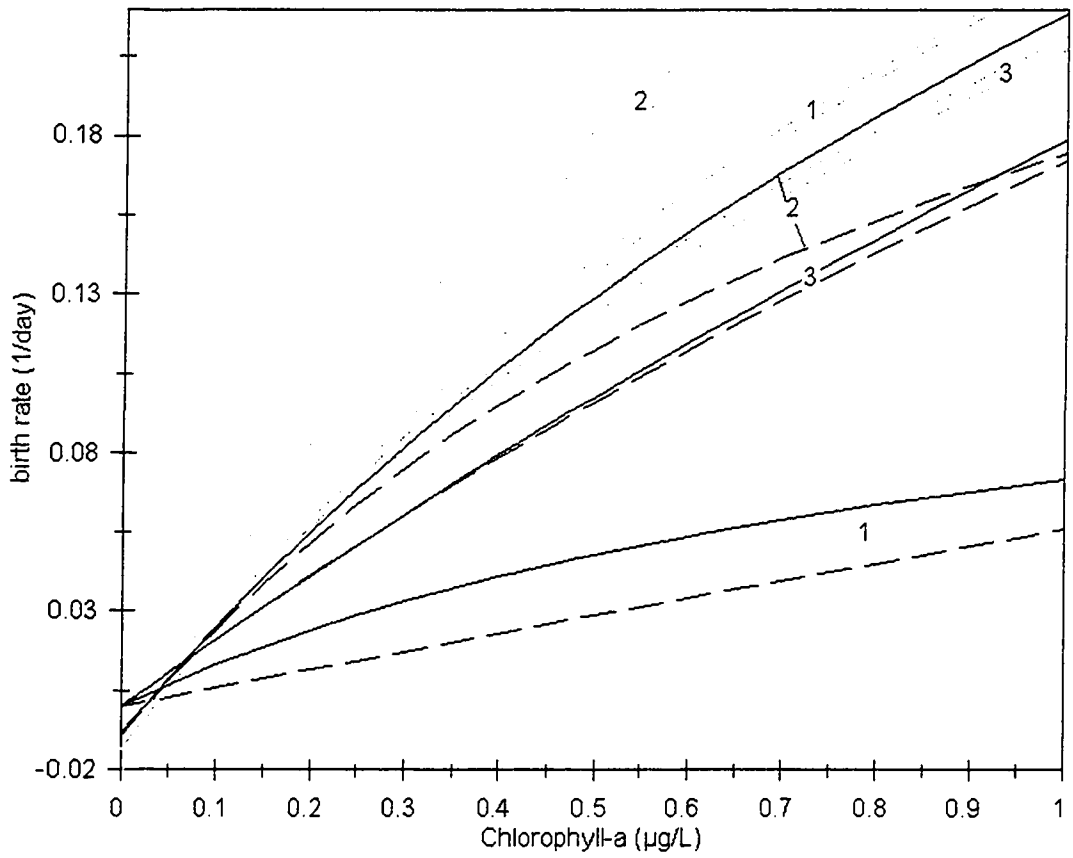

Figure 4.7. Comparison of birth rate curves between non-metapopulation and metapopulation systems fit using Model I and Model II when light is heterogeneous. The graph shows the birth rate curves of *Ceriodaphnia* fit using Model I in non-metapopulation (dashed grey) and metapopulation (dashed black) systems. Also shown are the birth rate curves fit using Model II in non-metapopulation (solid grey) and metapopulation (solid black) systems when $A_a=A_b$. The numbers shown are the replicate numbers.

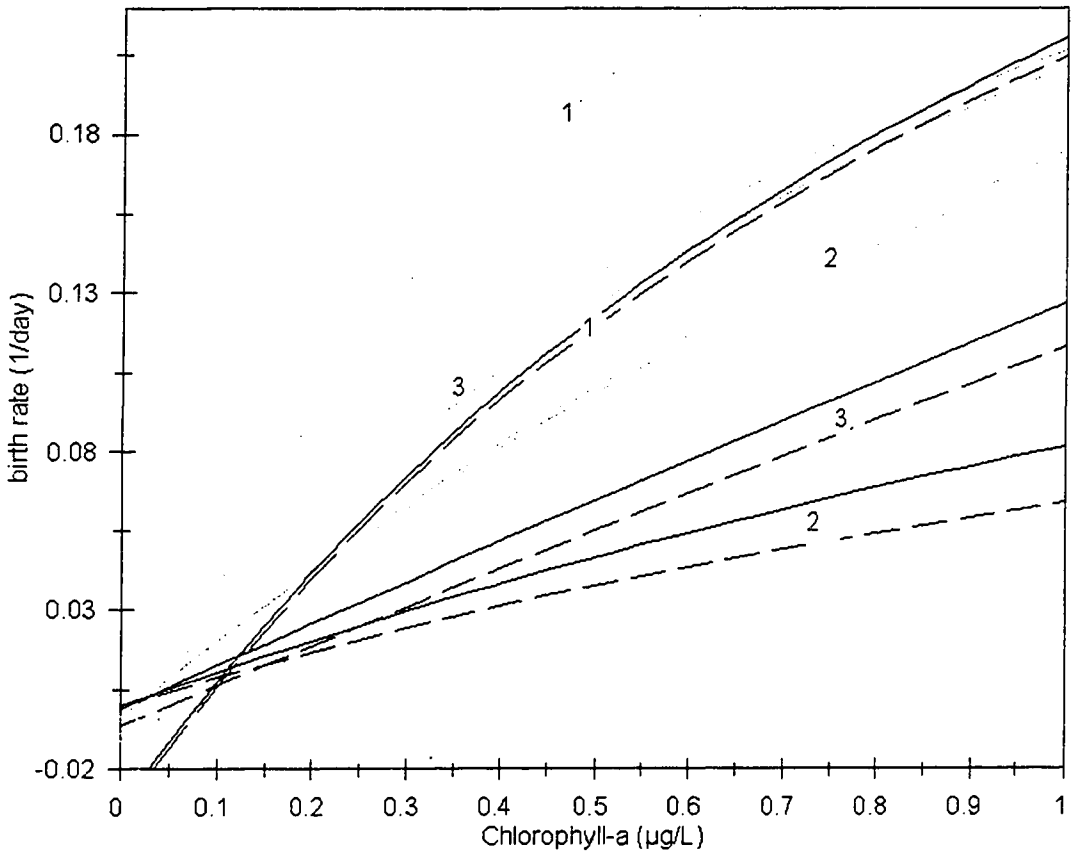

Figure 4.8. Comparison of birth rate curves between non-metapopulation and metapopulation systems fit using Model I and Model II when light is homogeneous. The graph shows the birth rate curves of *Ceriodaphnia* fit using Model I in non-metapopulation (dashed grey) and metapopulation (dashed black) systems. Also shown are the birth rate curves fit using Model II in non-metapopulation (solid grey) and metapopulation (solid black) systems when A_a=A_b. The numbers shown are the replicate numbers.

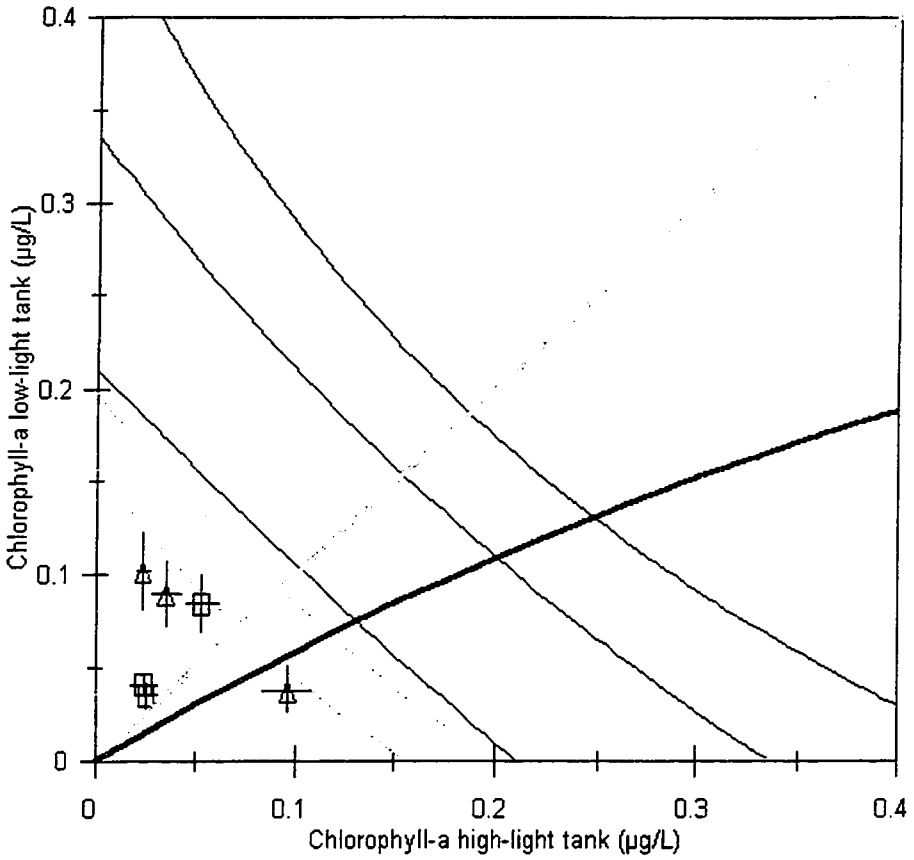

Figure 4.9. Observed and expected chlorophyll-*a* equilibria in heterogeneous systems. The negatively sloped curves show the expected equilibrium curves (equation 3.2) for non-metapopulation systems (grey) and metapopulation systems (black) based on parameters estimated from Model II. The non-metapopulation equilibria should fall on the positively sloped grey line and the metapopulation equilibria should fall on the bold black line (equation 2.11) (based on parameter estimates from Chapter 3) . The symbols are the observed equilibria for non-metapopulation systems (square) and metapopulation systems (triangle). Standard Error bars are shown.

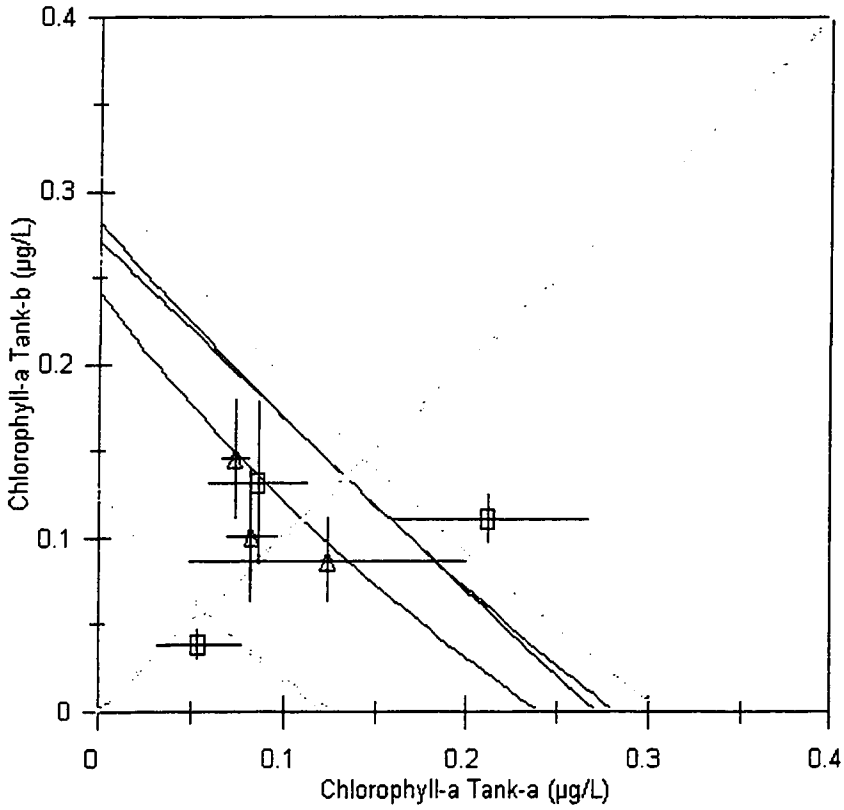

Figure 4.10. Observed and expected chlorophyll-*a* equilibria in homogeneous systems. The negatively sloped curves show the expected equilibrium curves (equation 2.11) for non-metapopulation systems (grey) and metapopulation systems (black) for parameters estimated using Model II. The symbols are the observed equilibria for non-metapopulation systems (square) and metapopulation systems (triangle). All equilibria should fall on the positively sloped grey line or on one of the axes in the case of metapopulations. Standard Error bars are shown.

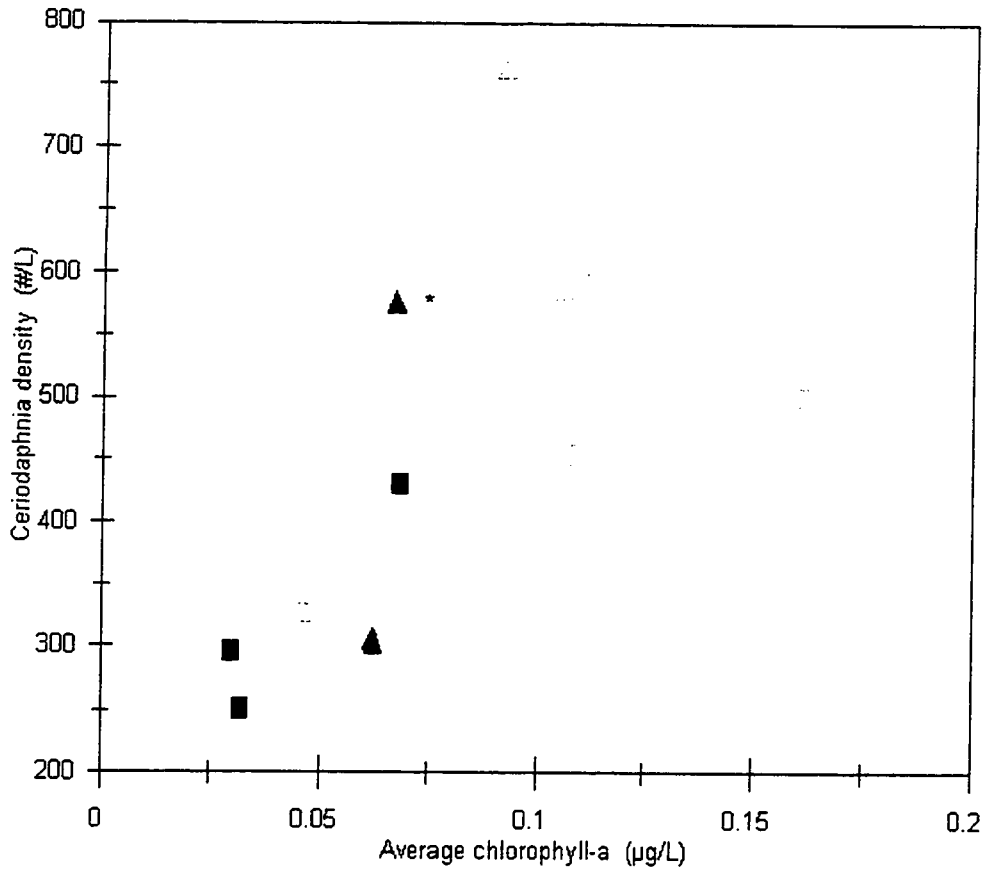

Figure 4.11. Observed *Ceriodaphnia* equilibria as a function of average chlorophyll-*a* equilibria between the two tanks. The figure show equilibria for heterogeneous non-metapopulations (black squares), heterogeneous metapopulations (black triangles), homogeneous non-metapopulations (grey squares) and homogeneous metapopulations (grey triangles). * indicates the one replicate from the heterogeneous metapopulations with a higher chlorophyll-*a* concentration in the high-light (low carrying-capacity) tank.

Table 4.5. The effect of increasing *Ceriodaphnia* parameters on the equilibrium of the non-metapopulation model. ↑- signifies increases the equilibrium value. ↓-signifies decreases the equilibrium value.

parameter	effect on chlorophyll-*a* concentration (A*)	effect on *Ceriodaphnia* density (C*)	In non-metapopulations this effect on C* is true for:
↑h	↑	↑	$A^* < k/2$
↑e	↓	↓	$A^* < (k-h)/2$
↑g	↓	↓	$A^* < k/2$
↑d	↑	↑	$A^* < (k-h)/2$

DISCUSSION

There are a number of results that were predicted by the model. A summary of the predictions and the relevant experimental results is given in Table 4.6. In heterogeneous systems, pattern formation occurred in metapopulations but not in non-metapopulations. In homogeneous systems pattern was observed in both metapopulations and non-metapopulations but other differences occur between metapopulations and non-metapopulations that are similar to those differences that are observed in heterogeneous systems, implying that a metapopulation structure can be important even in the absence of external heterogeneity. The birth rate for a given average chlorophyll-*a* concentration is lower in metapopulations than in non-metapopulations. Average chlorophyll-*a* concentration at equilibrium is lower in non-metapopulations than metapopulations in the heterogeneous systems.

There are a number of results that were not predicted by the model. Pattern in homogeneous metapopulations (1 replicate) and pattern with a higher chlorophyll-*a* concentration in the low-light (high carrying-capacity) tank (2 replicates) in heterogeneous metapopulations can both occur in the model, but not for parameter values close to the estimated values. The estimated quantity eg/h is smaller in metapopulations than in non-metapopulations in both heterogeneous and homogeneous light. Differences in parameter values which would give rise to a smaller value of eg/h would also produce higher equilibrium *Ceriodaphnia* density in metapopulations along with higher chlorophyll-*a*

Table 4.6 Predictions for heterogeneous and homogeneous systems and the relevant experimental result.

Prediction for heterogeneous systems	**Observed?**	**Prediction for homogeneous systems**	**Observed?**
non-metapopulations should be unstable. Metapopulations may or may not be unstable.	NO- all systems are stable.	All systems should be unstable.	NO- all systems are stable.
Over the entire time series, metapopulations should show pattern in chlorophyll-*a*, non-metapopulations should not.	YES	Metapopulations may or may not have pattern over the time series, non-metapopulations should not.	NO- both metapopulations and non-metapopulations show pattern but the quality of this pattern differs between treatments.
Metapopulations should have a lower birth rate than non-metapopulations for any average chlorophyll-*a* concentration between patches.	YES	The same prediction as for heterogeneous systems unless there is no pattern in a metapopulation, then it should be the same as the non-metapopulations.	YES
At equilibrium, metapopulations should have pattern.	YES	Metapopulations should have only the homogeneous equilibrium or pattern with zero chlorophyll-*a* concentration in one tank.	NO- at least one replicate has a pattern at equilibrium with a positive chlorophyll-*a* concentration in both tanks.
The average equilibrium chlorophyll-*a* concentration should be higher in metapopulations than in non-metapopulations.	YES	The average equilibrium chlorophyll-*a* concentration should be equal in metapopulations and non-metapopulations if pattern at equilibrium is not observed. If pattern is observed at equilibrium then the average equilibrium chlorophyll-*a* concentration should be lower.	YES

Table 4.6 continued.

In metapopulations, chlorophyll-*a* concentration should be higher in the high-light (low carrying-capacity tank). If a higher chlorophyll-*a* concentration is observed in the low light tank, this replicate should have the lower equilibrium *Ceriodaphnia* density.	NO- two replicates have a higher chlorophyll-*a* concentration in the low light tank. However, both of these replicates have much lower *Ceriodaphnia* density than the replicate with a higher chlorophyll-*a* concentration in the high light tank.	-	-
Metapopulations should have chlorophyll-*a* concentration higher in one tank and lower in the other tank, than the average equilibrium chlorophyll-*a* concentration of non-metapopulations.	NO- the chlorophyll-*a* concentration in both tanks at equilibrium is greater than the non-metapopulation chlorophyll-*a* concentration at equilibrium.	There should be no difference in chlorophyll-*a* concentrations between metapopulation and non-metapopulations (based on parameter values). If pattern is observed then the relationship between metapopulation and non-metapopulation concentrations should be the same as for heterogeneous systems.	NO- when pattern occurs the result is the same as for heterogeneous systems. Both tanks have a higher chlorophyll-*a* concentration.
Ceriodaphnia density at equilibrium should be smaller in metapopulations.	NO- *Ceriodaphnia* density, is higher in metapopulations.	There should be no difference in *Ceriodaphnia* density between metapopulations and non-metapopulations. If pattern is observed the prediction is the same as for heterogeneous systems.	NO- *Ceriodaphnia* density, is higher in metapopulations
The 'true' functional response should be the same in metapopulations and non-metapopulations. Parameter estimates using Model II should be identical for metapopulations and non-metapopulations.	NO - the quantity eg/h is lower in metapopulations.	Same as for heterogeneous systems.	NO- same result as in heterogeneous systems.

concentrations in both patches of heterogeneous metapopulations than in heterogeneous non-metapopulations. Both of these things are observed but not predicted by the model for equal parameter values in metapopulations and non-metapopulations. There are also results that suggest that the "within patch" model is not structurally correct and these are: (1) stability was observed for all treatments whereas instability was predicted by the model, (2) the average equilibrium chlorophyll-*a* concentration between the two tanks was greater in the systems with the higher average carrying capacity (i.e. the homogeneous systems), and (3) *Ceriodaphnia* densities were much higher than predicted. These three major groups of observations: the range of observed patterns, differences in parameters between treatments, and results that indicate structural errors of the "within patch" model, will be discussed independently, and then the possible relationships among them will be discussed in the synthesis section.

Range of observed patterns

Higher chlorophyll-*a* concentrations in the low-light tanks at equilibrium in the heterogeneous systems, and pattern in the homogeneous systems, were not expected to occur for the estimated parameter values.

It is unlikely that this result could be caused by inaccurate estimates of the *Ceriodaphnia* parameters (h,g,e,d_1,d_2) because parameter estimates from the literature and from the time series agree closely. Also, the average equilibrium chlorophyll-*a* concentrations, which are exclusively dictated by *Ceriodaphnia* parameters in the non-metapopulation model and primarily dictated by *Ceriodaphnia* parameters in the metapopulation model, are very close to those predicted by parameter estimates.

If the carrying capacity in low light is actually one half of the estimated value, then observed range of pattern at equilibrium in metapopulations would be expected. The algae-only tanks did show a decrease in chlorophyll-*a* concentration after the initial peak. It has also been suggested that the presence of inedible algae can reduce the effective carrying capacity of edible algae (McCauley and Murdoch, 1990; Kretchmar, Nisbet, and McCauley, 1993; Mudoch *et al.*, 1998). Decreasing the carrying capacity of the low light tanks in the model would have the effect of lowering the already drastically underestimated *Ceriodaphnia* equilibrium densities.

It is possible that some small change in model structure, as described in the following two sections, would also affect the type of pattern that could occur at equilibrium.

The difference in parameter estimates between metapopulations and non-metapopulations

Higher average equilibria in the metapopulation systems appear to be due to a decrease in the filtration rate at low chlorophyll-*a* concentration or the conversion efficiency. This could be due to one of two factors: either the 'shape' of the birth rate curve is different from what would be expected assuming that *Ceriodaphnia* have a type II functional response, or the metapopulation structure affects the algal community composition. It would be nice to identify a small change in the model, that would result in a model where metapopulation and non-metapopulations have the same "within patch" model with the same parameter values, and would explain the observed differences in parameter values estimated using the current model.

A first attempt to modify the model to accommodate the observed equilibria assumes that the following equation still describes *Ceriodaphnia* dynamics in both metapopulations and non-metapopulations:

$$\frac{dC}{dt} = (eI - d_1 - d_2)C \quad (4.1)$$

Now all that is needed is an ingestion function that gives the same average ingestion when both patches of the metapopulation have a higher chlorophyll-*a* concentration than the non-metapopulation. This type of functional response is shown in figure 4.12 along with the generally accepted form (a type II functional response). Given the range of chlorophyll-*a* concentrations, it is highly unlikely that the ingestion rate decreases with chlorophyll-*a* concentration in the region of observed chlorophyll-*a* concentrations, and this relationship is also not observed in the birth rate curves of the experimental systems. This explanation for the observed equilibria is rejected. There are other arguments that follow along similar lines but they all require that the per capita rate of increase of *Ceriodaphnia* can decrease with increasing chlorophyll-*a* concentration when chlorophyll-*a* is homogeneous, which is just not realistic for the low observed chlorophyll-*a* concentrations. A single predator equation with a per capita rate of change that is purely dependent on prey density cannot capture the observed dynamics.

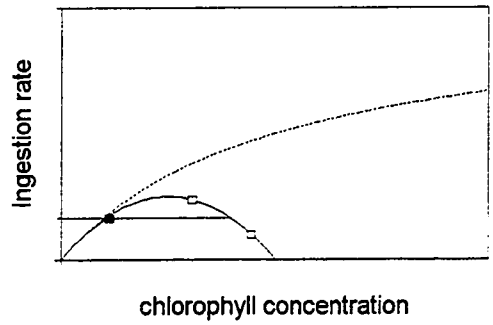

Figure 4.12. What the shape of the functional response curve would have to look like in order to produce the equilibria of metapopulations and non-metapopulations observed in the experiment. The top curve represents what the functional response has been shown to look like. The bottom curve is the required shape to produce the observed equilibria. The solid point shows the ingestion rate for a low chlorophyll-*a* concentration. The open points show the ingestion rate for two high chlorophyll-*a* concentrations that give the same average ingestion rate as the low chlorophyll-*a* concentration.

Another possible factor which might give rise to the observations is density dependence in the functional response or the birth rate. If the birth rate were density dependent, then the birth and ingestion rates may be described by:

$$b = eI - d_1 - f_1 C \quad (4.2.1) \qquad I = \frac{gA}{h + A} \quad (4.2.2)$$

Previously, density-dependence has been incorporated into the functional response assuming predator interference which results in a half saturation constant that is linearly related to predator density (Beddington, 1975). A more simplistic (non-mechanistic) form which is analogous to that described for the birth rate is:

$$b = eI - d_1 \quad (4.3.1) \qquad I = \frac{gA}{h + A} - f_2 C \quad (4.3.2)$$

Both of these types of density-dependence result in functionally identical predator growth equations. In either case, if *Ceriodaphnia* density is higher in the metapopulations, this would require a higher chlorophyll-*a* concentration in order for the birth rate to balance the death rate. Over the period when parameters were estimated, *Ceriodaphnia* density is higher in the metapopulations than the non-metapopulations for any given chlorophyll-*a* concentration (Figure 4.13). These two forms have the potential to capture the observed

differences between metapopulations.

Alternatively the observed differences in parameters between metapopulations and non-metapopulation could result from an effect of a metapopulation structure on the algal community composition. Chlorophyll-*a* was used to estimate edible algal density. If there was an increase in the amount of inedible algae in the metapopulation systems this would make it appear as though there were a decrease in the conversion efficiency or attack rate. In addition to this, the attack rate on edible algae can be reduced when there is an increase in inedible algae (McCauley, Murdoch, and Watson, 1988). It is unclear why there would be more inedible algae in the metapopulation systems. An explanation for the heterogeneous systems might be that inedible algae grow better (compared to edible algae) in high light than when they are mixed between high and low light or if they remain in low light. However, the same factors appear to operate in homogeneous systems to a lesser extent and the algae competition hypothesis does not work for them.

Results that indicate that there is a structural inaccuracy in the "within patch" model

All of these systems appear to be stable. This is in spite of the fact that parameter estimates from the literature and the experiment predict instability. This has been observed both for closely related system (Daphnia-algae) (McCauley and Murdoch, 1990) and for less closely related systems (red scale - *Aphytis*) (Murdoch, 1994). This is a general phenomenon in consumer-resource systems (Murdoch *et al.*, 1998), and research suggests simple structural changes that can account for the joint phenomena of a stable low equilibrium prey density in productive environments (McCauley *et al.*, in prep). Murdoch *et al.* (1998) tested possible reasons for stability in the Daphnia-algae system include density-dependence of the death rate or the functional response, both of which were rejected, and nutrient uptake by inedible algae.

Also not predicted by the model was the result that the equilibrium chlorophyll-*a* concentration was higher in the systems with the higher average carrying capacity. This has also been observed in previous studies (Watson and McCauley, 1988; Watson, McCauley, and Downing, 1992). Many of the hypothesized mechanisms of stability proposed by Murdoch *et. al.* (1998) also result in a positive relationship between equilibrium prey density and the prey carrying capacity.

Density-dependence in the birth rate or functional response of the predator, as discussed in the section on parameter differences between metapopulation and non-

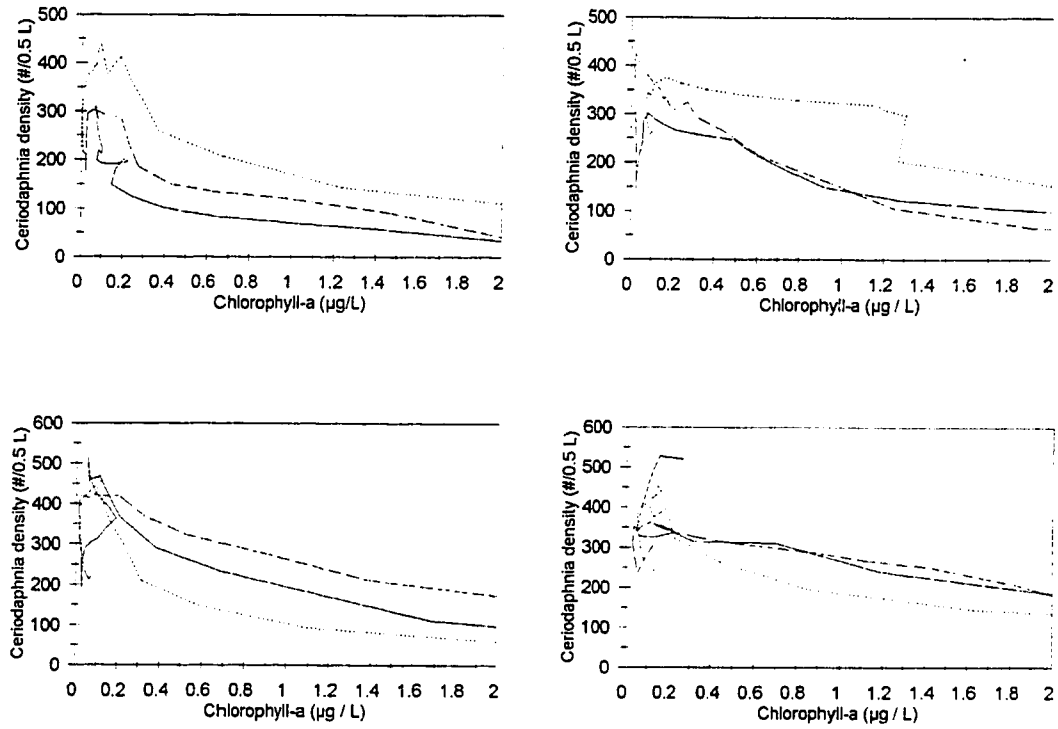

Figure 4.13. *Ceriodaphnia* density as a function of the average of the chlorophyll-*a* concentration between the two tanks in the heterogeneous systems (upper row) and homogeneous systems (lower row). On the left are the birth rate curves of the three replicates of the non-metapopulation systems. On the right are the birth rate curves of the three replicates of the metapopulation systems. Data points were obtained by linear interpolation of the natural-log transformed chlorophyll-*a* concentrations and the natural-log transformed *Ceriodaphnia* densities. Connected points are sequential in time.

metapopulations, could also introduce stability and a positive relationship between the equilibrium prey density and the carrying capacity.

There is another possible source of stability observed in these systems. In figure 4.5 and 4.6, in the non-metapopulation systems, the slope of the birth rate curve increases with increasing chlorophyll-*a* concentration in the region near the equilibrium. If the functional response also increases in this way (i.e. is a type III functional response) then this would introduce stability into the system. Experimental evidence does not support the hypothesis of a type three functional response for Cladocera (Murdoch *et al.*, 1998 and references therein) . *In situ* measurements of the functional response could test whether the functional response follows the same shape of curve as the birth rate.

It is also possible that density dependence appears to occur because of features of the size structure of the *Ceriodaphnia* population. This could be evaluated by studying the effect of a metapopulation structure on a more accurate, size-structured plankton model (for example the model described by McCauley, Nisbet, de Roos, Murdoch and Gurney, 1996). However, this approach is not particularly promising because the size structure of the metapopulations and non-metapopulations do not appear to differ for any given chlorophyll-*a* concentration.

Synthesis of differences between theory and experiment

Initially it appeared as though a fundamental assumption of many spatially-structured models, that metapopulation dynamics arise from simply adding migration to "within patch" dynamics, had been broken. However, it does appear as though there is potential to capture the dynamics of the metapopulation and non-metapopulation systems, with the same "within patch" model and parameter values, in metapopulations and non-metapopulations. If the birth rate is density-dependent then this might be able to explain all three major categories of deviation of the experimental systems from the existing model. This will require investigation of a substantially more complex model, even in the case of non-metapopulation model. Another component of this line of investigation would be to identify a potential mechanism for a density dependent birth rate or functional response. Density-dependence in the birth rate might arise as a result of the existence of some limiting nutrient that is vital for reproduction. Alternatively, the instantaneous birth rate depends on the food history and not just the current concentration. A faster depletion rate due to high predator density over the period of time when energy is being gathered for eggs

may reduce the amount of energy obtained. This argument is similar to those that have been used to construct ratio-dependent models (Arditi and Ginzburg, 1989) and a formal approach would need to be taken in order to determine whether a mechanistic food-dependent model could give rise to the proposed phenomenon. An experimental approach could also be used to determine whether or not the coincidence of higher predator density with lower birth rate for the same chlorophyll-*a* concentration was causal.

The next most promising approach would be to incorporate competition between edible and inedible algae and/or nutrient cycling. Theoretically, the effect of the presence of a predator on the competitive metapopulations and the effect of competitive metapopulations on the predator population are both of interest. Nutrient dynamics might be important because there is a net flow of *Ceriodaphnia* (and the nutrients they contain) from the high chlorophyll-*a* tank to the low chlorophyll-*a* tank in metapopulations. This type of study might also verify that the algae growth parameters were not accurately estimated and that for the proper estimates, the observations described in the section on 'details of observed patterns' are expected. Also, the approach might also explain the observed stability in these systems (Murdoch *et. al.*, 1998).

It may be found that incorporating a density-dependent birth rate, nutrient cycling or algal competition, can capture the apparent differences in parameter values between metapopulations and non-metapopulations, and that differences between these two types of systems cannot be captured by simply adding migration to the non-metapopulation model. Although this would mean that an empirical approach to studying metapopulations cannot mimic the theoretical approach, it does not mean that consideration of metapopulation features is not necessary to understand the dynamics of experimental metapopulations. There have been a number of studies where consideration of metapopulation features has contributed to the understanding of an ecological system in the absence of a non-metapopulation control system (Harrison and Taylor, 1997). In this study, variation in vital rates among replicates and within replicates at different points in time in the homogeneous systems, arise from differences in chlorophyll-*a* concentration between patches. In the heterogeneous metapopulations, all replicates have very similar average chlorophyll-*a* concentrations at equilibrium but the single replicate with a higher chlorophyll-*a* concentration in the high light (low carrying- capacity) tank has a much higher *Ceriodaphnia* density. These observations could not be understood without a spatially

structured model.

One of the specific areas of interest in this study was contrasting metapopulation dynamics in heterogeneous and homogeneous environments. As was expected, the large differences in the average carrying capacity, rather than the difference in the degree of environmental heterogeneity, between homogeneous and heterogeneous environments appears to be the major factor influencing the difference in dynamics between systems. It is unfortunate that the homogeneous systems had a higher average carrying capacity than the heterogeneous systems. An experiment where the heterogeneous systems have a higher average carrying capacity would more fully determine whether environmental heterogeneity can promote stability in spite of the destabilizing effect of an increased average carrying capacity. The model studied in Chapter 2 does not predict this, but it has been hypothesized from many other theoretical investigations (including for the Lotka-Volterra model described in Chapter 1), and has been, until recently, a widely held belief (Reeve, 1990). A very closely related question is whether or not spatial structure can be important in the absence of environmental heterogeneity. This experiment has demonstrated that it can be, because there are differences in the nature of pattern formation, parameter estimates, and equilibrium values, observed between metapopulations and non-metapopulations in homogeneous light. These differences are very similar to those differences observed in the presence of environmental heterogeneity.

CONCLUSION

This experiment has demonstrated that spatial structure can have an effect on a real predator-prey interaction in heterogeneous, and to a lesser extent, homogeneous environments. A metapopulation model has been shown to be useful in understanding spatially structured experimental systems.

In addition to testing predictions about the differences between metapopulations and non-metapopulations, this experiment has helped to identify promising approaches to more fully understanding the interaction both in metapopulations and well mixed systems. A new factor which might be important to the interaction, density-dependence in the predator birth rate, has been identified and theoretical and experimental approaches to investigating the role of this factor in metapopulation and non-metapopulations has been described.

References

Adler, F. R. 1993. Migration alone can produce persistence of host-parasitoid models. American Naturalist 141:642-650.

Anderson, D. H., and A. C. Benke. Growth and reproduction of the cladoceran Ceriodaphnia dubia from a forested floodplain swamp. Limnology and Oceanography 39:1517-1527.

Arditi, R., and L. R. Ginzburg. 1989. Coupling in predator-prey dynamics: ratio-dependence. Journal of Theoretical Biology 139: 311-326.

Beddington, J. R. 1975. Mutual interference between parasites or predators and its effect on searching efficiency. Journal of Animal Ecology 44:331-340.

Cowgill, U. M., and D. P. Milazzo, 1991. Demographic effects of salinity, water hardness and carbonate alkalinity of Daphnia magna and Ceriodaphnia dubia. Archive Hydrobiology 122:33-56.

Cuddington, K., and E. McCauley. 1994. Food-dependent aggregation and mobility of the water fleas *Ceriodaphnia dubia* and *Daphnia pulex*. Canadian Journal of Zoology 72:12-17-1226.

de Roos, A. M., J. A. J. Metz, E. Evers, and A. Leipoldt. 1990. A size dependent predator-prey interaction: who pursues whom? Journal of Mathematical Biology 28: 609-644.

de Roos, A.M., E. McCauley, and W. G. Wilson. 1991. Mobility versus density limited predator-prey dynamics on different spatial scales. Proceedings of the Royal Society of London B. 246:117-122.

de Roos, A.M., E. McCauley, and W. G. Wilson. 1998. Pattern formation and the spatial scale of interaction between predators and their prey. Theoretical Population Biology. In press.

Gurney, W. S. C., and R. M. Nisbet. 1998. Ecological Dynamics. Oxford University Press Inc. New York.

Hanski, I. A., and D. Simberloff. 1987. The metapopulation approach, its history, conceptual domain, and application to conservation. In: Hanski, I. A. and M. E. Gilpin (Eds). Metapopuation biology: ecology, genetics, and evolution. Academic Press. Toronto.

Harrison, S., and A. D. Taylor. 1997. Empirical evidence from metapopulation dynamics. In: Hanski, A. and M. E. Gilpin (Eds). Metapopuation biology: ecology, genetics, and evolution. Academic Press. Toronto.

Hassell, M. P. , H. N. Comins, and R. M. May. 1991. Spatial structure and chaos in insect population dynamics. Nature 353:252-258.

Hastings, A. 1978. Global stability of a two species system. Journal of Mathematical Biology 5:399-403.

Jansen, V. A. A. 1994. On the bifurcation structure of two diffusively coupled predator-prey systems. In: Theoretical aspects of metapopulation dynamics. Ph.D Thesis, Leiden University. Leiden.

Jansen, V. A. A. 1995. Regulation of predator-prey systems through spatial interactions: a possible solution to the paradox of enrichment. Oikos 74:384-380.

Kirk, K. L., and J. J. Gilbert. 1990. Suspended clay and the population dynamics of planktonic rotifers and cladocerans. Ecology 71:1741-1755.

Kretchmar, M., R. M. Nisbet, and E. McCauley. 1993. A predator-prey model for zooplankton grazing on competing algal populations. Theoretical population Biology 44:32-66.

Kuznetsov, Y. A. 1995. Elements of applied bifurcation theory. Springer-Verlag. New York.

Levins, R. 1969. Some demographic and genetic consequences of environmental heterogeneity for biological control. Bulletin of the Entomological Society of America 15:237-240.

Lynch, M., L. J. Weider, and W. Lampert. 1986. Measurement of the carbon balance in *Daphnia*. Limnology and Oceanography 31:17-33.

Matvee, V. F, and E.G. Balseiro. 1990. Contrasting responses of two cladocerans to changes in the nutritional value of nannoplankton. Freshwater Biology 23: 197-204.

May, R. M. 1993. Stability and Complexity in Model Ecosystems. Second Edition. Monographs in population biology 6. Princeton University Press. Princeton.

McCauley, E. 1984. Estimating zooplankton biomass. In: Downing J. and F. Rigler (Eds). Assessing Secondary Productivity. Blackwell. Oxford.

McCauley, E. and W. W. Murdoch. 1990. Predator-prey dynamics in environments rich and poor in nutrients. Nature 343:455-457.

McCauley, E., W. W. Murdoch, R. M. Nisbet, and W. S. C. Gurney. 1990. The physiological ecology of *Daphnia*: development of a model of growth and reproduction. Ecology 71:703-715.

McCauley. E., W. W. Murdoch, and S. Watson. 1988. Simple models and variation in plankton densities among lakes. American Naturalist 132:383-403.

McCauley, E., R. M. Nisbet, A. M. de Roos, W. W. Murdoch, and W. S. C. Gurney. 1996. Structured population models of herbivorous zooplankton. Ecological Monographs 66:479-501.

McCauley *et al.* In prep.

Mourelatos, S., and G. Lacroix. In situ filtering rates of Cladocera: effect of body length, temperature, and food concentration.

Murdoch, W. W., C. J. Briggs, R. M. Nisbet, W. S. C. Gurney, and A. Stewart-Oaten. 1992. Aggregation and stability in metapopulation models. American Naturalist 140:41-58.

Murdoch, W. W. 1994. Population regulation in theory and practice. Ecology 75: 271-287.

Murdoch, W. W., R. M. Nisbet, E. McCauley, A. M. de Roos, and W. S. C. Gurney. 1998. Plankton abundance and dynamics across nutrient levels: test of hypotheses. Ecology 79:1339-1356.

Nisbet, R. M., C. J. Briggs, W. S. C. Gurney, W. W. Murdoch, and A. Stewart-Oaten. 1992. Two-patch metapopulation dynamics. In: Levin, S. A., J. H. Steele, and T. Powell. (Eds). Patch dynamics in terestrial , freshwater and marine ecosystems. Lecture Notes in Biomathematics 96. Springer, Berlin.

Nisbet, R. M., E. McCauley, W. S. C. Gurney, W. W. Murdoch, and A.M. de Roos. 1997. Simple representations of biomass dynamics in structured populations. In: H. Othmer, F.R. Adler, M.A. Lewis (Eds.). Case Studies in Mathematical Biology. Prentice-Hall.

Nisbet, R. M., E. McCauley, A.M. de Roos, W. W. Murdoch, and W. S. C. Gurney. 1991 Population dynamics and Element Recycling in an Aquatic Plant-Herbivore System. Theoretical Population Biology 40:125-147.

Pace, L. P., K. G, Porter, and Y. S. Feig. 1983. Species- and age-specific differences in bacterial resource utilization by two co-occurring cladocerans. Ecology 64: 1145-1156.

Paloheimo, J. I. 1974. Calculation of instantaneous birth rate. Limnology and Oceanography 19: 692-694.

Reeve, J. D. 1988. Environmental variability, migration, and persistence in host-parasitoid systems. American Naturalist 132:810-836.

Reeve, J. D. 1990. Stability, Variability, and persistence in host-parasitoid systems. Ecology 71:422-426.

Rosenzweig, M. L. 1971. Paradox of enrichment: destabilization of exploitation ecosystems in ecological time. Science 171:385-387.

Taylor, B. E., and M. Slatkin. 1981. Estimating birth and death rates of zooplankton. Limnology and Oceanography 261:143-158.

Taylor, A. D. 1988. Large-scale spatial structure and population dynamics in arthropod predator-prey systems. Annales Zoologici Fennici 25:63-74.

Watson, S., and E. McCauley. 1988. The regulation of phytoplankton community size-structure along gradients of enrichment. Canadian Journal of Fisheries and Aquatic Sciences 45:915-920.

Watson, S., E. McCauley, and J. A. Downing. 1992. Sigmoid relationships between phosphorus, algal biomass, and algal community structure. Canadian Journal of Fisheries and Aquatic Sciences 49: 2605-2610.

Appendix I

Lotka-Volterra model with diffusive migration

The model can be scaled using the following variables:

$A_a' = efA_a \quad A_b' = efA_b \quad C_a' = fC_a \quad C_b' = fC_b$

None of the original variables are used so the primes are dropped to give the following scaled model:

$$\frac{dA_a}{dt} = r_a A_a - A_a C_a \qquad \frac{dA_b}{dt} = r_b A_b - A_b C_b$$

$$\frac{dC_a}{dt} = A_a C_a - dC_a - m(C_a - C_b) \qquad \frac{dC_b}{dt} = A_b C_b - dC_b - m(C_b - C_a)$$

There is only one equilibrium with positive prey and predator density in both patches:

$$C_a^* = r_a \qquad C_b^* = r_b$$

$$A_a^* = d + m - m\frac{C_b^*}{C_a^*} \qquad A_b^* = d + m - m\frac{C_a^*}{C_b^*}$$

If $r_b > r_a$ then the prey equilibrium is positive in both patches if:

$$m < \frac{d}{\left(\frac{r_b}{r_a} - 1\right)}$$

Small deviations from equilibrium can be described by:

$$\frac{dx}{dt} = Mx \qquad x = \begin{bmatrix} A_a - A_a^* \\ C_a - C_a^* \\ A_b - A_b^* \\ C_b - C_b^* \end{bmatrix} \qquad M = \begin{bmatrix} 0 & -A_a^* & 0 & 0 \\ C_a^* & A_a^* - (d+m) & 0 & m \\ 0 & 0 & 0 & -A_b^* \\ 0 & m & C_b^* & A_b^* - (d+m) \end{bmatrix}$$

The characteristic equation can be put in the following form:

$$\lambda^4 + m\left[\frac{C_b^*}{C_a^*} + \frac{C_a^*}{C_b^*}\right]\lambda^3 + \left[A_a^* C_a^* + A_b^* C_b^*\right]\lambda^2 + m\left[\frac{A_a^* C_a^{*2}}{C_b^*} + \frac{A_b^* C_b^{*2}}{C_a^*}\right]\lambda + A_a^* C_a^* A_b^* C_b^* = 0$$

By using this form without yet substituting in for the prey and predator equilibrium expressions it can be seen that the coefficients of the characteristic equation are positive as long as the equilibrium values are all positive. The only additional requirement for local stability reduces to a factor which is always positive as long as the predator equilibrium density in the two patches is not equal:

$$m^2\left(C_a^* - C_b^*\right)^2 (d+2m)^2 > 0$$

When r_a=r_b this factor is zero and the equilibrium is neutrally stable.

There are two other interesting equilibria each with prey density equal to zero in one of the patches. If the prey density is zero in patch-a then the equilibrium is:

$$C_a^* = \frac{m}{d+m} C_b^* \qquad C_b^* = r_b$$

$$A_a^* = 0 \qquad A_b^* = d + m - m\frac{C_a^*}{C_b^*}$$

Small deviations from this equilibrium can be described by:

$$\frac{dx}{dt} = Mx \qquad x = \begin{bmatrix} A_a - A_a^* \\ C_a - C_a^* \\ A_b - A_b^* \\ C_b - C_b^* \end{bmatrix} \qquad M = \begin{bmatrix} r_a - C_a^* & 0 & 0 & 0 \\ C_a^* & -(d+m) & 0 & m \\ 0 & 0 & 0 & -A_b^* \\ 0 & m & C_b^* & A_b^* - (d+m) \end{bmatrix}$$

In this case the characteristic equation is:

$$\left(\lambda - r_a + C_a^*\right)\left[\lambda^3 + m\left(\frac{C_b^*}{C_a^*} + \frac{C_a^*}{C_b^*}\right)\lambda^2 + mC_b^*\left(\frac{C_b^*}{C_a^*} - \frac{C_a^*}{C_b^*}\right)\lambda + m^2\frac{C_b^{*2}}{C_a^*}\left(\frac{C_b^*}{C_a^*} - \frac{C_a^*}{C_b^*}\right)\right] = 0$$

If $r_b > r_a$ then the first eigenvalue is negative when:

$$m > \frac{d}{\left(\frac{r_b}{r_a} - 1\right)}$$

Therefore this equilibrium can only be stable when the equations for the previous equilibrium give negative prey density in patch-a. As long as the predator equilibrium value in the second patch is greater than in the first patch the coefficients of the unfactored portion of the characteristic equation are always positive the additional condition for stability reduces to:

$$\frac{m^2\left(C_b^* - C_a^*\right)\left(C_b^* + C_a^*\right)}{C_b^*} > 0$$

Again this is true if the predator equilibrium value in the second patch is greater than in the first patch. This occurs when $r_b > r_a$.

Lotka-Volterra "separation of scales" model

Using the same scaling as in the previous section gives:

$$\frac{dA_a}{dt} = r_a A_a - A_a C \qquad \frac{dA_b}{dt} = r_b A_b - A_b C$$

$$\frac{dC_a}{dt} = \frac{1}{2}\left(A_a C + A_b C\right) - dC$$

It is clear that if $r_a \neq r_b$ then the prey equilibrium cannot be positive in both patches. In the case where prey density is zero in patch a the equilibrium is:

$$A_a^* = 0 \qquad C^* = r_b \; A_b^* = 2d$$

Small deviations from equilibrium can be described by:

$$\frac{dx}{dt} = Mx \qquad x = \begin{bmatrix} A_a - A_a^* \\ A_b - A_b^* \\ C - C^* \end{bmatrix} \qquad M = \begin{bmatrix} r_a - C^* & 0 & 0 \\ 0 & 0 & -A_b^* \\ \frac{C^*}{2} & \frac{C^*}{2} & 0 \end{bmatrix}$$

The characteristic equation is:

$$(\lambda - r_1 + r_2)(\lambda^2 + r_2 d) = 0$$

The first eigenvalue is negative if $r_b > r_a$ but the second two eigenvalues have zero real part like the nonmetapopulation counterpart.

Rosensweig-MacArthur "seperation of scales" model

The following scaled variables and parameters are used:

$$r' = \frac{2r}{eg} \quad k' = \frac{k}{h} \quad d' = \frac{2d}{eg}$$

$$A_a' = \frac{A_a}{h} \quad A_b' = \frac{A_b}{h} \quad C_a' = \frac{2C_a}{eh} \quad t' = \frac{eg}{2}t$$

Again the prime notation is not necessary and the following model results:

$$\frac{dA_a}{dt} = rA_a\left(1 - \frac{A_a}{k}\right) - \frac{A_a C}{1 + A_a} \qquad \frac{dA_b}{dt} = rA_b\left(1 - \frac{A_b}{k}\right) - \frac{A_b C}{1 + A_b}$$

$$\frac{dC}{dt} = \frac{A_a C}{1 + A_a} + \frac{A_b C}{1 + A_b} - dC$$

Assuming that densities in each patch are not equal to zero, the equilibria are described by the following relationships:

$$C^* = r\left(1 - \frac{A_a^*}{k}\right)\left(1 + A_a^*\right) \qquad C^* = r\left(1 - \frac{A_b^*}{k}\right)\left(1 + A_b^*\right)$$

$$\frac{A_a^*}{1+A_a^*}+\frac{A_b^*}{1+A_b^*}-d=0$$

Equating the two expressions for the predator equilibrium gives the following:

$$\left(k-A_a^*\right)\left(1+A_a^*\right)=\left(k-A_b^*\right)\left(1+A_b^*\right)$$

which has two solutions:

$$A_b^*=A_a^* \qquad A_b^*=k-1-A_a^*$$

The first specifies the homogeneous equilibrium:

$$A_a^*=A_b^*=\frac{d}{2-d}$$

This equilibrium has the same local stability properties as the equilibrium of the mixed model. The second is an equilibrium with prey density positive in both patches but not equal. Analysis of the two symmetrical equilibria specified by this equation has some factors in common with the next equilibrium which will be analyzed first.

It is possible that the prey density is zero in one of the patches. This is a symmetric solution and only the case where patch-a has zero prey density will be considered. The equilibrium is:

$$A_a^*=0 \qquad A_b^*=\frac{d}{1-d} \qquad C^*=\frac{r}{k}\left(k-A_b^*\right)\left(1+A_b^*\right)$$

Dynamics near the equilibrium can be described by:

$$\frac{dx}{dt}=Mx \qquad x=\begin{bmatrix}A_a-A_a^*\\A_b-A_b^*\\C-C^*\end{bmatrix} \qquad M=\begin{bmatrix}-a_a & 0 & 0\\0 & -a_b & -b_b\\C^* & c_b & 0\end{bmatrix}$$

where:

$$a_a=-\frac{\partial}{\partial A_a}\frac{dA_a}{dt}\bigg|^*=r-C^* \qquad\qquad a_b=-\frac{\partial}{\partial A_b}\bigg|^*=\frac{r}{k}A_b^*\left[1-\frac{k-A_b^*}{1+A_b^*}\right]$$

$$b_b = -\frac{\partial}{\partial A_b}\frac{dC}{dt}\bigg|^{*} = \frac{A_b^*}{1+A_b^*} \qquad c_b = \frac{\partial}{\partial A_b}\frac{dC}{dt}\bigg|^{*} = \frac{r}{k}\frac{k-A_b^*}{1+A_b^*}$$

the characteristic equation is:

$$(\lambda + a_a)\left(\lambda^2 + a_b\lambda + b_b c_b\right) = 0$$

Therefore the equilibrium is stable as long as $a_a>0$ and $a_b>0$. That is:

$$\frac{k-1}{2} < A_a^* < k-1$$

When the prey density is positive in both patches but not equal between the two patches there are two symmetric solutions. The first one is:

$$A_a^* = \frac{k-1}{2} - \frac{\sqrt{(k+1)(2-d)\left[2(k-1)-d(k+1)\right]}}{2(2-d)}$$

$$A_b^* = \frac{k-1}{2} + \frac{\sqrt{(k+1)(2-d)\left[2(k-1)-d(k+1)\right]}}{2(2-d)}$$

For the other solutions the prey equilibria densities are equal to the opposite quantities. The quantity inside the square root sign is positive as long as $d<2$, which is also the upper boundary on d required to make the prey density positive, and that:

$$\frac{d}{2-d} < \frac{k-1}{2}$$

This is also the condition for instability of the homogeneous solution so when the homogeneous solution becomes unstable this equilibrium becomes positive.

Small deviations from equilibrium can be described by:

$$\frac{dx}{dt} = Mx \qquad x = \begin{bmatrix} A_a - A_a^* \\ A_b - A_b^* \\ C - C^* \end{bmatrix} \qquad M = \begin{bmatrix} -a_a & 0 & -b_a \\ 0 & -a_b & -b_b \\ c_a & c_b & 0 \end{bmatrix}$$

where:

$$a_a = -\frac{\partial}{\partial A_a}\frac{dA_a}{dt}\bigg|^* = \frac{r}{k}A_a^*\left[1-\frac{k-A_a^*}{1+A_a^*}\right] \qquad a_b = -\frac{\partial}{\partial A_b}\frac{dA_b}{dt}\bigg|^* = \frac{r}{k}A_b^*\left[1-\frac{k-A_b^*}{1+A_b^*}\right]$$

$$b_a = -\frac{\partial}{\partial C^*}\frac{dA_a}{dt}\bigg|^* = \frac{A_a^*}{1+A_a^*} \qquad b_b = -\frac{\partial}{\partial C^*}\frac{dA_b}{dt}\bigg|^* = \frac{A_b^*}{1+A_b^*}$$

$$c_a = \frac{\partial}{\partial A_a}\frac{dA_a}{dt}\bigg|^* = \frac{r}{k}\frac{k-A_a^*}{\left(1+A_a^*\right)} \qquad c_b = \frac{\partial}{\partial A_b}\frac{dA_b}{dt}\bigg|^* = \frac{r}{k}\frac{k-A_b^*}{\left(1+A_b^*\right)}$$

The characteristic equation is then:

$$\det(\lambda I - M) = \lambda^3 + (a_a + a_b)\lambda^2 + (a_a a_b + b_a c_a + b_b c_b)\lambda + a_a b_b c_b + a_a b_b c_b = 0$$

If the predator density is to be positive then $k_a > A_a^*$ and $k_b > A_b^*$. Under these conditions c_a and c_b will be positive and b_a and b_b are always positive. All of the coefficients of the characteristic equation are positive. Of special note is the coefficient of λ^2 which shows that although the prey equilibrium in one of the patches would be unstable in isolation, this coefficient can still be positive for the heterogeneous equilibrium. The other condition that is necessary for stability is:

$$(a_a + a_b) * a_a a_b + a_a b_a c_a + a_b b_b c_b > 0$$

After substituting in the prey equilibria and doing a significant amount of algebra this can be reduced to the following form:

$$-\left(\frac{r^2}{k^3(2-d)}\right)\left(2(k-1)-d(k+1)\right)\times$$

$$\left[\left(d-(1-d)(k-1)\right)\left(2d-(2-d)(k-1)\right)r + k(1-d)(2-d)\left(2d-(1-d)(k-1)\right)\right] > 0$$

The second term is negative if the prey equilibrium values are positive so the term in

square brackets must be positive for the equilibrium to be stable. The coefficient of r is always negative as long as the prey equilibrium values are positive so the condition can be put in the following form:

$$r < k(1-d)\frac{\left[\frac{d}{1-d}-\frac{k-1}{2}\right]}{\left[\frac{k-1}{2}-\frac{d}{2-d}\right]\left[\frac{d}{1-d}-(k-1)\right]}$$

Surprisingly, this condition can be interpreted in terms of characteristics of the homogeneous equilibrium and the equilibrium when one patch is zero. The upper term is the deviation of the equilibrium value in one patch when the other patch is zero from the prey density where the predator density is maximized. The lower left term is the deviation of the mixed equilibrium from the point that gives maximum predator density.

Appendix II

Logistic growth in a heterogeneous environment

The logistic model can be solved explicitly for prey density as a function of time and the initial density. The dynamics of the single population in environment-a are described by:

$$A_a(t) = \frac{k_a A(0)}{A_a(0) + (k_a - A_a(0))e^{-r_a t}}$$

If there are two populations with different parameters that are mixed together, and the interval between mixing (in days) is m and a migration occurs at time 0 then the dynamics can be described by:

$t = xm + T \quad 0 < T \leq m, \quad x = 1,2,3,4.....$

$$A_a(t) = \begin{cases} \dfrac{k_a A_a(mx)}{A_a(mx) + (k_a - A_a(mx))e^{-r_a T}} & T < m \\ \dfrac{1}{2}\dfrac{k_a A(xm)}{A_a(mx) + (k_a - A_a(xm))e^{-r_a m}} + \dfrac{1}{2}\dfrac{K_b A_b(xm)}{A_b(mx) + (k_b - A_b(xm))e^{-r_b m}} & T = m \end{cases}$$

$$A_b(t) = \begin{cases} \dfrac{k_b A(mx)}{1 + (k_b - A_b(mx))e^{-r_b T}} & T < m \\ \dfrac{1}{2}\dfrac{k_a A_a(xm)}{A_a(xm) + (k_a - A_a(xm))e^{-r_a m}} + \dfrac{1}{2}\dfrac{k_b A_b(xm)}{A_b(xm) + (k_b - A_b(xm))e^{-r_b m}} & T = m \end{cases}$$

The density just after migration can be written in terms of the density just after the previous migration (the density will then be equal in both patches):

$$A_{mix}(xm + m) = \frac{1}{2}\frac{k_a A_{mix}(xm)}{A(xm) + (k_a - A_{mix}(xm))e^{-r_a m}} + \frac{1}{2}\frac{k_b A_{mix}(xm)}{A_{mix}(xm) + (k_b - A_{mix}(xm))e^{-r_b m}}$$

The case where mixing occurs continuously and when it is finite are both of interest. The differential equation for A_{mix} when m approaches 0 can be found by using the definition of derivative:

$$\frac{df(a)}{da} = \lim_{h \to 0} \frac{f(a+h) - f(a)}{h}$$

If t is taken as the time of the previous migration and the time to the next migration as m then the derivative would be:

$$\frac{dA_{mix}}{dt} = \lim_{m \to 0} \frac{A_{mix}(t+m) - A_{mix}(t)}{m}$$

In this case the result is:

$$\frac{dA_{mix}}{dt} = \frac{1}{2} r_a A_{mix}\left(1 - \frac{A_{mix}}{k_a}\right) + \frac{1}{2} r_b A_{mix}\left(1 - \frac{A_{mix}}{k_b}\right)$$

Heterogeneous non-metapopulation model

The following scaled variables and parameters are used:

$$r_a' = \frac{2r_a}{eg} \quad r_b' = \frac{2r_b}{eg} \quad k_a' = \frac{k_a}{h} \quad k_b' = \frac{k_b}{h} \quad d' = \frac{2d}{eg}$$

$$A_{mix}' = \frac{A_{mix}}{h} \quad C_{mix}' = \frac{2C_{mix}}{eh} \quad t' = \frac{eg}{2} t$$

Again the prime notation is not necessary and the following model results:

$$\frac{dA_{mix}}{dt} = \frac{r_a}{2} A_{mix}\left(1 - \frac{A_{mix}}{k_a}\right) + \frac{r_a}{2} A_{mix}\left(1 - \frac{A_{mix}}{k_b}\right) - \frac{A_{mix} C_{mix}}{1 + A_{mix}}$$

$$\frac{dC_{mix}}{dt} = 2\frac{A_{mix} C_{mix}}{1 + A_{mix}} - dC_{mix}$$

There is a single equilibrium with positive predator density:

$$A_{mix}^{*} = \frac{d}{2 - d}$$

$$C^*_{mix} = \frac{r_a}{2}\left(1-\frac{A^*_{mix}}{k_a}\right)\left(1+A^*_{mix}\right)+\frac{r_b}{2}\left(1-\frac{A^*_{mix}}{k_b}\right)\left(1+A^*_{mix}\right)$$

The stability analysis for this model can be found in many places but it is useful to go through it here because of its relationship to the next model. Small deviations from equilibrium can be described by:

$$\frac{dx}{dt} = Mx \qquad x = \begin{bmatrix} A_{mix} - A^*_{mix} \\ C_{mix} - C^*_{mix} \end{bmatrix} \quad M = \begin{bmatrix} -a & -b \\ c & 0 \end{bmatrix}$$

where:

$$a = -\frac{\partial}{\partial A_{mix}}\frac{dA_{mix}}{dt}\bigg|^* = \frac{r_{mix}A^*_{mix}}{k_{mix}}\left[1-\frac{k_{mix}-A^*_{mix}}{1+A^*_{mix}}\right] = a_a + a_b$$

$$a_a = \frac{r_a A^*_{mix}}{2k_a}\left[1-\frac{k_a - A^*_{mix}}{1+A^*_{mix}}\right] \qquad a_b = \frac{r_b A^*_{mix}}{2k_b}\left[1-\frac{k_b - A^*_{mix}}{1+A^*_{mix}}\right]$$

$$b = -\frac{\partial}{\partial C_{mix}}\frac{dA_{mix}}{dt}\bigg|^* = \frac{A^*_{mix}}{1+A^*_{mix}}$$

$$c = \frac{\partial}{\partial A_{mix}}\frac{dC_{mix}}{dt}\bigg|^* = 2\frac{r_{mix}}{k_{mix}}\frac{k_{mix}-A^*_{mix}}{1+A^*_{mix}} = \frac{r_a}{k_a}\frac{k_a - A^*_{mix}}{1+A^*_{mix}} + \frac{r_b}{k_b}\frac{k_b - A^*_{mix}}{1+A^*_{mix}}$$

The characteristic equation is :

$$\det(\lambda I - M) = \lambda^2 + a\lambda + bc = 0$$

The equilibrium is stable if the predator equilibrium is positive and a>0. The latter condition is satisfied if :

$$A^*_{mix} > \frac{k_{mix}-1}{2}$$

A sufficient condition for stability is that the following two inequalities are true, if they are both false then the system is unstable:

$$A^*_{mix} > \frac{k_a - h}{2} \quad \text{And} \quad A^*_{mix} > \frac{k_b - h}{2}$$

Homogeneous metapopulation model

Again, the number of parameters can be reduced. Parameters are scaled in the same way as the last section and state variables are scaled as follows:

$$A_a' = \frac{A_a}{h} \; A_b' = \frac{A_b}{h} \; C' = \frac{2C}{eh} \; t' = \frac{eg}{2} t$$

Again the prime notation is not necessary and the following model results:

$$\frac{dA_a}{dt} = \frac{r_a}{2} A_a \left(1 - \frac{A_a}{k_a}\right) + \frac{r_b}{2} A_a \left(1 - \frac{A_a}{k_b}\right) - \frac{A_a C}{1 + A_a}$$

$$\frac{dA_b}{dt} = \frac{r_a}{2} A_b \left(1 - \frac{A_b}{k_a}\right) + \frac{r_b}{2} A_b \left(1 - \frac{A_b}{k_b}\right) - \frac{A_b C}{1 + A_b}$$

$$\frac{dC}{dt} = \frac{A_a C}{1 + A_a} + \frac{A_b C}{1 + A_b} - dC$$

The analysis using the new parameters does not give any new information of interest. The results of this model from Chapter 1 with the parameters r_{mix} and k_{mix} are sufficient. Because the homogeneous equilibrium of this model has the same stability boundaries as the mixed model the homogeneous equilibrium is stable if the equilibrium is stable in both types of environment and unstable if the equilibrium in each environment is unstable as shown for the heterogeneous non-metapopulation model.

Heterogeneous Metapopulation Model

Using the same parameter and variable scaling as the homogeneous metapopulation model gives the following heterogeneous metapopulation model:

$$\frac{dA_a}{dt} = r_a A_a \left(1 - \frac{A_a}{k_a}\right) - \frac{A_a C}{1 + A_a} \qquad \frac{dA_b}{dt} = r_b A_b \left(1 - \frac{A_b}{k_b}\right) - \frac{A_b C}{1 + A_b}$$

$$\frac{dC}{dt} = \frac{A_a C}{1+A_a} + \frac{A_b C}{1+A_b} - dC$$

As long as the prey density is not zero in one of the patches the equilibria satisfy the following relationships:

$$C^* = r_a\left(1-\frac{A_a^*}{k_a}\right)\left(1+A_a^*\right) \qquad C^* = r_b\left(1-\frac{A_b^*}{k_b}\right)\left(1+A_b^*\right)$$

$$\frac{A_a^*}{1+A_a^*} + \frac{A_b^*}{1+A_b^*} - d = 0$$

Small deviations from equilibria with prey density not equal to zero in either patch can all be described by:

$$\frac{dx}{dt} = Mx \qquad x = \begin{bmatrix} A_a - A_a^* \\ A_b - A_b^* \\ C - C^* \end{bmatrix} \qquad M = \begin{bmatrix} -a_a & 0 & -b_a \\ 0 & -a_b & -b_b \\ c_a & c_b & 0 \end{bmatrix}$$

where:

$$a_a = -\frac{\partial}{\partial A_a}\frac{dA_a}{dt}\bigg|^* = \frac{r_a}{k_a}A_a^*\left[1-\frac{k_a - A_a^*}{1+A_a^*}\right] \qquad a_b = -\frac{\partial}{\partial A_b}\frac{dA_b}{dt}\bigg|^* = \frac{r_b}{k_b}A_b^*\left[1-\frac{k_b - A_b^*}{1+A_b^*}\right]$$

$$b_a = -\frac{\partial}{\partial C^*}\frac{dA_a}{dt}\bigg|^* = \frac{A_a^*}{1+A_a^*} \qquad b_b = -\frac{\partial}{\partial C^*}\frac{dA_b}{dt}\bigg|^* = \frac{A_b^*}{1+A_b^*}$$

$$c_a = \frac{\partial}{\partial A_a}\frac{dA_a}{dt}\bigg|^* = \frac{r_a}{k_a}\frac{k_a - A_a^*}{\left(1+A_a^*\right)} \qquad c_b = \frac{\partial}{\partial A_b}\frac{dA_b}{dt}\bigg|^* = \frac{r_b}{k_b}\frac{k_b - A_b^*}{\left(1+A_b^*\right)}$$

The characteristic equation is then:

$$\det(\lambda I - M)$$
$$= \lambda^3 + (a_a + a_b)\lambda^2 + (a_a a_b + b_a c_a + b_b c_b)\lambda + a_a b_b c_b + a_a b_b c_b = 0$$

If the predator density is positive ($A_a^* < k_a$ and $A_b^* < k_b$) then c_a and c_b will be positive and b_a and b_b are always positive. The Routh-Hurwitz criteria are:

$$a_a + a_b > 0 \qquad a_a b_b c_b + a_b b_a c_a > 0 \qquad (a_a + a_b)a_a a_b + a_a b_a c_a + a_b b_b c_b > 0$$

It is clear that if a_a and a_b are positive then the equilibrium is stable and if they are both negative then the equilibrium is unstable. The condition for a_a and a_b to be positive respectively are:

$$A_a^* > \frac{k_a - 1}{2} \quad \text{and} \quad A_b^* > \frac{k_b - 1}{2}$$

This is analogous to the mixed and isolated patches except that the equilibrium densities of prey are different than they are for mixed or isolated systems. From this it can be seen that equilibrium #1 is stable as long as it is on the right branch on the upper part of the hyperbola. And likewise if equilibrium #3 falls on the left branch of the hyperbola then it is unstable.

When the prey density is zero in the first patch the equilibrium is:

$$A_a^* = 0 \qquad A_b^* = \frac{d}{1-d} \qquad C^* = r_b\left(1 - \frac{A_b^*}{k_b}\right)\left(1 + A_b^*\right)$$

The equilibrium for this model is the same as if patch B were isolated but with twice the normal death rate. Small deviations from the equilibrium can be described by:

$$\frac{dx}{dt} = Mx \qquad x = \begin{bmatrix} A_a - A_a^* \\ A_b - A_b^* \\ C - C^* \end{bmatrix} \qquad M = \begin{bmatrix} -a_a & 0 & 0 \\ 0 & -a_b & -b_b \\ 0 & c_b & 0 \end{bmatrix}$$

where:

$$a_a = -\frac{\partial}{\partial A_a}\frac{dA_a}{dt}\bigg|^* = r_a - C^* \qquad a_b = -\frac{\partial}{\partial A_b}\frac{r_b}{K_b}\bigg|^* = A_b^*\left[1-\frac{K_b - A_b^*}{1+A_b^*}\right]$$

$$b_b = -\frac{\partial}{\partial A_b}\frac{dC}{dt}\bigg|^* = \frac{A_b^*}{1+A_b^*} \qquad c_b = \frac{\partial}{\partial A_b}\frac{dC}{dt}\bigg|^* = \frac{r_b}{K_b}\frac{K_b - A_b^*}{1+A_b^*}$$

The characteristic equation is:

$$\det(\lambda I - M) = \left(\lambda + a_a\right)\left(\lambda^2 + a_b\lambda + b_b c_b\right) = 0$$

Therefore the equilibrium is stable as long as $a_a>0$ and $a_b>0$. Thus the lower stability boundary (when changing d) is the same as that of the isolated model with twice the death rate. The point where the upper part of the hyperbola intersects the A_b axis coincides with $a_a=0$. The values of this point are given in Table 2.1. Therefore the upper stability boundary of this equilibrium occurs when the heterogeneous equilibrium with prey positive in both patches becomes negative. Analysis of the equilibrium with prey density equal to zero in patch-b is identical.

Appendix III

The egg stage duration and the average starvation time, which were used for estimation of parameters, were obtained from supporting experiments.

Individual Ceriodaphnia were grown in 25 mL of Big Hill Spring water which was changed daily. Individuals were fed a constant amount of food daily throughout their lifetime. Food concentrations ranged from 1.5×10^4 and 1.2×10^5 cells / mL . A total of 16 individuals reached reproductive age. Juveniles ranging in age from 0 - 2 days were placed in 25 mL of water without food and placed in the incubator. Water was changed daily and it was noted whether or not individuals were dead. A total of 21 individuals were starved to death.

The egg stage duration was always observed to be 2 days at all food levels. The mean starvation time was 2.73 days ($s^2 = 3.42$).